Molecular Mechanisms controlling the Precision of Chemokine Guided Cell Migration

Dissertation

zur Erlangung des akademischen Grades
eines Doktors der Naturwissenschaften (Dr. rer. nat.)

im Fachbereich 18 Naturwissenschaften
der Universität Kassel

vorgelegt von
Sofia Minina

Kassel, April 2007

Supervisors: Prof. Dr. Mireille A. Schäfer
PD Dr. Reinhard Schuh

Committee: Prof. Dr. Mireille A. Schäfer
PD Dr. Reinhard Schuh
Prof. Dr. Markus Maniak
Prof. Dr. Wolfgang Nellen

Date of Defense: June. 13. 2007

To my parents.

Table of contents

Abbreviations

AB	antibody
BSA	bovine serum albumin
cas	*Casanova*
cDNA	complementary DNA
DNA	deoxyribonucleic acid
E. coli	Escherichia coli
EDTA	ethylendiamine tetraacetate
EGFP	enhanced green fluorescent protein
fkd-2	*forkhead-2*
GFP	green fluorescent protein
hpf	hours post fertilization
IgG	immunoglobulin G
mRNA	messenger RNA
nos1	*nanos1*
ody	*Odysseus*
o/n	over night
ORF	open reading frame
PBS	phosphate buffered saline
PBT	phosphate buffered saline containing Tween20
PCR	polymerase chain reaction
PGC	primordial germ cell
RNA	ribonucleic acid
rpm	revolutions per minute
RT	room temperature
RT-PCR	reverse transcription polymerase chain reaction
Wt	wild-type

1.0 Introduction

1.1 Germ cells

The continuity of the germ cell lineage ensures the transmission of genetic information between generations. Primordial germ cells (PGCs) are a small population of cells that set aside from other cell lineages early in embryogenesis and typically migrate to the site where they coalesce with supporting somatic tissues and undergo differentiation into gametes [1-3]. Consequently, the gametes would fuse to give rise to the next cycle of life.

Zebrafish is an attractive model system for investigating PGC biology due the availability of genetic mutations, the reverse genetic tools as well as the translucent nature of the embryos. Below we will summarize the current knowledge about PGCs in zebrafish and describe the development of this cell lineage in other model organisms. In the last parts of the introduction we will focus on the molecular aspects implicated in PGC guidance.

1.2 Primordial germ cell specification and development

Although PGCs are usually set aside as a distinct cell population early in embryogenesis, the mechanisms of their specification are different in different organisms. PGC specification can be a result of inheritance of maternally provided determinants or be controlled by cell-cell interaction where the PGC fate is induced by secreted factors.

In mouse and urodele amphibians germ cells are specified by inductive signals provided by neighbouring cells (reviewed in [4-6]). This induction results in *de novo* transcription of specific genes in presumptive PGCs, which initiates their differentiation into cells belonging to the germline [7-9].

PGC induction in mouse occurs before stage E6.5 when PGCs can first be detected as a cluster of cells expressing *fragilis* at the base of allantois [8]. The inductive signals responsible for PGC induction were identified as members of the BMP family of secreted factors that activate the intercellular signalling cascade of the TGF-beta family. Experiments with 6.5 days epiblast cells from which PGCs arise suggest that BMP4/8 signaling is required and sufficient for the initial specification of germ cell fate [10]. Germ cell specification in the mouse is closely linked to the initiation of germ cell-specific transcription. Gene expression controlled by the distal enhancer of the Oct4 promoter, for example, begins in the germ cells as early as E7.0. Later on these precursors migrate to the primitive streak where they segregate into PGC and allantois lineages.

In *Drosophila*, *C.elegans*, *Xenopus*, chick, and zebrafish (*Danio rerio*), germline discriminates from other (somatic) cells by inheritance of maternal factors deposited in the egg during oogenesis that contain germ cell determinants [11-13]. These determinants, specific RNAs and proteins, together comprise so-called germ plasm and are organised in germ granules, which due to their electron density were described in zebrafish as a characteristic feature of germ cells even before their molecular components were identified. It is possible that germ plasm RNAs localise to the germ plasm through *cis*-acting elements in their 3'-untranslated regions (UTR) as it was first shown for the *vasa* RNA [14]. Germ cell specific expression of those RNA molecules is achieved also through selective stabilization and preferential translation in PGCs as compared to somatic cells [15-18]. Certain *cis*-elements in the 3' UTRs of RNA molecules of *vasa* and *nanos-1* were shown to be utilised as a signal for degradation in somatic cells where the remaining germ plasm components that were not incorporated into PGCs can be observed until early epiboly [17, 19-23]. Specifically, *nanos-1* 3'UTR was recently described as a target of microRNA-mediated repression [23]. These posttranscriptional mechanisms lead to establishment of a specific protein expression profile in germ cells, which in turn determines their fate.

The number of proteins identified to be specifically expressed in PGCs is constantly growing, although their particular role is not always clear. *vasa*, a gene originally identified in *Drosophila* [24], is the first found PGC specific gene in

zebrafish. An RNA-helicase, it belongs to a DEAD-box family. *vasa* is expressed and stabilized in PGCs from the earliest time point of specification [20]. Products of *nanos*-1 and *deadend* genes were identified as prominent components of germ plasm in different organisms [17, 25-30]. In zebrafish, RNA of these genes can be seen in the distal parts of the embryonic cleavage furrow as early as at 2-cell stage and stays there for a number of divisions until it is inherited by 4 blastomeres, which then undergo assymetrical divisions so that only one of two daughter cells obtains germ plasm and the number of presumptive PGCs harbouring germ plasm remains constant [22]. At the late blastula stage (4 hpf, 4 k cell, late sphere stage) PGC specification occurs and the symmetrical divisions start to multiply the net number of PGCs at four random positions in the embryo [22].

1.3 Primordial germ cell migration

As mentioned above, in most organisms PGCs specify early in embryonic development and away from the site where gonad will form. To reach the region where the gonad develops the cells actively migrate from their site of origin in response to directional cues provided by the somatic environment along the migration path. Below, we provide an overview of PGC migration in different organisms.

1.3.1 Drosophila

PGCs in *D. melanogaster* are specified at the posterior pole of the embryo (Figure 1A) [2]. During gastrulation, PGCs do not actively migrate and are rather transported along with the midgut primordial that they are associated with and become internalized into the forming posterior midgut (Figure 1B). Next, reorganization of the cell-cell contacts among the endodermal cells comprising the gut wall allow the PGCs to acively migrate through the midgut epithelium in a process termed transendothelial migration (Figure 1C). From there, the cells reorient on the midgut toward the overlying mesoderm (Figure 1D). Subsequently, the PGCs leave the midgut and sort into two bilateral clusters within the mesoderm, where they associate with the somatic gonadal precursors (SGPs)

(Figure 1E). Finally, the two tissues coalesce to form the embryonic gonad (reviewed in [3, 31]).

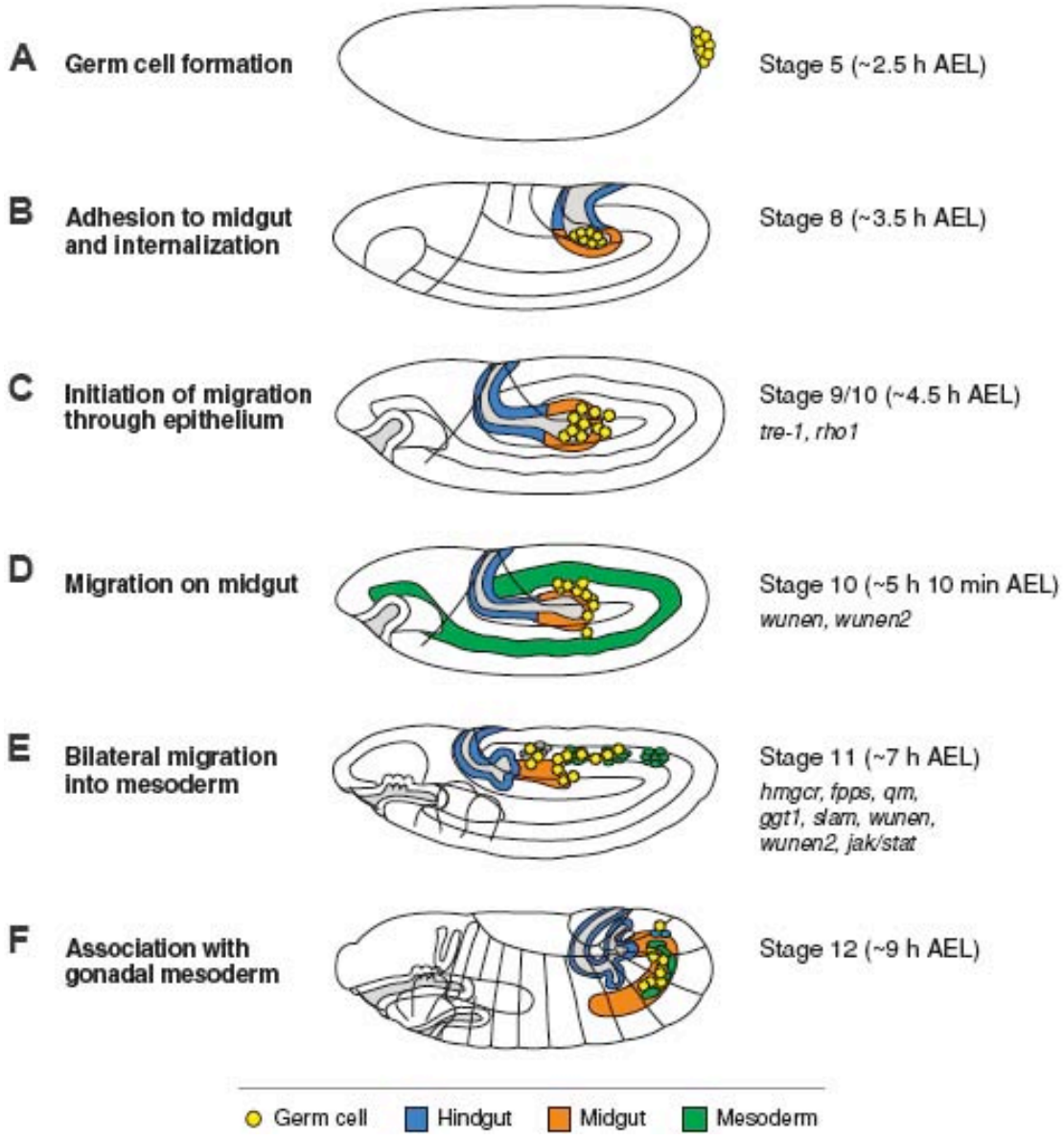

Figure 1. Stages of germ cell migration in *Drosophila*. The time of onset of each step is indicated at the top right of each panel. AEL stands for after egg laying at 25°C. The genes required for each step are shown in the bottom right of each panel. This figure is adapted from [31]. (A, B) Germ cells are formed at the posterior pole of the embryo and are internalized into the blindfold of the midgut epithelium during gastrulation movements. (C) Subsequently, at stages 9/10 germ cells migrate out of the midgut. (D) Germ cells have moved to the dorsal surface of the midgut by late stage 10. (E) At stage 11, germ cells migrate bilaterally to reach the gonadal mesoderm from the

dorsal surface of the midgut. (F) Subsequently, germ cells associate with the gonadal mesoderm to form the gonad at stage 14.

Several genes regulating these processes were identified as a result of mutational screens. Whereas the actual guidance molecules that guide PGC migration are not known, enzymes thought to be important for their synthesis or destruction have been identified. 3-hydroxy-3methylglutaryl coenzyme A reductase (HMGCoAR) was found to regulate generation of the presumptive attractant [32]. This gene is expressed in the target mesoderm and PGCs in embryos lacking HMGCoAR function do not reach their target properly. Conversely, HMGCoAR expression in ectopic locations is sufficient for attracting the cells to those sites [32].

Two members of the family of lipid phosphate phosphatase proteins, WUNEN1 and WUNEN2, were shown to be expressed in regions in the embryo that the PGCs avoid and were found to generate environment that is repulsive for the migrating cells. In *wunen* mutant embryos the germ cells are found in locations that they normally avoid and therefore their overall migration is abnormal. When expressed in the PGC migration target sites, the Wunen proteins can prevent PGC from entering those sites [33, 34].

Recently, a G-protein coupled receptor Trapped in endoderm-1 (Tre-1) was shown to play a role in PGC migration in *Drosophila*. In Tre-1 mutants the PGCs fail to exit the gut, suggesting that the cells require its function to perform transendothelial migration [35]. The Tre1 GPCR belongs to a novel group of GPCRs of the rhodopsin family, and the ligand has yet to be identified. Hence, the definite role of Tre-1 in PGC migration or guidance is still not known.

1.3.2 Mouse

PGCs in the mouse are motile from their inception (around E7.0) to the point when they colonize the genital ridge (E11.5). Shortly after their formation, individual PGCs that at this stage already show polarized morphology and send protrusions move through the posterior primitive streak and disperse into the adjacent posterior embryonic endoderm, which gives rise to the hindgut. (Figure 2A) [3, 8, 36]. At

E8.0 - E9.0, the cells are incorporated into the hindgut (Figure 2B) and then leave the hindgut towards the genital ridge as individual cells via transepithelial migration (E9.5–E10.5) (Figure 2C) [37]. Between E10.5 and E11.5, germ cells reach the genital ridges, where they coalesce with somatic gonadal cells to form the gonads (Figure 2D) [38]. The role of endoderm as a migration substrate for PGCs in mouse is reminiscent of such in PGC migration in *Drosophila* and therefore it is tempting to speculate that this role of endoderm in PGC migration is conserved throughout the phylogenetic tree.

The molecular mechanism by which cell motility is initiated in mouse PGCs is not well understood. Regulated adhesion and repulsion mechanisms mediated by the interferon-induced transmembrane protein IFITM1 (IFITM/Mil/Fragilis), which plays a role in mouse PGC specification may regulate this step [9, 39]. The gene *Ifitm1* is required for PGC migration from the mesoderm into the endoderm and supposedly plays a repulsive role since when IFITM1 is depleted, germ cells remain in the posterior mesoderm [9].

Recent analysis of mouse mutants for the chemokine SDF1 and for its receptor CXCR4 revealed that the migration of germ cells toward the genital ridges is mediated by SDF1, which is highly expressed in the mesenchyme and genital ridges, and its receptor CXCR4, which is expressed in germ cells [40, 41]. In mutant embryos lacking either the CXCR4 receptor or the SDF1 ligand, germ cells fail to reorient on the hindgut, and only a few of them reach the genital ridges, where they survive and divide at a rate similar to that of wild type. This suggests that SDF1/CXCR4 regulate germ cell migration and is probably not involved in PGC survival.

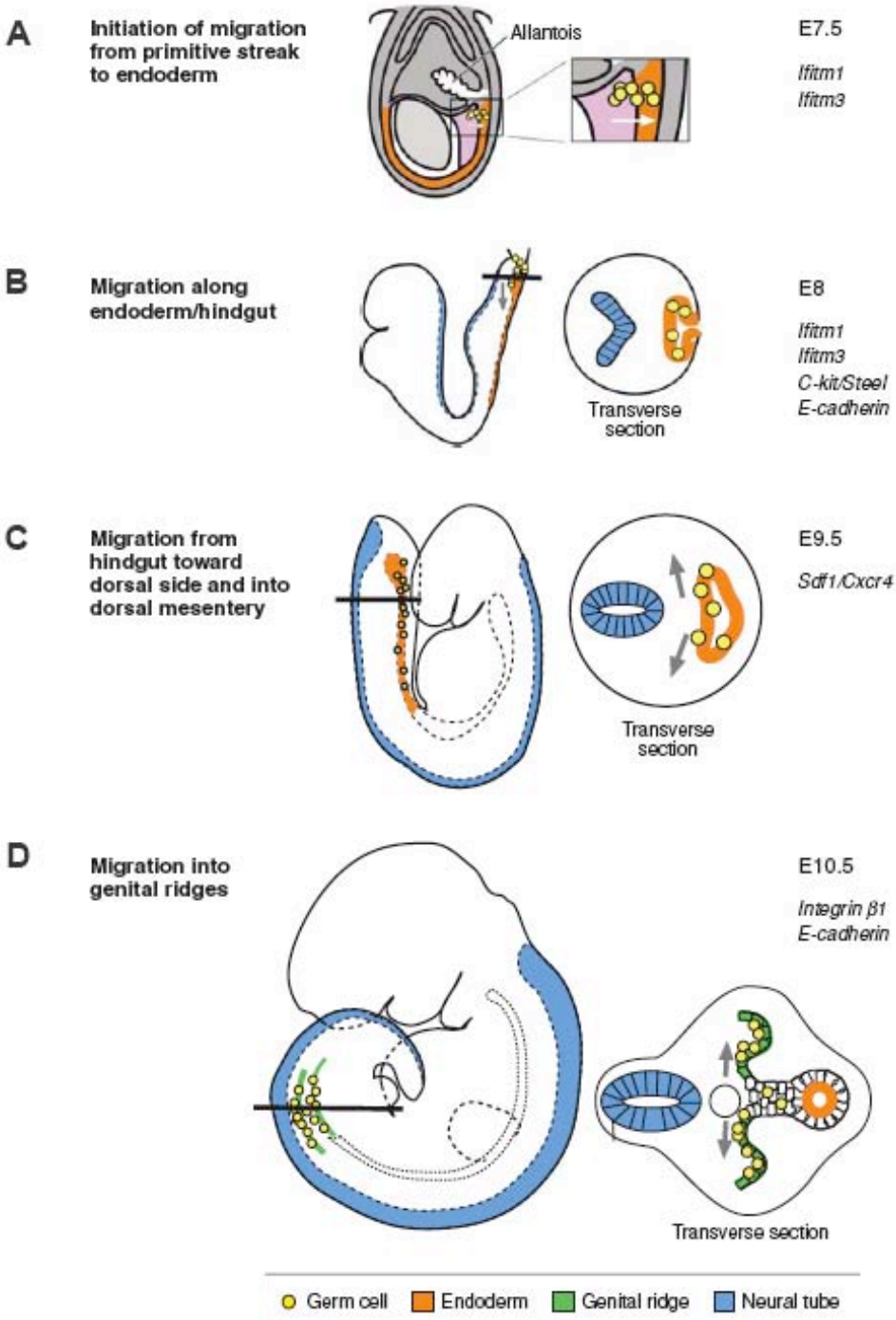

Figure 2. Stages of germ cell migration in mice. The time of onset of each step is indicated at the top right of each panel. E stands for embryonic day. The genes required for each step are shown in the bottom right of each panel. (A) Germ cells (yellow) are specified in the primitive streak. At E7.5, they initiate their migration to the endoderm (orange). An enlargement of the boxed area is shown on the right. In B-D a transverse section (straight black line) is shown at the right of each panel. (B) At E8, germ cells start migrating within the endoderm (which now becomes hindgut). (C) At E9.5, germ cells can be seen migrating from the hindgut toward the dorsal body wall. (D) By

E10.5, germ cells reach the genital ridges (green) from the body wall to form the gonad; germ cells at the base of the mesentery will be lost. This figure is adapted from [31].

1.3.3 Zebrafish

Zebrafish PGCs are specified at four different positions that are randomly located in respect to the embryonic axis by maternally provided cytoplasmic determinants, commonly called germ plasm [12, 17, 20, 21, 42]. After having been specified germ cells acquire motility and start migrating directionally to arrive at the site of the future gonad by the end of the first day of fish development [42, 43] (Figure 3). In the course of their migration germ cells crawl on top of the yolk syncitial layer where endodermal layer is also located at gastrulation stages [27, 42] (Figure 4F, 4G). Nevertheless, the role of the endoderm for PGC migration in zebrafish despite the importance of this germ layer for PGC migration in *Drosophila* and mouse has never been tested.

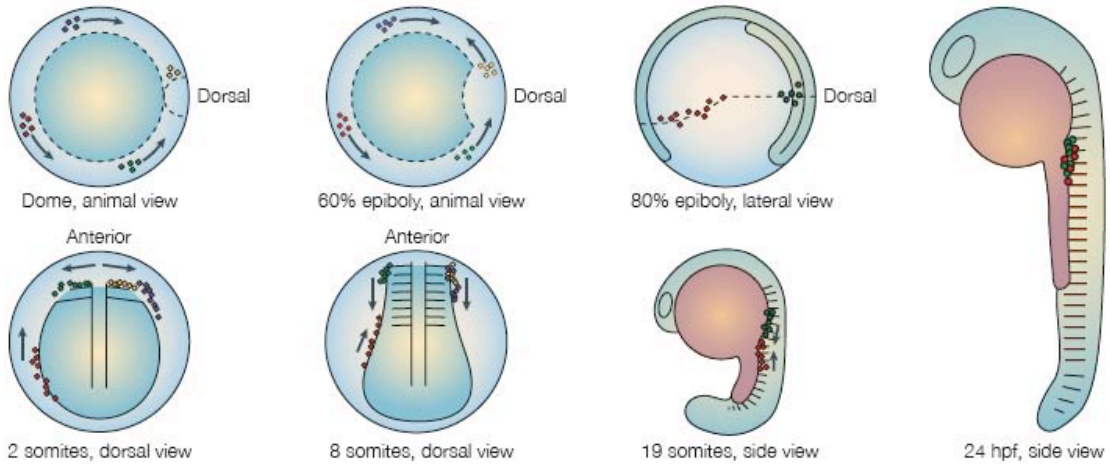

Figure 3. The steps of primordial germ cell (PGC) migration in zebrafish. Schematic drawings of embryos from dome stage to 24-hours post fertilization (hpf), which show the positions and movements of the four PGC clusters from one of the possible starting positions.

dome stage: four clusters of PGCs are found close to the blastoderm margin in a symmetrical 'square' shape. All possible orientations of the square relative to the dorsal side of the embryo can be observed. Here, an intermediate arrangement is shown with one cluster close to, but not directly at the dorsal side.

60%-epiboly stage: loss of the 'square' arrangement of PGC clusters, PGCs from the ventral move in direction to the dorsal and dorsal located PGC clusters exclude the dorsal midline where the notocord will form.

80%-epiboly stage: dorsally located PGCs align along the border between the head and trunk paraxial mesoderm marked by the dashed line. Ventrally located PGC clusters align at the lateral border of the mesoderm.
2-somite stage: most PGCs arrived in two lines at the level of the first somite. These anterior located PGCs migrate towards the lateral and form two lateral clusters. Cells that were initially located ventrally migrate towards the anterior along the anlage of the pronephros (anterior migration of trailing PGCs). In this illustration, the positions of the PGCs are drawn relative to the adaxial cells, the somites and the lateral border of the pronephric anlage.
8-somite stage: all anterior PGCs are found lateral to the paraxial mesoderm in a cluster extending from the 1st to the 3rd somite. These clusters start to move towards the posterior while the trailing cells tightly align on the lateral border of the pronephros and continue to migrate anteriorly.
19-somite stage: the main clusters have shifted to more posterior positions and in 60% of embryos some trailing cells are still seen.
24 hpf: the PGC clusters are located at the anterior end of the yolk extension, which corresponds to the 8th to 10th somite level. In most embryos, all PGCs have reached this region, only a few trailing cells are found close to the main clusters. (Adapted after [44])

The analysis of PGC migration during the first 24 hour of development was done by following the RNA expression pattern of a germ cell marker (*vasa*) [42] and later by following GFP-labelled migrating PGCs [17, 45]. Analysis of PGC migration in specific mutants revealed that the migration of PGCs towards their targets depended on proper differentiation of somatic mesodermal cells in that region, whereas faulty development of tissues vacated by PGCs proved to be of no consequence to the process. Taken together, these results supported the idea that attractive cues provided by somatic cells are responsible for directing the germ cells towards their targets [45].

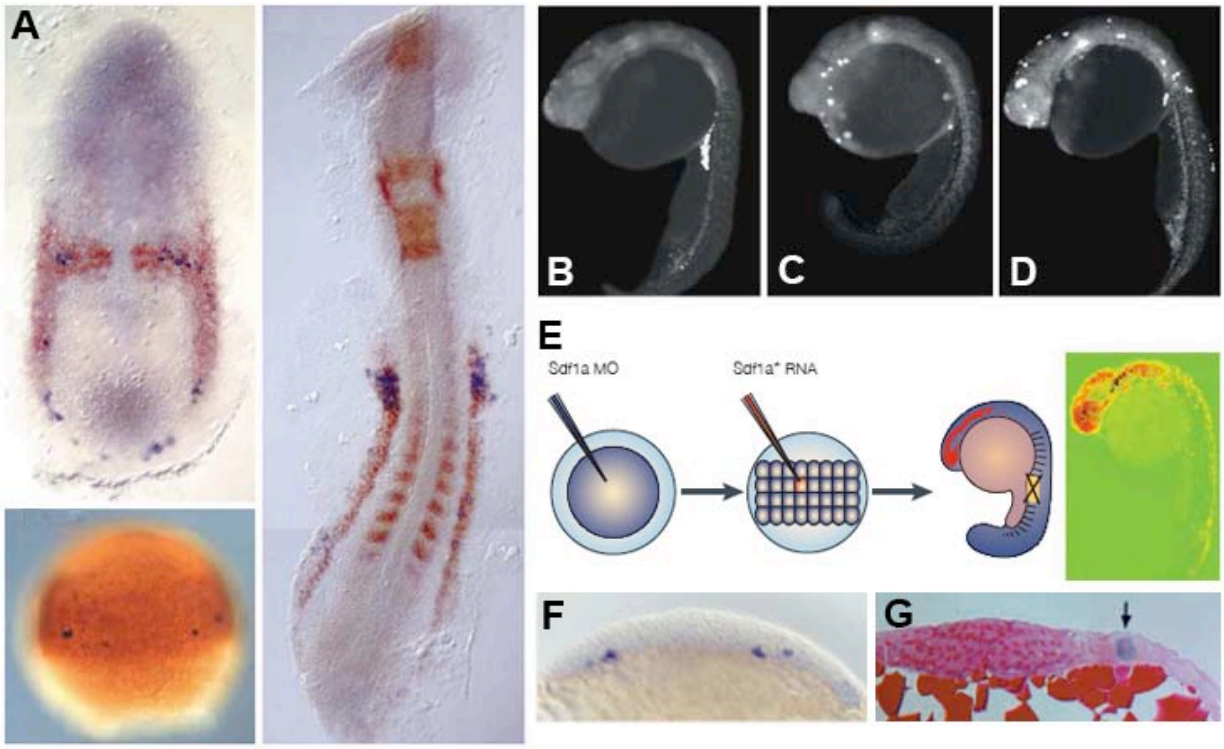

Figure 4. SDF-1a and CXCR4b control PGC migration. (A) The expression pattern of *sdf-1a* RNA (brown) relative to the position of the migrating *nanos-1*-positive germ cells (blue). In wild-type embryos, the germ cells are found in positions where the *sdf-1a* RNA is highly expressed. (B-D) Alterations in the level of Sdf1a signalling in the primordial germ cells (PGCs) result in defects in germ-cell migration. In contrast to wild-type embryos, in which most of the germ cells are found in the region of the gonad by the end of the first day of development (B), inhibiting the translation of *cxcr4b* (C) or overexpressing Sdf1a in the germ cells (D) results in migration defects. Germ cells can be attracted towards an ectopic Sdf1a source. Global inhibition of *sdf-1a* translation by early injection of a modified antisense oligonucleotide (blue; Sdf1a MO) is followed by injection of morpholino-resistant *sdf-1a* RNA into one cell at a later stage, thereby generating a clone of cells that express Sdf1a (red; Sdf1a* RNA). By the end of the first day of development, the germ cells are found in ectopic positions, mainly in the clone that expresses Sdf1a. (F, G) Optical cross-sections of embryos at dome stage (4.3 hpf) (F) and 7-somite stage show that *nanos-1*-positive PGCs (blue) are confined to the yolk surface. This figure is adapted after [27, 42, 46].

The molecular identity of the receptor for these cues was revealed in two genetic screens [46, 47]. In these studies, a crucial role was demonstrated for CXCR4b, a chemokine receptor that is expressed in PGCs. Germ cells with reduced expression of the receptor maintain their motile behaviour but fail to migrate towards the targets and therefore arrive at ectopic locations in the embryo [46, 47]. The ligand of this receptor, the chemokine SDF-1a, is dynamically expressed in the

regions towards which the PGCs migrate (Figure 4A) [46]. In line with the idea that the PGCs are attracted to sites of SDF-1a expression within the embryo, somatic cells engineered to express SDF-1a introduced into ectopic locations are able to attract PGCs there (Figure 4E) [43, 46].

In a recent study it was shown that throughout their migration the PGCs alternate between 'run' phases, during which they are polarized and actively migrate, and 'tumble' phases, in which they lose their polarity and remain on the spot protruding in all directions. The loss of cell polarity during tumbling phases is followed by reacquisition of cellular polarity and resumption of the migration. The fact that the majority of the changes in the course of PGC migration occur at the exit from 'tumble' phase suggested that the function of tumbling is to allow for corrections in the route of migration and, thus, to facilitate precise arrival at the target.

One of the first responses to CXCR4 activation is calcium elevation within cells. It was shown that polarized calcium influx close to the leading edge of PGCs makes their migration more persistent. PGCs with lower calcium levels in the protrusion (those lacking CXCR4b signalling or cells in which calcium was specifically buffered) although still able to migrate perform shorter run phases [48]. Calcium influx in the part of the cell facing up the chemokine gradient leads to myosin contraction in this part of the cell which in turn results in bleb formation which contributes to persistent displacement in the direction of the chemokine source [48].

Although the mechanism that controls the alternation between run and tumbling phases or phase duration seems to be an important factor regulating PGC arrival at the site of the gonad, the nature of the mechanism is not known.

1.4 CXCR4 signaling

The chemokine receptor CXCR4b that guides PGC migration in zebrafish is highly homologous to human CXCR4. Both receptors belong to a large superfamily of G protein-coupled receptors, which comprise the largest family of cell-surface

receptors. Receptors of this family mediate the responses to a wide variety of signalling molecules, including hormones, neurotransmitters, and local mediators (chemokine receptors are reviewed in [49]). All G-protein-linked receptors have a similar structure. They consist of a single polypeptide chain that threads back and forth across the lipid bilayer seven times and are therefore called 7-transmembrane receptors. In addition to their characteristic orientation in the plasma membrane, they transmit their signal to the cell interior using G proteins they associate with.

Controlling cell migration and signalling, CXCR4 is directly involved in a number of biological processes including organogenesis (including PGC migration), hematopoiesis, and immune response. Recent evidence has demonstrated the role of CXCR4 in a variety of diseases including HIV, cancer, and WHIM syndrome [50-55]. Importantly, the involvement of CXCR4 in cancer metastasis and WHIM syndrome appears to be due to deregulation of the receptor (at expression or protein level correspondingly) leading to enhanced signalling.

CXCR4 binds its ligand, chemokine SDF-1 that induces conformational changes in receptor molecule thereby activating multiple signalling pathways. There is some evidence that chemokine binding triggers receptor dimerization [56, 57] as well as translocation of the receptor into lipid rafts, thus providing more efficient signalling by the receptor [58, 59].

Directionally migrating cells exhibit clear morphological polarity, which is often manifested in elongated cell shape and extensive protrusive activity at the cell front [60, 61]. An obvious factor that could contribute to cell polarity is the spatial distribution of the receptor guiding the process. Indeed, several chemokine receptors, such as the formylmethionylleucylphenylalanine (fMLP) receptor in neutrophils, CCR2 and CCR5 in T lymphocytes, and CXCR4 in B and T lymphocytes and in human hematopoietic progenitor cells have been reported to be enriched at the leading edge in response to polarized application of the corresponding ligands *in vitro* [62-66]. In contrast, the distribution of other receptors such as C5a receptor in neutrophils and cAMP receptor in *Dictyostelium discoideum* during chemotaxis was shown to be uniform [67, 68]). The distribution of zebrafish CXCR4b on the surface of migrating PGCs has not been tested.

Following SDF-1 binding, CXCR4 (as well as its zebrafish homologue CXCR4b [69]) couples to Gi family of proteins. The vast majority of signaling pathways and biological outcomes of CXCR4 is mediated by Gi proteins (Figure 5). All G proteins are composed of alpha, beta and gamma subunits. When the alpha subunit is bound to GDP the G protein is inactive and is found in complex with beta and gamma subunits. When stimulated by an activated receptor, the alpha subunit releases GDP, allowing GTP to bind in its place. This exchange causes the trimer to dissociate into two activated components – an alpha subunit and a beta/gamma complex. In this form, they are able to activate their downstream effectors.

GTP bound Galphai subunit inhibits adenylyl cyclase and activates the Src family of tyrosine kinases, while the released Gbeta/gamma dimer activates phospholipase C-beta (PLC-beta) and phosphoinositide-3 kinase (PI-3K) [70] thus, inducing cascades of signaling events ultimately leading to regulation of processes such as gene transcription, cell migration, and cell adhesion. It was shown that altered PI3K activity or reduced levels of phosphorylated phosphoinositides affected germ cell motility and cell morphology [69]. Calcium elevation elicited by SDF-1 stimulation of CXCR4 has been utilized as an important experimental indicator of receptor activation. Among Gi associated signaling events of SDF-1/CXCR4 signaling axis is phosphorylation of focal adhesion components as well as activation of p44/42 MAP kinases (ERK 1 and 2) and NF-kappaB (Figure 5) ([70] and reviewed in [71]).

In addition to G protein activation, SDF binding to CXCR4 induces transient association of JAK2 and JAK3 with the receptor, which leads to the activation and nuclear translocation of a number of STAT proteins [56]. As judged by inhibition of Gi protein signaling by PTX, CXCR4 interaction with JAK proteins is G protein independent. Furthermore, pretreatment with PTX leads to a prolonged association of JAK with CXCR4 notifying that G protein coupling may negatively regulate CXCR4/JAK/STAT signaling [56].

Non-visual arrestins 2 and 3 (also called beta-arrestin-1 and beta-arrestin-2) are considered to be involved in receptor desensitization i.e., shutting down signal

transduction following receptor activation [72]. Indeed, in the absence of arrestin-3 CXCR4, desensitization is attenuated and G protein coupling to the receptor is enhanced [73]. However, the cells devoid of this molecule exhibit decreased chemotactic response to SDF-1, which possibly reflects the ability of arrestin-3 to promote signaling [73]. Consistent with this notion, arrestins are able to act as scaffolds for a number of signaling molecules and therefore could propagate signaling or serve as a platform for induction of certain signaling cascades [74-76]. In addition, it has been reported that arrestin-2 and arrestin-3 enhance CXCR4-mediated ERK activation [77] and arrestin-3 is involved in p38 MAPK activation independent of G protein activity [78].

Different signaling activities were assigned to different CXCR4 domains by assaying the function of mutated intracellular loops or the C-terminus of CXCR4 [79]. This study shows that coupling of Gi proteins solely depends on the third intracellular loop, which at the same time is involved in calcium mobilization and MAPK p42/44 activation. The second intracellular loop was found dispensable for Galphai signaling. The second and the third intracellular loops as well as the C-terminal domain were essential for SDF-1-mediated chemotaxis. Involvement of several CXCR4 domains in this process evidences that chemotaxis is mediated by convergence of several signaling pathways rather than by activation of one signaling pathway alone [79].

1.5 Regulation of CXCR4 signaling

In addition to activation of signalling cascades, ligand binding to GPCRs initiates a series of processes that regulate GPCR activity: 1) desensitization (homologous and heterologous), 2) internalization, and 3) degradation (reviewed in [80]).

1.5.1 Desensitization

Desensitization is an adaptive cellular response whereby receptor becomes refractory to repeated stimulation by the ligand, which is used to prevent the harmful effects of persistent receptor activation resulting from prolonged agonist

exposure. Almost all GPCRs that were studied including CXCR4 were shown to undergo homologous desensitization and all cells use a universal mechanism for desensitizing GPCRs. Homologous desensitization involves the coordinated actions of two families of proteins, the G protein-coupled receptor serine/threonine kinases (GRKs) and arrestins [72, 81-83]. After binding to its agonist, a GPCR assumes a conformation that allows it to bind one or more of the GRKs, which in turn initiate desensitization via phosphorylation of serine/threonine residues of the third intracellular loop or of the cytoplasmic tail (C-tail) [72]. Subsequently, non-visual arrestin-2 and/or arrestin-3 bind to the phosphorylated receptor molecule and uncouple the receptor from G proteins [84-86] often targeting the receptor for internalization.

Many GPCRs also undergo a process termed heterologous desensitization, whereby the activation of one GPCR can result in the inhibition of another, heterologous GPCR. Activation of second messenger-dependent protein kinases, such as protein kinase A and protein kinase C (PKC), by one GPCR can result in the phosphorylation of other GPCRs in the same cell and result in heterologous desensitization. Second messenger-dependent protein kinase-mediated phosphorylation of serine and threonine residues within the intracellular domains of GPCRs is presumed to sterically interdict G protein coupling. Sequence analysis of CXCR4 shows that multiple serines in the C-tail are potential PKC phosphorylation sites. Consistent with this, direct activation of PKC using phorbol esters as well as more physiologically relevant stimuli that lead to PKC activation such as T or B cell receptor engagement [87, 88], formyl peptide receptor activation [89, 90], CXCR1 activation [91], CXCR2 activation [92], or CCR5 activation [93] result in phosphorylation and internalization of CXCR4 [94-97].

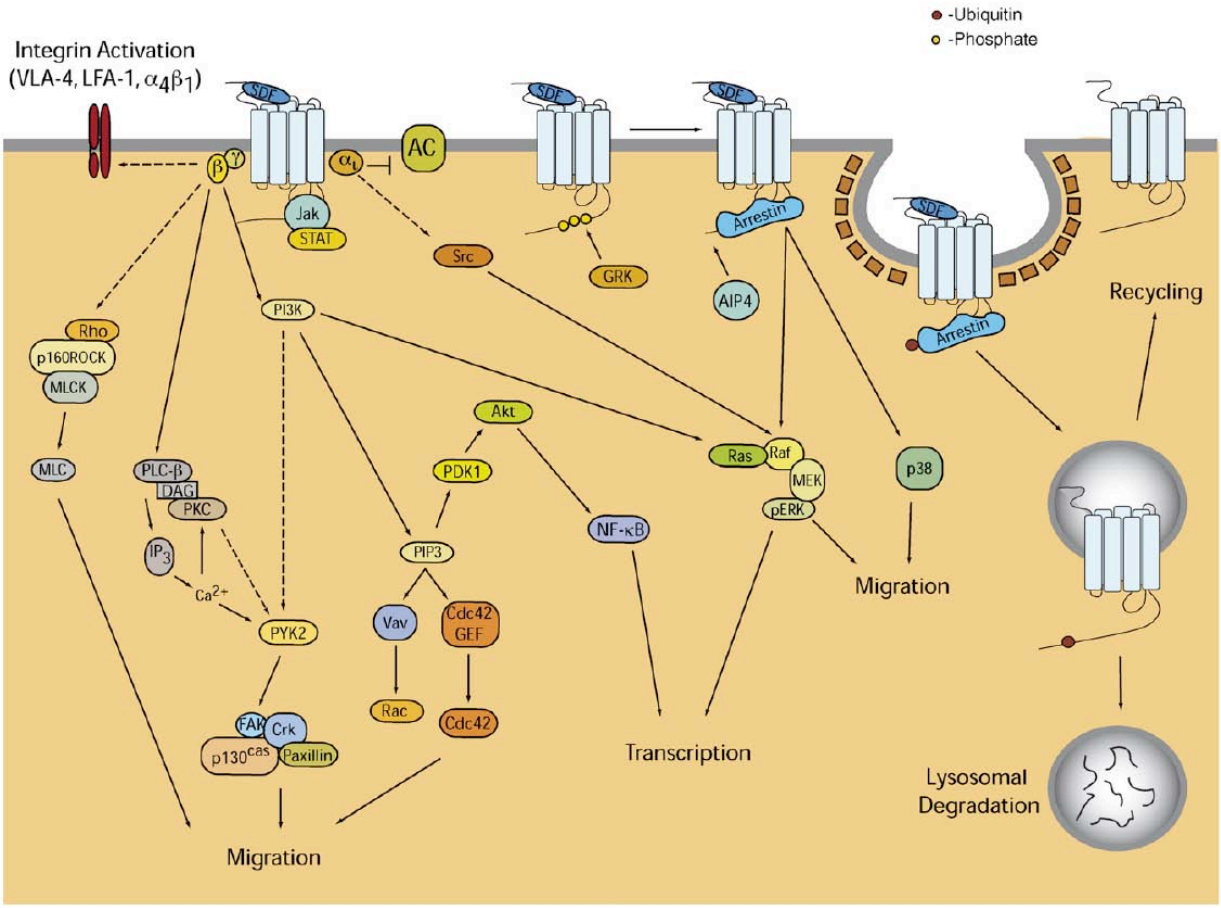

Figure 5. Signal transduction pathways and regulation of CXCR4. SDF binding to CXCR4 leads to the activation of multiple G protein-dependent signaling pathways, resulting in diverse biological outcomes such as migration, adhesion, and transcriptional activation. Pathways activated and outcomes elicited may differ between $CXCR4^+$ cell types. Two potential G protein-independent pathways have been described. Tyrosine phosphorylation of CXCR4 results in the recruitment and activation of the JAK/STAT pathway, while p38 and ERK activation has been shown to be partially dependent on arrestin-3. Following activation, GRK phosphorylation results in the recruitment of arrestin 2/3 and subsequent internalization. CXCR4 is also ubiquitinated by AIP4 at the plasma membrane, which results in its sorting to and degradation in lysosomes. However, a portion of the internalized receptor may also recycle back to the plasma membrane. Adapted from [80].

1.5.2 Internalization and degradation

GPCR internalization or sequestration of activated GPCRs from the plasma membrane into internal cellular compartments is an important part of the regulation of the receptor signalling cycle (reviewed in [98]). Upon internalization, GPCRs can be recycled back to the plasma membrane or sorted to the lysosomes for

degradation [99]. Following PKC-mediated internalization, CXCR4 was shown to recycle back to the plasma membrane [96]. In contrast, recycling of internalized CXCR4 was not efficient following SDF stimulation [100]. In fact, CXCR4 has been shown to be ubiquitinated, sorted to the lysosomal compartment, and degraded [101], a process mediated by the E3 ubiquitin ligase AIP4 [102].

The only clearly delineated endocytic route utilized by GPCRs is the clathrin-mediated endocytic pathway. The targeting of many GPCRs to clathrin-coated pits for internalization involves both GRK-mediated phosphorylation and β-arrestin binding. β-arrestins function as intermediary endocytic adaptor proteins that target GPCRs to coated pits via their association with both AP2 adaptor complex and clathrin. Although there is considerable evidence supporting the notion that CXCR4 also employs the arrestin-dependent internalization pathway [95], in a recent paper it was shown that CXCR4 utilizes the alternative endocytic route through caveolae and this process is majorly dependent on caveolin, a component of these membranal structures [103]. These discrepancies can be attributed to cell line differences. At least the importance of CXCR4 incorporation into lipid rafts for CXCR4 internalization was reported for T-cells [104] and not for HeLa cells [105].

GPCR internalization requires intact serine/threonine rich cytoplasmic C-terminus and specific amino acids within CXCR4 C-terminus essential for this process were identified [94, 95]. These were serines 324, 325, 338, and 339 and the dileucine motif at the position 328 and 329 [95, 106].

1.5.3 Deregulation of CXCR4 signaling

As described above, the regulatory units contributing to CXCR4 signaling control are concentrated in the C-terminal domain of the receptor molecule. Both desensitization and internalization were also shown to require the same region of CXCR4 molecule, which is the receptor C-tail. Thus it is eligible to think of these two processes as two consequent steps when phosphorylation and arrestin binding lead to both uncoupling of G-proteins from CXCR4 and CXCR4 sequestration from plasma membrane. Both processes directly regulate receptor signalling level by

shutting down G-protein signalling (desensitization) or by removal of the receptor from the membrane (internalization). Therefore, it could be expected that removal of the C-terminal domain or interference with C-terminal phosphorylation would have an impact on SDF-1-controlled signalling and cell behaviour. Indeed, enhanced calcium response as well as more G-protein activity was observed in cells expressing CXCR4 unable to internalize. Moreover, a rare combined immunodeficiency characterized by warts, hypogammaglobulinemia, recurrent bacterial infection, and myelokathexis, known as WHIM syndrome was identified as a first immunological disease associated with mutations to a chemokine receptor. The mutations identified to date (one frameshift and three nonsense mutations) all truncate the C-terminal tail of CXCR4 eliminating a number of potential phosphorylation sites [53, 107]. Therefore, regulation of the mutant receptor is altered as compared to wild-type molecule as indicated by a lack of desensitization [55, 107], an increase in F-actin polymerization [55], enhanced calcium mobilization [108], and a decrease in internalization [55, 108] in response to SDF induced activation.

The ability of cells expressing C-tail defective CXCR4 for chemotaxis was assessed as well. Here, the results appeared to be controversial. Whereas a number of *in vitro* studies suggested that the carboxyl terminus of CXCR4 positively regulate chemotaxis (e.g. [79]), others reached the opposite conclusion [55, 107, 109]. These conflicting results highlight the importance of investigating this process under physiological conditions in the live animal.

1.6 Aim of the present work

1) The aim of this thesis was to investigate the mechanisms controlling the precision of PGC arrival at the site of the gonad and in particular, the role of CXCR4b internalization in this process.

2) The other focus of this thesis was to assess the role the endoderm plays in primordial germ cell migration.

2.0 Results

2.1 Zebrafish PGCs migrate in close association with the endoderm

Zebrafish PGCs are formed in vegetal positions of the blastula in proximity to the yolk cell. It has been previously shown that during somitogenesis stages PGCs frequently contact mesodermal tissues as well as the yolk syncytial layer (YSL), cellular layer enveloping the yolk [27, 42]. To determine the cellular context within which zebrafish PGCs migrate at higher resolution we followed the position of the cells using tissue sections and confocal microscopy. We performed this analysis during gastrulation stages when extensive PGCs migration takes place.

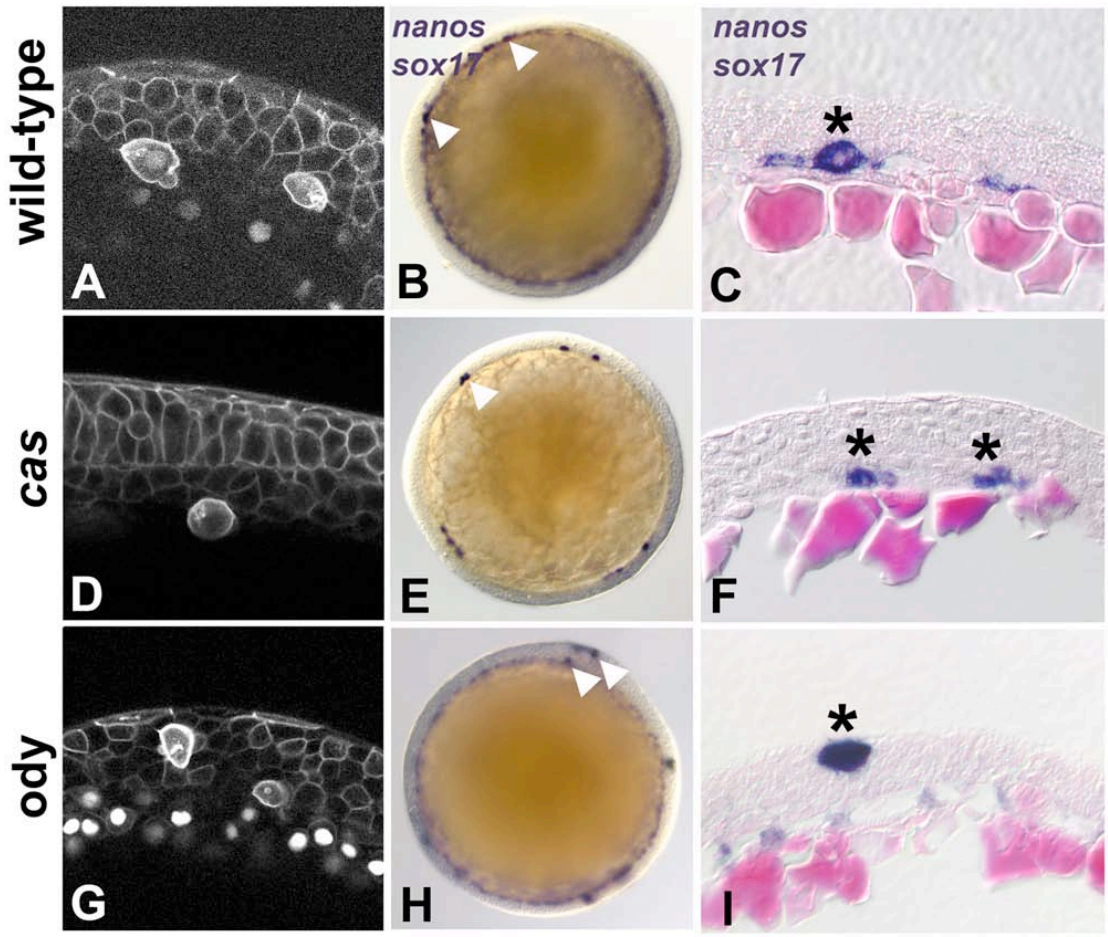

Figure 6. Location of PGCs in wild-type and mutant embryos. (A-C) Wild-type PGCs migrate in close proximity to the yolk in close contact with endoderm. (D-F) PGC in *casanova* mutant migrate in close proximity to the yolk in the absence of endoderm. (G-I) PGC in *odysseus* mutant lose their

contact with the deep embryonic layers and can be found in various locations in respect to the yolk and endoderm. (A, G) Endodermal cells are engineered to express nuclear marker H1M (See Materials and Methods). (A, D, G) PGCs are marked with farnesylated EGFP used as lineage marker and driven to PGCs by 3' UTR of *nanos*. Live embryos are visualized with confocal microscope (See Materials and Methods). (B, E, H) RNA *in situ* hybridization of *nanos* (PGC marker) and *sox17* (endodermal marker) both stained in blue. White arrowheads are pointing at PGCs. In (B) and (H) endodermal cells form a rim around the yolk. Wild-type PGCs are not found away from this rim (B) while the PGCs in *ody* mutant are found also in the unstained part of the embryo i.e., away from endoderm. (C, F, I) Cross-sections of embryos after whole-mount *in situ* hybridization of *nanos* and *sox17*. PGCs are marked with black asterisks. Embryos at 70-80% epiboly were used in all experiments.

In wild-type embryos the germ cells are found in the deepest layers of the gastrula contacting both endodermal cells and YSL (Figure 6A-6C). The cells were never found away from the yolk and endodermal cells in the embryos (Figure 6B). On sections, it is visible that germ cells share their position close to the yolk with endodermal cells and therefore, may contact with them (Figure 6C). To determine the dynamic features of PGC migration relative to tissues that surround them, we extend the analysis to live embryos using confocal microscopy.

We found that PGCs migrate along the endoderm. Interestingly, they appear to migrate in a corridor between endoderm and the mesoderm layers touching both but not invading them (Figure 6A). This corridor appears to be formed by the PGCs themselves as it is not seen in positions devoid of migrating PGCs. Additionally, similar to other phenomenon that could only be observed in live material (e.g., [110]) this corridor was not visible in sections of fixed material.

Together, these results obtained using different experimental approaches demonstrate that in the course of their migration PGCs are confined to the deep embryonic tissues making their way on top of the YSL while making contact with endoderm.

2.2 The endoderm does not constitute a preferred migration substance for PGCs

As in different organisms including zebrafish PGCs migrate over endodermal tissues [1], it is possible that the cells exhibit affinity to this germ layer by virtue of specific cell-cell or cell-matrix adhesion. To examine this notion we followed the migration of PGCs relative to the endoderm in embryos that can not respond to the guidance cue, namely in *odysseus* mutant embryos (*ody*) that lack the functional chemokine receptor CXCR4b [47].

Interestingly, PGCs lacking the guidance cue were not confined to the more vegetal parts of the embryos and readily lost contact with the endoderm (Figure 6G-6I). In such embryos the cells were found in ectopic positions in the embryo (e.g. head, tail) in association with cells of other germ layers. Notably, we could not observe any tendency of the cells to remain in association with the normally developing endoderm. The migrating cells exhibited normal cell morphology and behaviour despite the foreign environment within which they were migrating (e.g. Figure 6G).

2.3 The endoderm is not required for the position of the PGCs relative to other germ layers

Whereas the endoderm is not sufficient for maintaining the PGCs in close proximity to the yolk cell, it could be required for it. For instance, endodermal cells could produce extracellular matrix important for SDF-1a stability or accessibility. To check this point we sought to follow the behaviour of PGCs in embryos lacking endodermal cells. To this end we made use of the c*asanova* mutation. *casanova* is a transcription factor of Sox family [111] which is essential for endoderm differentiation from the onset of gastrulation in zebrafish [112, 113].

In the absence of endodermal cells, the PGCs still migrate in close proximity to the YSL not entering outer layers (Figure 6D-6F). Confocal live imaging indicates that cell morphology is normal and migration is not affected by elimination of this germ layer (Figure 6D).

Therefore, endoderm is not required for normal location of PGCs within the embryo during the migration phase.

2.4 Endodermal cells do not express the guidance cue SDF-1a

As shown above, the endoderm is neither required nor sufficient for the positioning of PGCs close to the yolk. The dominant factor dictating the localization of the PGCs could thus be SDF1a, the ligand of CXCR4b. To check if SDF-1a is expressed in the endoderm, we combined whole mount in situ hybridization and immunostaining and showed that consistent, SDF1a was indeed not expressed in the endoderm, but rather in mesodermal tissues (Figure 7). Interestingly, SDF1a is expressed only in those mesodermal cells that are located in the close proximity to the yolk (Figure 7). This can explain the fact that PGCs migrate so close to the yolk but leave it readily once they do not respond to the SDF-1a guidance.

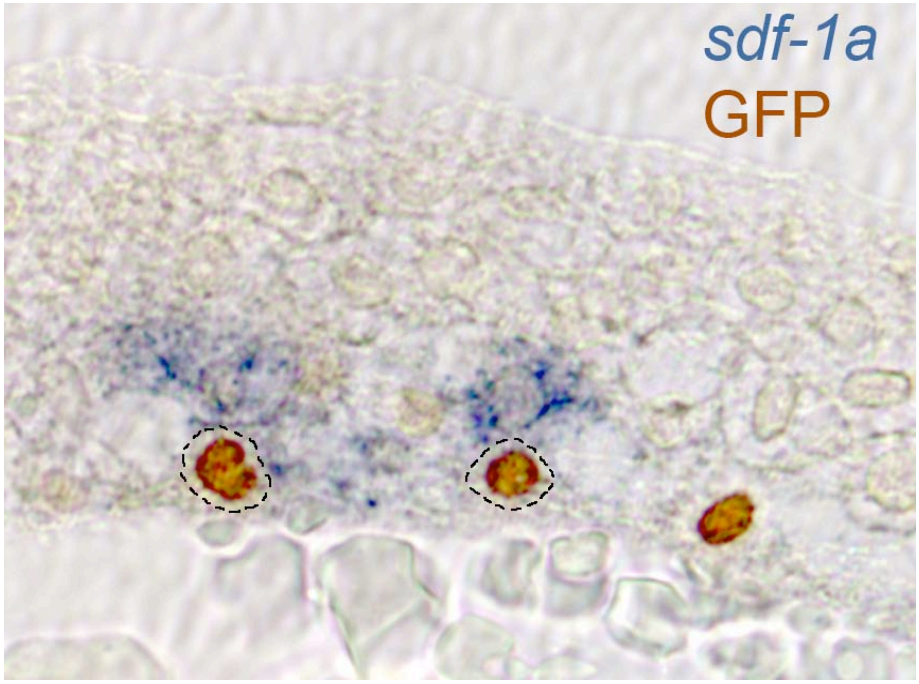

Figure 7. SDF-1a is expressed in mesodermal cells and not in the endoderm. *sdf-1a* RNA (blue pattern) is excluded from the cytoplasm of endodermal cells which are contoured with dashed lines. Only the deepest mesodermal cells express *sdf-1a*. Nuclei of endodermal cells were engineered to express GFP and then GFP was detected with anti-GFP antibodies (brown nuclei).

2.5 Endodermal mutants fail to locate germ cells properly at gonad position.

Based on the results presented above endoderm does not seem to be important for PGC migration. To determine whether this germ layer plays a role during later development of the germline, we followed the germ cells in the endoderm deficient *cas* mutants up to 30 hours post fertilization (hpf). In wild type embryos, PGCs form two clusters at the stage of one somite [42]. From this stage on they start migrating posteriorly to arrive to the site of the future gonad as two separate clusters on both sides from the yolk extension by the end of the first day of development [42]. In 30 hpf *cas* mutant embryos the PGCs appear as a single cluster, which is extended over the embryonic midline (Figure 8A). Interestingly, *sdf-1a* expression is not detectable at the site of the gonad at this stage (Figure 8A, red arrowheads).

To determine at which time point the fusion of the two clusters occurs we followed the germ cells at stages preceding the observed phenotype (Figure 8B). We found that at 18 hpf the PGCs appear to form two cluster in *cas* mutant embryos, but these come closer together at 24 hpf, and eventually fuse into a single cluster by 28 hpf (Figure 8B).

Together, our results demonstrate that although endoderm is not essential for PGCs arrival at their correct target, it is required for the maintenance of two separate clusters of germ cells at the site where later the gonad will form.

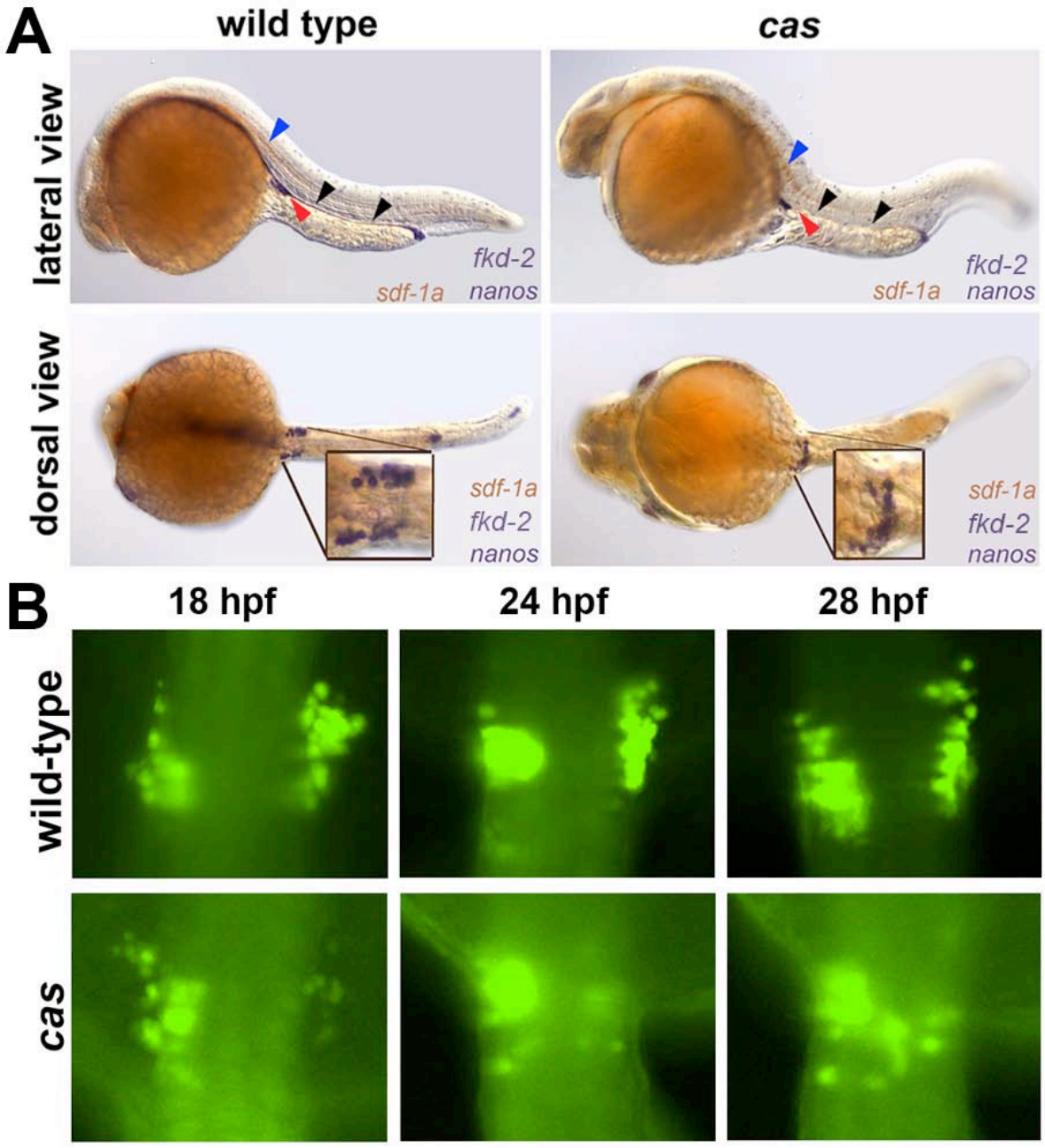

Figure 8. PGCs are mislocated at gonad position in *casanova* mutant embryos. (A) *In situ* hybridization of floating head (*fkd-2*, late endodermal marker) and nanos. In *cas* mutant embryos in which gut is absent (see *fkd-2* staining, black arrowheads) PGCs fail to form two bilateral clusters (lower right panel) as compared to the wild-type PGCs (lower left panel) and instead form one cluster. *Sdf-1a* expression is not detectable at the site of the gonad (red arrowheads) at this stage (30 hpf). It is still present at other sites e.g., in the lateral line (blue arrowheads). (B) PGCs form a single cluster in *cas* mutant by 28 hours of development. PGCs in embryos born from *cas* heterozygous fish were marked with GFP and snapshots of the gonad region were taken at indicated time points.

2.6 CXCR4b is uniformly distributed on the PGC plasma membrane

In wild-type embryos, PGCs express the chemokine receptor CXCR4b and directionally migrate towards sites in the embryo at which the ligand SDF-1a is expressed [43, 46, 114]. To determine if polarized PGC morphology during their migration originates from CXCR4b distribution on the plasma membrane we monitored the distribution of CXCR4b within migrating PGCs in developing zebrafish embryos expressing a CXCR4b-EGFP fusion protein in these cells. Based on the efficiency in guiding PGCs lacking the endogenous receptor towards their target, the level of CXCR4b-EGFP used in this experiment is optimal for its function as a guidance receptor [46]. CXCR4b was found to be uniformly distributed on the plasma membrane in a similar manner to that of a membrane marker (farnesylated Ds-Red) throughout the migration process (Figure 9 and Supplemental Movie S1).

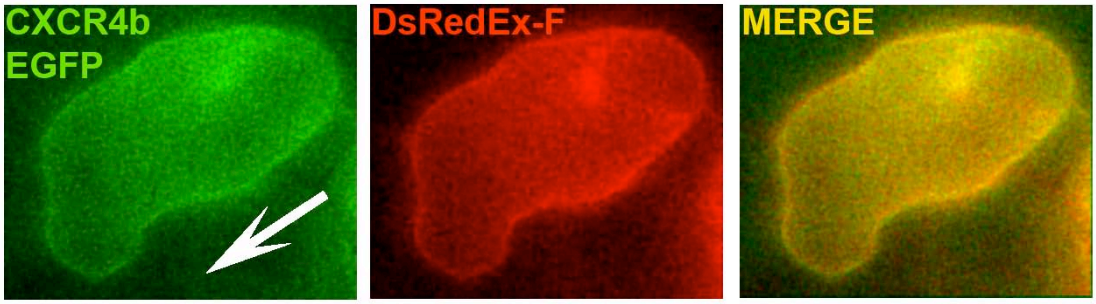

Figure 9. CXCR4b-EGFP (green) is evenly distributed on the plasma membrane as compared to the membrane marker farnesylated Ds-Red (red). The arrow indicates the direction of cell migration.

2.7 CXCR4b internalizes in response to SDF-1a

The uniform distribution of CXCR4b on the plasma membrane implies that polarization of migrating PGCs depends on asymmetric receptor activation rather than on its distribution (e.g., [48]). }). An important process that was implicated in localizing receptor activation to the leading edge is endocytosis [115]. Defects in receptor internalization were also implicated in abnormal migration of leukocytes

derived from patients with WHIM syndrome in which truncation of the cytoplasmic tail of CXCR4 was identified [53, 55].

To determine whether CXCR4b undergoes internalization in response to its ligand, we have transplanted SDF-1a-expressing cells as a source of the chemokine in close proximity to PGCs expressing CXCR4b-EGFP. This manipulation led to a gradual reduction in CXCR4b signal on the plasma membrane and concomitant appearance of intracellular GFP signal, thus providing evidence for receptor internalization *in vivo* (Figure 10, Supplemental Movie S2).

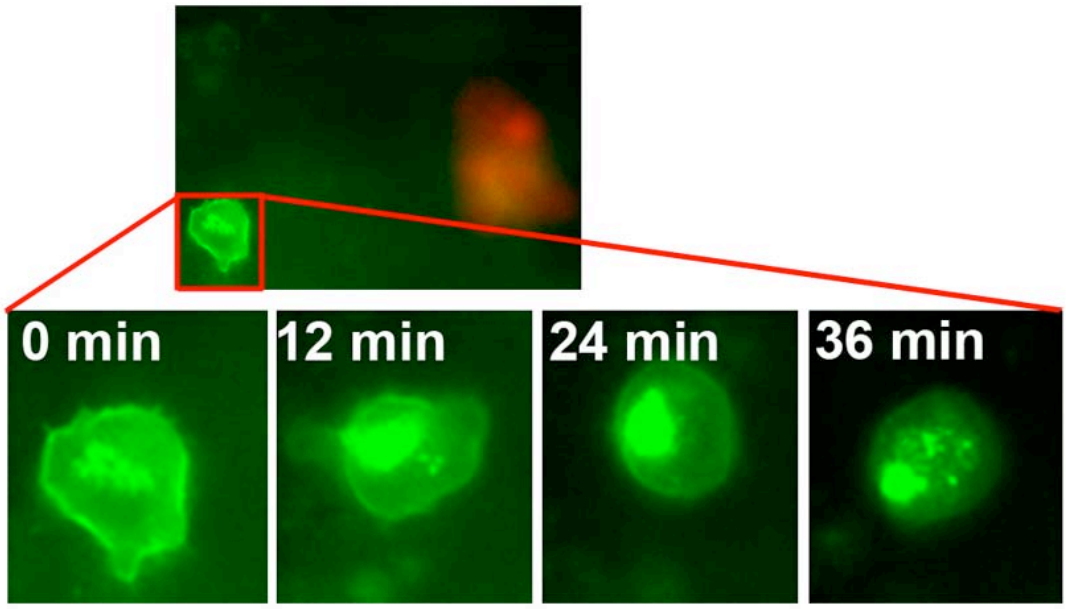

Figure 10. *In vivo* internalization of CXCR4b in response to SDF-1a. CXCR4b-EGFP (green) is initially observed on the plasma membrane (0 minutes) and internalizes following transplantation of SDF-1a expressing cells in close proximity (12 to 36 minutes, SDF-1a expressing cells labelled in red).

The CXCR4b-EGFP fusion protein could therefore allow us to define domains or specific amino acids that are essential for CXCR4b internalization. This would in turn enable us to determine the role this process plays in chemokine regulated signalling and guided cell migration.

2.8 CXCR4b internalization requires functionally redundant serine residues located at the C-terminus of the protein

Conserved serine phosphorylation sites within the cytoplasmic C-terminus were shown to regulate endocytosis in different experimental systems [95, 96, 116-122]. To determine whether these findings pertain also to CXCR4b in the context of germ cell migration *in vivo,* we have generated deletion and point mutations in the EGFP tagged receptor and examined the effect of these manipulations on receptor internalization (Figure 11, 12).

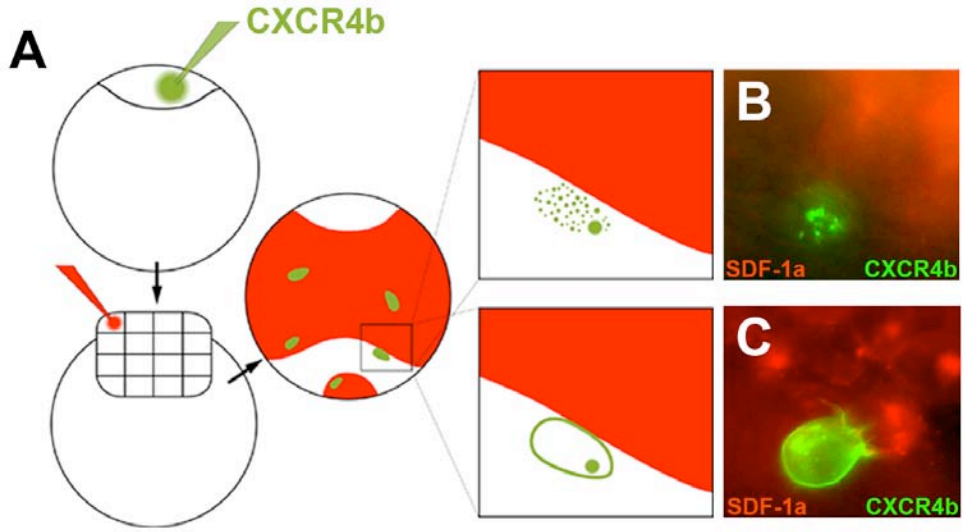

Figure 11. Assaying receptor internalization by expression of SDF-1a in the endoderm. (A) To assess the internalization potential of different mutant CXCR4b molecules (presented in Figure 12), PGCs expressing the different versions of CXCR4b fused to EGFP (green) were exposed to high levels of SDF-1a produced by endodermal cells (labelled in red, see Methods). (B) Wild type CXCR4b-EGFP (green) internalizes when found in proximity to the SDF-1a source (red). (C) Specific mutations in the receptor that inhibit internalization of the CXCR4b-EGFP fusion protein (green) result in persistence of the signal on the membrane despite the exposure to SDF-1a expressing cells (red).

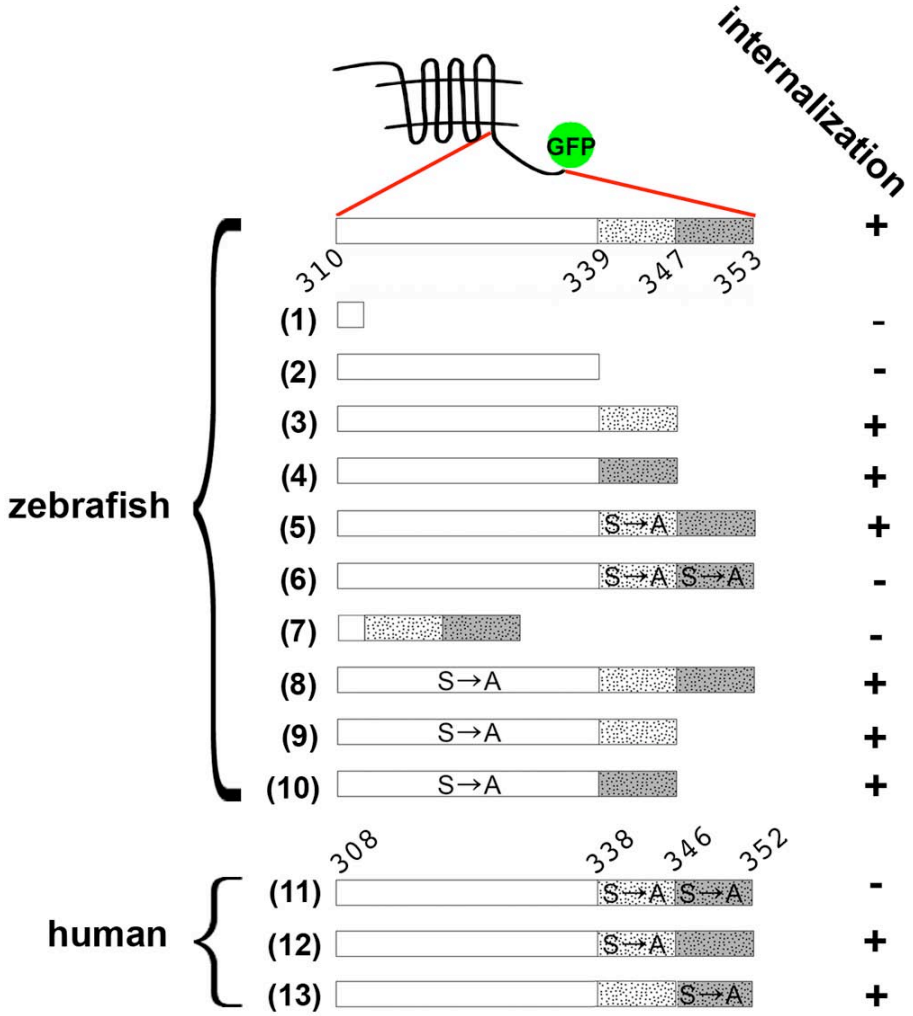

Figure 12. Mutations in the C-terminal domain of CXCR4 and their effect on internalization. The C terminus of CXCR4 was mutated by introducing deletions (constructs 1-4, and 7), by substitution of serines for alanines (constructs 5, 6, 8 and 11-13), or by both (constructs 9 and 10). The effect of these mutations on receptor internalization was assayed as described in panel C. Internalization appearing as shown in panel D is marked "+" and lack of internalization as shown in panel E is marked "-". 'S->A' signifies the serine-to-alanine exchange mutations in the region where this sign is positioned. The internalization potential of the human CXCR4 mutants (constructs 11, 12, and 13 as well as the wild-type form) was assayed as shown in Figure 14B.

As depicted in Figure 11, PGCs expressing the various mutated CXCR4b forms were exposed to SDF-1a, which was provided by endodermal cells engineered to express high levels of the chemokine (Figure 11 and see Experimental Procedures). In this experiment, wild-type CXCR4b-EGFP fusion protein, as well as mutants that were capable of undergoing internalization were not found on the plasma membrane (Figure 11B), whereas mutated proteins that could not

internalize remained on the plasma membrane (Figure 11C). In this analysis (Figure 12) we identified serine residues located within a 15 amino-acid span at the C-terminus (serines 339, 340, 342, 345, 347, 348, 349 located within the shaded area in Figure 12) that together were crucial for receptor internalization. Interestingly, serine residues within this region are functionally redundant (compare mutant (3, 4, 5) and (2, 6) in Figure 12), so that different parts of the C-terminus of CXCR4b could provide the platform for phosphorylation required for internalization.

Producing a CXCR4b mutant lacking the part of the C-terminus preceding the last 15 amino acids (mutant 7 in Figure 12) we showed that although the most distal 15 amino acid span is required for internalization it is not at the same time sufficient for this process. Exchange mutant in which all the serines in the part of CXCR4b C-terminus upstream to the last 15 amino acids (mutant (8) in Figure 12) showed the internalization potential indicating that serines in this region are not required for the receptor internalization. To exclude the possibility that this proximal part of CXCR4b C-tail provides phosphorylation sites when some of the last seven serines are compromised we showed that mutants lacking some serines in the distal part and all of the serines in the proximal part of the C-terminus (mutants (9) and (10) in Figure 12) still pertained the ability to internalize.

To determine if the difference in internalization potential between wild-type and ‘non-internalizable’ mutant CXCR4b described above is relevant for cells responding to physiological levels of SDF-1a, we compared the subcellular localization of the two receptor versions in germ cells migrating to a source of SDF-1a expressing physiological amounts of the chemokine (Figure 13, left panels) or when the cells form clusters in response to the endogenous SDF-1a signal (Figure 13, right panels). In both cases, the wild-type receptor was found at the plasma membrane as well as in intracellular vesicles, while the mutant receptor was detected exclusively on the plasma membrane.

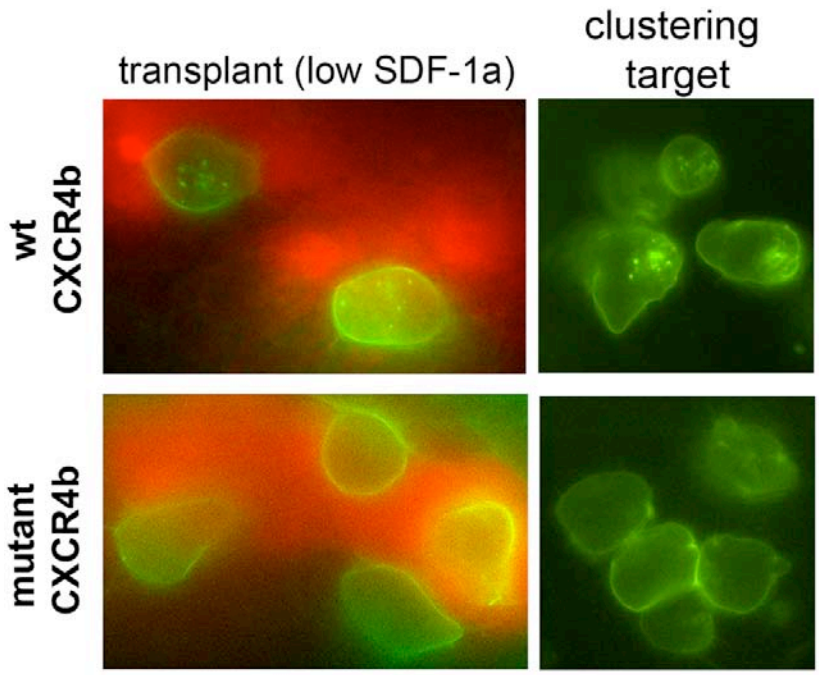

Figure 13. Serine mutations in C-terminus of CXCR4b prevent the receptor internalization at physiological levels of SDF-1a. Wild-type CXCR4b is observed on plasma membrane and intracellular vesicles whereas mutant receptor is located exclusively on plasma membrane. PGCs have arrived to a group of cells (red) secreting physiological levels of SDF-1a (left panels). PGCs are at their clustering target (right panels).

2.9 The amino acid requirements for internalization are conserved between zebrafish and human

The most distal part of the C-terminus of CXCR4 is highly conserved between *Danio rerio* and *Homo sapiens* and the seven serine residues that we have shown to be critical for CXCR4b internalization exist in the human protein as well (Figure 14A). To determine whether the serines in zebrafish and human C-terminus of CXCR4 exert similar function, we have generated mutants of the human receptor in which either all seven serines in the critical region were exchanged with alanines (mutant (11) in Figure 12) or only serines in specific parts of this region (mutants (12) and (13) in Figure 12). We then examined the internalization potential of these mutants in transfected HEK-293 cells. Following application of SDF-1 to the medium, the level of wild-type CXCR4 on the plasma membrane was strongly reduced, while the GFP signal became detectable in large cytoplasmic vesicles (yellow in Figure 14B). These vesicles contained fluorescent dextrane that was applied along with SDF-1 confirming the endocytic origin of those vesicles. In

contrast, human CXCR4 lacking the seven serines (mutant (11) in Figure 12) largely remained on the plasma membrane (Figure R5 B). Similar to our finding in zebrafish, human CXCR4 molecules that retained some serines in this critical region (mutants (12) and (13) in Figure 12) underwent internalization in response to SDF-1. These results demonstrate the functional conservation of the amino acids required for internalization of fish and human CXCR4 receptors and reinforce the notion that serines within the most distal region of the cytoplasmic tail of CXCR4 are redundant in supporting internalization.

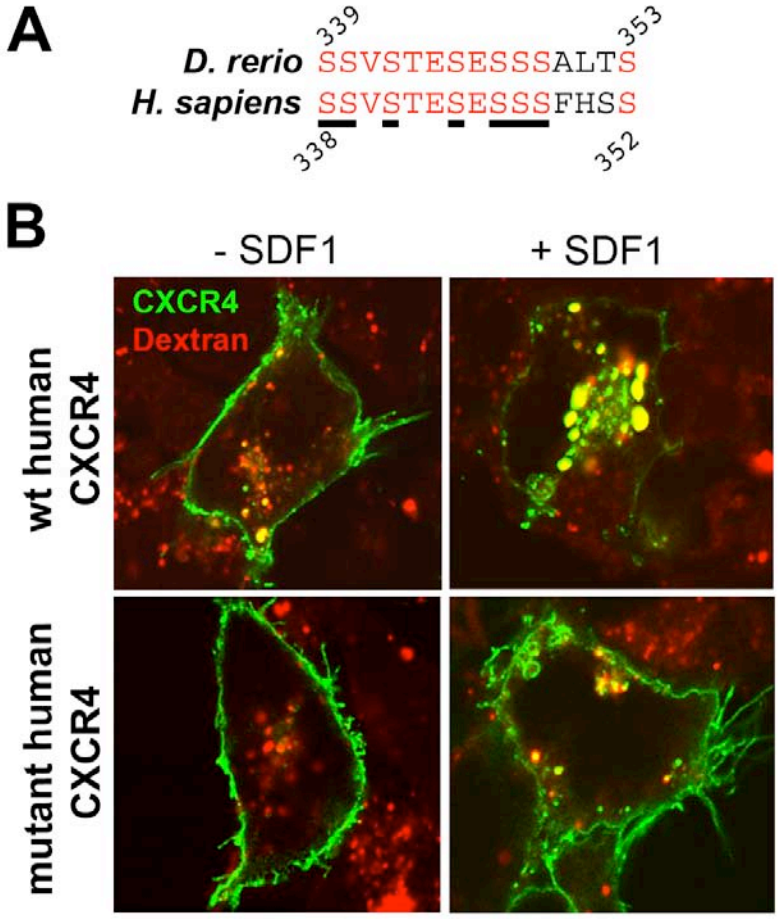

Figure 14. Genetic and functional conservation in the C-termini of CXCR4 between zebrafish and human. (A) High conservation in the C-terminus of CXCR4b between zebrafish and human (identical residues labelled in red). Serines that were mutated into alanine residues (Figure 12) are underlined. (B) The alanine-exchanged mutant of human CXCR4 (construct 11 in Figure 12) demonstrates defective internalization. The wild-type form of human CXCR4 expressed in HEK-293 cells internalizes efficiently upon exposure to recombinant SDF-1 and translocates into vesicles that contained red fluorescent dextran that was added to the medium along with SDF-1 (signal colocalization appears yellow). In contrast, a mutated version of the human CXCR4 where 7 serines

were exchanged with alanine residues (mutant 11 in Figure 12) fails to undergo internalization upon application of SDF-1.

2.10 Enhanced signalling by internalization defective CXCR4b

To determine whether preventing internalization alters the signalling level by CXCR4b, we have assayed the potency of the relevant mutants in mobilizing calcium, one of the earliest cellular responses to activation of CXCR4 by SDF-1 [123, 124]. Importantly, we found that the level of calcium in pseudopods of cells expressing the mutant CXCR4b (construct (6) in the Figure 12) was significantly higher than that in control cells expressing the wild-type form (Figure 15).

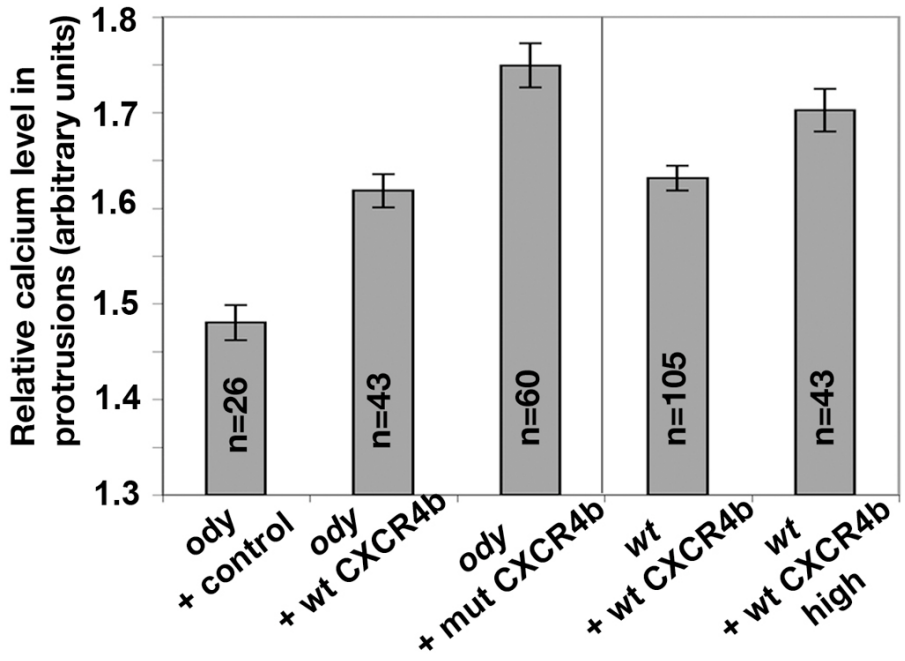

Figure 15. Relative calcium level in protrusions of PGCs expressing different amounts or types of CXCR4b. *ody* PGCs expressing the "non-internalizable" mutant (mut) form of CXCR4b (construct (6) in (F), left part of the panel) and wild type cells expressing high amounts of wild type CXCR4b (right part of the panel) show significantly higher calcium level in protrusions as compared to that in *ody* PGCs expressing the wild type form of the receptor and wild type cells expressing low amounts of wild type receptor correspondingly. The error bars represent the standard error of the mean (SEM) and 'n' is the number of protrusions analyzed. The first three measurements (the left part of the panel) were compared using the Tukey HSD test. The different treatments of wild-type embryos (the right part of the panel) were compared using the T-test. $P < 0.005$ for both comparisons.

2.11 Precise arrival of the PGCs at their target requires internalization and control of signalling level

To determine the functional significance of internalization in guided cell migration in the context of the intact organism, we evaluated the ability of the PGCs guided by the 'non-internalizable' version of CXCR4b (e.g. construct (6) in the Figure 12; hereafter referred to as 'mutant receptor') to arrive at the position where the gonad develops, a site they normally colonize within 24 hours after fertilization [42, 45].

To this end, we have made use of *odysseus (ody)* embryos, which carry a loss of function mutation in the *cxcr4b* locus [47]. Wild type or mutant forms of the receptor were expressed in *ody* mutant embryos and the position of the germ cells in 1-day old mutants was monitored. Unable to respond to SDF1a, germ cells of the *ody* mutants are found at random positions throughout the embryo rather than as a cluster at the site where the gonad develops (Figure 16A, 16D and [47]). Introduction of the wild-type receptor into *ody* mutant germ cells dramatically reverted this phenotype as 88% of the cells arrived at the region of the gonad (Figure 16B and 16D) (considered as 100% in the Figure 16D). Interestingly, in this assay, the mutant receptor was significantly less potent in rescuing the *ody* phenotype as compared with the wild-type version (Figure 16C and 16D). Furthermore, the cells that are guided by the mutant receptor that nonetheless arrived at the region of the gonad, formed a distinctly dispersed cell cluster as compared with cells directed by the wild-type receptor (Figure 16B, 16C and Figure 17).

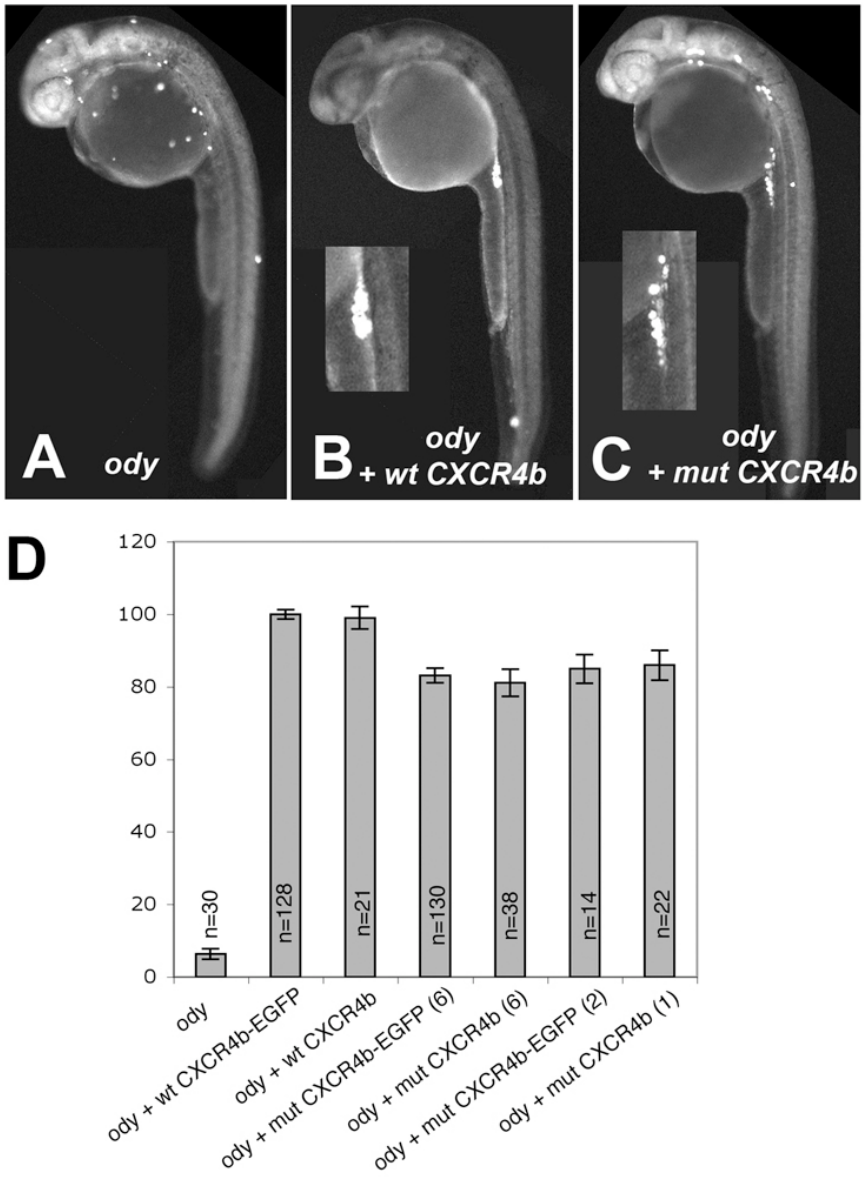

Figure 16. CXCR4b internalization is required for precise arrival of PGCs at the region where the gonad develops. (A-C) Wild type and mutant (mut) form of CXCR4b differ in the ability to complement the *ody* mutation. Expression of wild-type CXCR4b in *ody-/-* PGCs allows the cells to arrive at their target by the end of the first day of development (B), while the mutated internalization-defective receptor (mut CXCR4b, construct 6 in Figure R4) is less effective (C). Insets in panels B and C are enlarged images of the area where the gonad develops in the corresponding embryos. Cells expressing the mutant CXCR4b often form a loose cluster. (D) The percentage of correctly migrating PGCs (cells that have arrived at the region where the gonad develops) in *ody* embryos and in *ody embryos* expressing the wild type or mutant forms of CXCR4b (numbers given in parenthesis corresponds to mutant numbers in Figure R4) fused or not fused to EGFP. The error bars represent the standard error of the mean (SEM) and 'n' is the number of embryos examined.

Figure 17. Cells expressing mutant CXCR4b arrive at different SDF-1a expression domains. Whole mount in situ hybridization of an embryo whose PGCs (*nanos-1* in blue) express a mutant form of CXCR4b. PGCs arrive at various sites of *sdf-1a* expression (labelled in red), other than the site of the gonad. The inset shows *sdf-1a* expressed along the lateral line that attracts PGCs located away from their correct target.

Notably, the cells expressing the mutant receptor that were found at ectopic positions in 24 hours old embryos were not located at random positions. Rather, such cells arrived at other SDF-1a expression domains, such as a region between the midbrain-hindbrain boundary and the otic vesicle [42, 46] and along the lateral line [125, 126] (Figure 16C, Figure 17).

It is noteworthy to mention that similar results were obtained when other internalization-defective mutant forms of the receptor (construct (1) and (2) in Figure 12) were assayed for complementing the *ody* mutation (Figure 16D). In addition, the potency of the CXCR4b-EGFP protein fusions to guide the PGCs towards their targets was in all cases similar to that of the non-EGFP-fused versions (Figure 16D).

The increased calcium level in cells expressing the mutant CXCR4b (Figure 15) and the enhanced G-protein activity induced by C-terminus mutated CXCR4 [55, 109] are consistent with the notion that this domain is important for controlling receptor signalling. Expressing an over-activated internalization-defective mutant receptor in wild type cells is therefore expected to interfere with normal migration. Indeed, increasing the level of the non-internalizable receptor to the amount previously used for complementation of *ody* embryos (i.e., 90 pg of RNA, Figure 16D) resulted in arrival of otherwise wild-type cells at ectopic locations as observed in 24 hours old wild-type embryos (Figure 18). This effect was concentration dependent such that further increase in the amount of the mutant receptor led to a corresponding increase in the percentage of misguided cells (Figure 18). In this assay, expression of very high levels of the wild-type receptor (i.e., 240 pg of RNA, Figure 18) resulted in imprecise cell migration as well, presumably due to higher levels of CXCR4b signalling as manifested by higher calcium level in protrusions of these cells (Figure 15). The wild-type receptor was however significantly less potent in inducing ectopic cell migration as compared with the mutant receptor (e.g., no phenotype is observed at the 90 pg level, Figure 18).

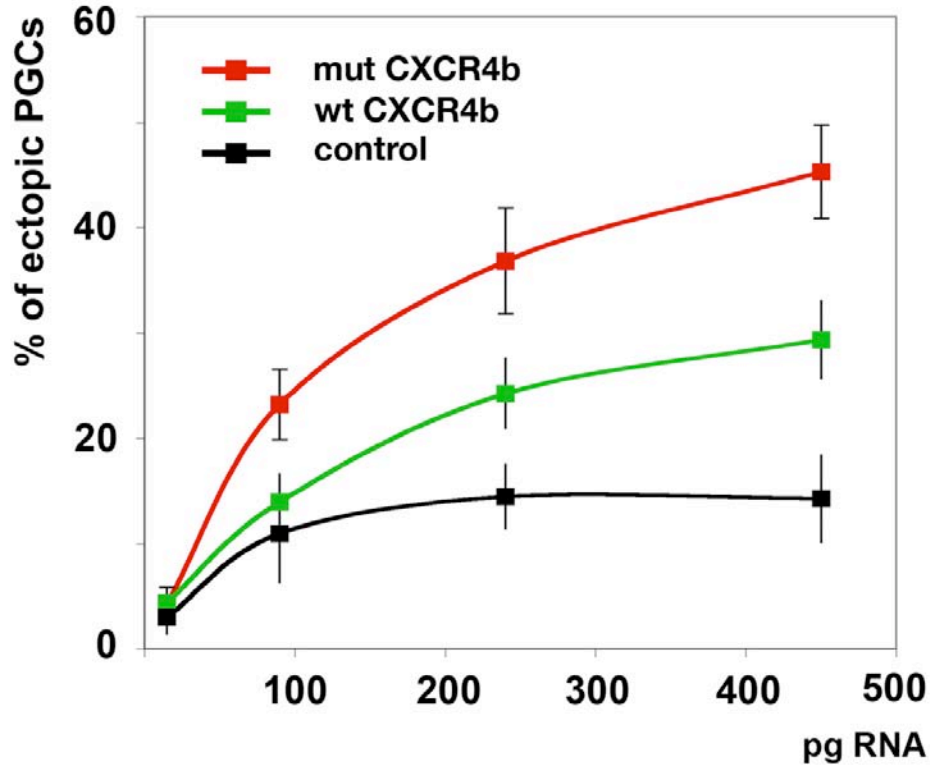

Figure 18. Increased signalling by CXCR4b results in mis-migration of PGCs. Increasing the amount of wild type *CXCR4b* (green), or mutant *CXCR4b* (red) RNA in the wild type PGCs result in an increase in the percentage of ectopic PGCs as assessed at the end of the first day of development. Error bars represent SEM. 20 to 40 embryos were analyzed for each point and the control RNA is *vasa-DsRed*-3'UTR.

Together, our results suggest that chemokine receptor internalization and signalling level are important for proper chemotaxis of germ cells. We show that although germ cells guided by CXCR4b harbouring defective C-tail are able to sense and respond to SDF-1a, a large proportion of the cells arrive at ectopic locations and even when reaching their correct target, do not cluster properly.

The critical role of receptor internalization and control of signalling level in PGC arrival at their target prompted us to investigate PGC migration at a higher resolution under conditions in which these processes are abnormally regulated.

2.12 Restricting active migration requires internalization and control of signalling level

To determine the basis for the defects in migration described above, we have monitored the behaviour of PGCs that express the mutated receptor and compared it to that of cells that express the wild-type form. It has been previously shown that zebrafish PGCs migrate in a characteristic bimodal fashion alternating between run and tumbling which constitute an intrinsic property of the migrating cells ([114] and see Introduction).

To determine whether the run-and-tumbling behaviour is controlled by receptor internalization, we have analyzed the migration of *ody* germ cells expressing the mutant receptor as compared to *ody* cells expressing the wild-type receptor. Specifically, we examined the duration of run and tumbling as well as the migration speed of experimental and control cells (Figure 19 and Supplemental Movie S3 and S4). We found that whereas the speed of run (Figure 19A) and the duration of tumbling (Figure 19B) were similar between the two cell populations, PGCs expressing the internalization-defective mutant receptor performed longer runs relative to their control counterparts (Figure 19B and Supplemental Movie S3 and S4). In an additional analysis, we grouped the run phases according to their duration (one group of 1-15 minute runs and a second group of runs lasting longer than 15 minutes) and found that lack of CXCR4 internalization resulted in a striking increase in percentage of PGCs that performed at least one long run; from 33% of cells guided by the wild type form of the receptor to 81% of cells when guided by the mutant receptor (Figure 19C). Importantly, the effect on the run and tumbling behaviour described above for the mutant receptor (construct (6) in Figure 12) were replicated in a similar experiment in which the *ody* mutation was complemented with a receptor lacking the serine-rich region (construct (2) in Figure 12) (Figure 19B).

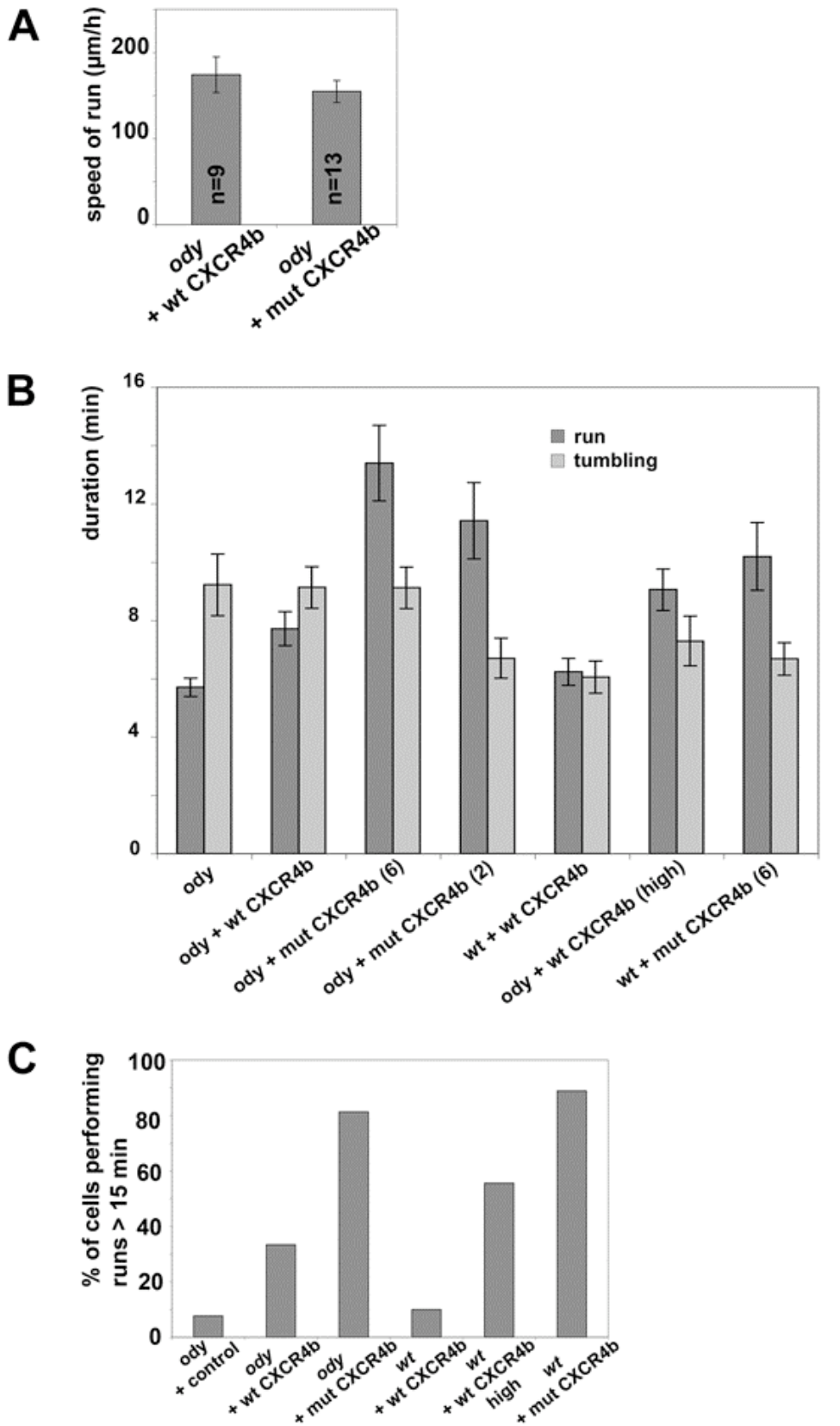

Figure 19. CXCR4b internalization controls PGC run-and-tumbling behavior by prolonging the phase of active migration. (A) The migration speed of *ody* PGCs expressing wild type or the

internalization defective mutant CXCR4b does not differ significantly (P > 0.4, n = number of cells examined). (B) Duration of run and tumbling of *ody* or wild type PGCs expressing the wild type or the internalization defective CXCR4b (construct (6) or (2) in figure R4) tagged with EGFP. *vasa-DsRed*-3'UTR RNA was used as a control. The amount of control and CXCR4b (wild type or mutant) RNA injected was 90 pg in all treatments except for the "wild-type + wild-type CXCR4b high" where 240 pg of wild-type CXCR4b RNA was injected. The error bars represent the standard error of the mean (SEM). Number of run and tumbling phases analyzed for each point > 50. "ody + control" and "ody + wild-type CXCR4b" as well as "wild-type +wild type CXCR4b" and "wild-type + wild-type CXCR4b high" differ significantly as judged by T-test. P-value < 0.004 and P < 0.02 respectively. (C) Percentage of cells performing at least one run lasting more than 15 minutes in the experiment described in panel C (n=9 to 16 cells for each experimental point).

Consistent with the findings obtained examining *ody* mutant embryos, wild type cells expressing the mutant receptor or high amounts of the wild type CXCR4b performed extended run phases, as well (Figure 19B and 19C).

Together, our results indicate that the C-terminus of CXCR4 regulates the run and tumbling behaviour by restricting the duration of run phases.

Whereas increased receptor activation resulted in long run phases, reducing the signalling level led to the opposite result. For example, PGCs lacking a functional receptor (as is the case in *ody* mutant embryos) performed shorter runs compared to the same cells complemented by wild type CXCR4b (Figure 19B). Similarly, PGCs migrating in an environment devoid of SDF-1a, as well as cells knocked down for CXCR4b also performed shorter runs as compared with wild-type cells [114].

2.13 The "run" phases shorten as the germ cells approach their target

According to our findings, cells in which CXCR4b signalling is reduced spend less time actively migrating i.e., in run mode, relative to cells experiencing normal signalling levels (Figure 19B and [114]). Conversely, increasing the level of the directional signal (as manifested by enhanced calcium mobilization (Figure 15)) dramatically prolongs the duration of runs (Figure 19B, 19C and Supplemental

Movies S3 and S4). It would therefore be expected that as the cells approach their target, where the level of SDF-1a is the highest, the duration of runs would be further increased. Considering the above results, prolonged runs at the vicinity of the target would reduce the precision of arrival and interfere with efficient clustering. In contrast to these expectations, as wild type PGCs approach a group of transplanted cells engineered to express high levels of SDF-1a, the duration of the run phases is decreased while the duration of the tumbling phase remains the same (Figure 20). Importantly, wild-type PGCs expressing the mutant CXCR4b increase the duration of run phases as they approach the transplant (Figure 20).

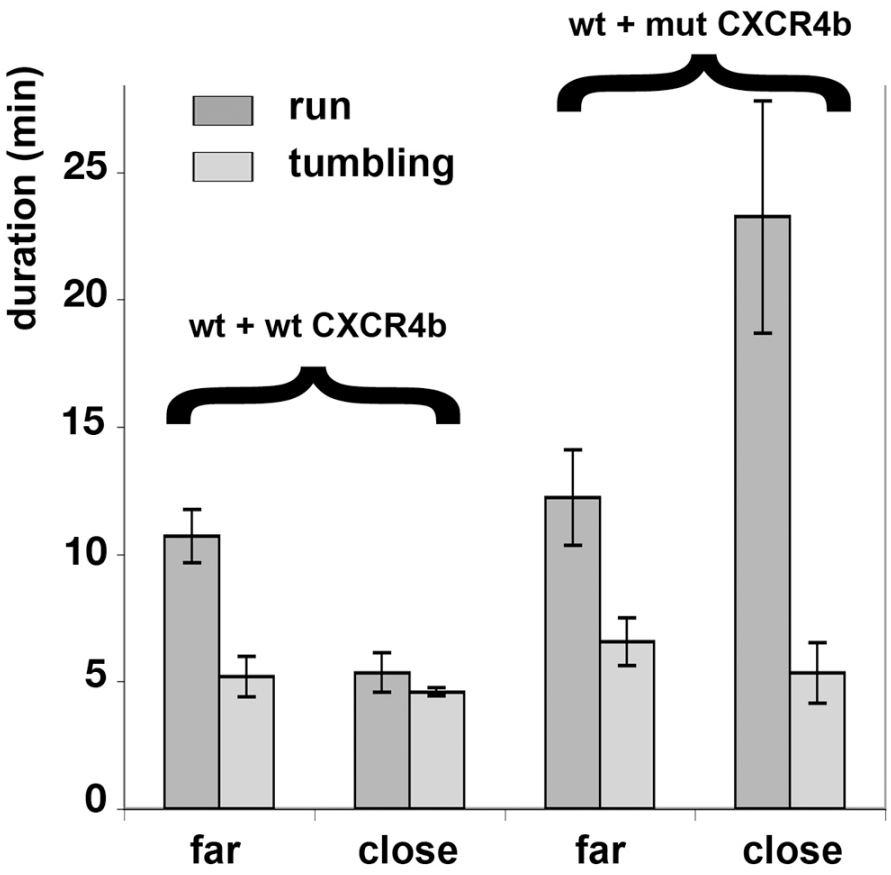

Figure 20. Internalization is required for reducing the duration of run phases in the vicinity of the target. The duration of run and tumbling phases was extracted from tracks of wild-type cells that express exogenous wild-type (left) or mutant CXCR4b (right) as they migrate towards a transplant of cells producing SDF-1a. The duration of the run phases of cells expressing wild-type CXCR4b far from the transplant (90 mm or more) was higher compared to the duration of the run phases close to the transplant (60 mm or less). In contrast, germ cells expressing the mutant CXCR4b increased the duration of the run phases as they arrived closer to the transplant.

3.0 Discussion

In this work we investigate the mechanisms responsible for precise arrival of zebrafish primordial germ cells at the site of the future gonad. We show that in contrast to its role in *Drosophila* and mouse, endoderm does not play an important role in zebrafish germ cell migration although it is essential for proper cluster formation after the cells have arrived at their final target. Aiming to study mechanisms controlling the precision of PGC arrival at this target we have moved our research focus to the molecular machinery regulating PGC migration throughout the stages when they actively migrate. To this end, we demonstrate the importance of CXCR4b internalization and signalling down-regulation for the precision of PGC arrival at the site of the future gonad.

3.1 Role of endoderm in zebrafish PGC migration

Endoderm has long been shown to be a germ layer crucial for germ cell migration in *Drosophila* and mouse as germ cells reside in the forming gut (an organ of endodermal origin) and then migrate through the gut epithelium towards mesodermal structures where they participate in gonad formation (reviewed in [31]). In contrast, another germ layer, mesoderm, was identified as crucial for zebrafish PGC migration [42], although it had not been shown that endoderm does not play a role in this process. Fly and mouse are quite remote in the phylogenetic tree and it was appealing to hypothesize that the mechanism conserved between these two might pertain in fish as well.

To address the functional role of endoderm in germ cell migration we first studied the localization of cells belonging to these two lineages. It has previously been shown that PGCs migrate in close proximity to the yolk on top of the yolk syncytial layer [27]. In our study we show that indeed, in wild-type embryos germ cells are never found away from this location. Additionally, we discovered that they are sharing this location with endoderm, the germ layer most proximal to the yolk. Imaging live embryos in which both endoderm and germ cells were marked, we

could see that germ cells migrate in a corridor, on top of endoderm and below the overlaying tissues not intermingling with any of them. Interestingly, this corridor could be observed only at the spots where germ cells were crawling and not in the adjacent regions. This tendency to migrate on top of endoderm is reminiscent of mouse germ cells that having arrived into the hindgut migrate along it. There, regulated adhesion mediated by IFITM3 expressed in the mouse germ cells and E-cadherin expressed in the hindgut but not in germ cells during this stage, may play an important role in keeping germ cells within the hindgut [9, 39, 127]. Nevertheless, zebrafish germ cells did not alter their spatial behaviour in *cas* mutant embryos. They remained confined to the deepest embryonic layers although endoderm lacked altogether in these mutants [112, 113]. It would be interesting to follow the behaviour of mouse or *Drosophila* germ cells in the absence of the endoderm. Unfortunately, mutations that would eliminate this germ layer without affecting the body plan are not available for those organisms.

Next we found that PGC location near the yolk depends on SDF-1a/CXCR4b signalling. In *ody* mutant embryos lacking functional CXCR4b PGCs would readily leave their “corridor” and be found at random locations in the embryo not only relative to *sdf-1a* expression sites but relative to the yolk, as well. Germ cells lacking CXCR4b signalling are known to maintain their ability to migrate although they are unable to respond to the chemical gradient [114]. Therefore, the “corridor” formation as well as their spatial disposition *per se* is not required for germ cell migration. Intuitively it would be tempting to suggest that a cell-free space could facilitate PGC migration positively affecting their speed. Nevertheless, it has been previously shown that in the absence of SDF-1a/CXCR4b signalling, PGCs migrate at the same speed during the run phases as there wild-type counterparts.

A likely explanation for the germ cells’ preferred location in the gastrulating embryo follows from our finding showing that *sdf-1a* is expressed exclusively in the deepest layers of embryonic mesoderm and not in the mesodermal cells located further away from the yolk. Hence, the secreted SDF-1a molecules could be presented by extracellular matrix underneath most proximal mesoderm. Conversely, endodermal cells do not express *sdf-1a* and taken together these results suggest that the close proximity of PGCs and endoderm might be a mere coincidence. To substantiate

our hypothesis it would be important to visualize SDF-1a secreted protein. Molecular mechanisms that promote germ cell migration into endoderm (in mouse) [9, 39] or induce their departure from this embryonic tissue (in *Drosophila,* in mouse) [33, 34, 40, 41, 128] but not those retaining them there have been discovered. Therefore, it would be interesting to check if similarly to the situation in zebrafish, in *Drosophila* and mouse PGC gut residence depends on local expression of an attractant molecule there.

Together, our results demonstrate that endoderm does not play a role in positioning PGCs during the period of their active migration. Similarly, it is not important for PGC arrival at the site where the gonad develops. Interestingly, although *cas* germ cells migrate as two separate clusters during late somitogenesis, as soon as two clusters come close together at around 28 hours post fertilization they fuse at the midline and form one cluster. Regularly, in the entire course of their migration germ cells avoid the midline [42]. When lacking CXCR4b/SDF-1a signalling PGCs can enter this zone suggesting that avoiding the midline is a result of lack of the attractive cue at this position [46]. We performed an RNA *in situ* hybridization to check if *cas* mutation has an effect on *sdf-1a* expression at the gonad region thereby providing the basis for the observed germ cell phenotype. Surprisingly, *sdf-1a* is not expressed in the area of the gonad in both wild-type and mutant embryos after 24 hours post fertilization when *cas* germ cell phenotype is observed. This finding points to an unknown mechanism that would retain germ cells at their final position that is likely to be disturbed by the lack of endoderm.

The germ cell phenotype in *cas* mutant embryos could stem from lack of specific tissues or organs. For example, the gut could normally control the movement of the germ cells as they cluster on both sides of this organ. The defects in endoderm formation could result in a lack of a barrier and fusion of the germ cell clusters. It would be important to determine the precise mechanism by which endoderm controls germ cell position within the developing gonad.

3.2 Control of active cell migration by chemokine receptor internalization and signalling level promotes precise arrival at the target

Many types of cells respond to extracellular directional cues with asymmetric changes in cell morphology and motility. The process in which a chemical gradient serves as a directional signal that organizes cell movement is called chemotaxis and plays a central role in development, immunity, and tissue homeostasis [129-132]. Directional sensing as well as directional cell movement involves cell polarization. In many studies the question of how chemotactic cells establish and maintain polarization has been addressed [133]. The first candidate molecule to be asymmetrically distributed in a polarized cell migrating according to a chemical gradient would be the molecule detecting the chemical signal i.e., chemokine receptor. Indeed, several *in vitro* studies performed on fMLPR in neutrophils, CCR2 and CCR5 receptors in T lymphocytes, and on CXCR4 in B and T lymphocytes and in hematopoietic progenitor cells demonstrated chemokine receptor relocalization to the leading edge of cells in response to the exposure to their corresponding chemokines [62-66]. Other groups demonstrated opposite results showing that cAR1 in *Dictiostelium* and C5aR in neutrophils are distributed evenly on the membrane. Similarly, when we expressed CXCR4b-EGFP fusion in PGCs it was found to be distributed evenly on cell plasma membrane during cell migration. To avoid possible saturation of the protein on the plasma membrane we expressed the amounts of CXCR4b-EGFP optimal for complementation of CXCR4b knock-down [46] or knock-out, levels that we considered close to physiological CXCR4b levels. Importantly, the optimal amounts of the fusion receptor was equimolar to the amounts of the untagged protein needed to rescue the phenotype caused by the lack of CXCR4b, which indicates that the CXCR4b-EGFP fusion is functionally intact. Furthermore, polarized distribution of CXCR4 on the membrane of hematopoietic progenitors was demonstrated visualizing CXCR4-GFP fusion protein [66] as we did in our studies, which proves that this method is sensitive enough to detect receptor accumulation at the leading edge when it takes place. Still it would be useful to confirm our findings using an immunofluorescence approach. Unfortunately, antibodies against CXCR4b are not available. Discrepancy in results from different studies could be attributed either to the

difference among the cell types examined or to differences between the *in vitro* experimental systems and the *in vivo* situation where the cells are exposed to physiological amounts of the ligand. In this case, our results obtained *in vivo* provide an important insight in the problem. However, we did not observe CXCR4b polarization to the front even when PGCs were exposed even to very high amounts of SDF-1a and cAR1 as well appears distributed uniformly on *Dictyostelium* membrane when cells are exposed to steep gradients of cAMP [67].

Several groups suggested another mechanism of cellular polarization acting through phosphatidylinositol-3 kinase (PI-3K) as manifested by recruitment of products of this enzyme selectively to the leading edge [134, 135]. Nevertheless, uniform distribution of these agents was demonstrated in a recent study from our lab [69].

Another mechanism responsible for maintenance of cellular polarization emerged from a study of *Drosophila* border cells [115]. Here, authors suggest that endocytosis of guiding receptors serves as a mechanism for spatial restriction of intracellular signalling in the direction of the guidance cues. It is hypothesized that the receptors are localized to the leading edge *via* re-delivery to this membranal domain following receptor internalization. We did not obtain any evidence for or against this data in our experiments. Apart from the role in localizing active receptors in *Drosophila* border cells guidance receptor internalization was implicated in chemotaxis in other systems as indicated by migration abnormalities when the chemotactic signal is transmitted through internalization defective mutant receptors [55, 79, 107, 109, 136]. However, in these studies receptor internalization was linked to receptor signalling regulation rather than spatial polarization.

To determine if CXCR4b internalization is involved in PGC migration, we first checked if this process occurs in germ cells or not. Introducing a group of cells secreting high amounts of SDF-1a in close proximity to germ cells expressing CXCR4b-EGFP, we could observe the green fluorescence gradually being reduced on the germ cell plasma membrane with concomitant appearance of particles that supposedly correspond to endocytic vesicles. Interestingly, germ cells exposed

very high doses of SDF-1a (300 pg of injected RNA into donor embryos in this experiment) was not attracted to the transplant for 40 minutes that we observed it while cells exposed to a transplant secreting much lower levels of SDF-1a (60 pg of injected RNA) started to crawl to the transplant immediately after transplantation. Presumably, this was due to the inability of germ cells to detect the gradient under conditions of very high SDF-1a levels.

Altogether, we showed that we could induce full CXCR4b internalization in vivo, validate the effect of SDF-1a on the process and demonstrate that CXCR4b internalization could be visualized using the CXCR4b-EGFP fusion. We then used this system of exposing cells expressing the CXCR4b-EGFP fusion to high SDF-1a levels by expressing the ligand in endodermal cells to identify the domains or specific amino acids within the receptor molecule that are essential for receptor endocytosis. CXCR4 internalization is mediated by a group of proteins that interact with the receptor through phosphorylated amino acids located at the C-terminal part of the molecule ([94-96, 119, 137] and reviewed in [98]). This region is also involved in desensitization of the receptor and down regulation of G-protein signalling [80]. In our mutant analysis we discovered that serine residues within last 15 amino acids of CXCR4b C-tail provide the phosphorylation platform required for receptor internalization. Interestingly, these serines appeared to be redundant i.e., a certain number of them was sufficient to allow CXCR4b internalization to happen. The redundancy among the phosphorylation sites could indicate a potential for integrating multiple inputs that would modulate the process. Next we showed that the part of CXCR4b cytoplasmic tail upstream from the critical region is also essential for internalization. Nevertheless, the serine residues within this part of receptor molecule are not required for receptor endocytosis. It would be interesting to find out the exact role this region of the molecule plays in the process.

Importantly, we demonstrated that serine exchange mutations inhibiting CXCR4b internalization when PGCs were exposed to high amounts of SDF-1a prevented internalization of CXCR4b also at physiological levels of the chemokine. In a recent study conducted on CXCR1 and CXCR2 in human primary neutrophils Rose et al. showed that ligand concentrations necessary for internalization are 10-fold higher than concentrations that induce chemotaxis [138]. We could propose that these

receptors internalize at higher ligand concentration than CXCR4b or alternatively, normal levels of SDF-1a in zebrafish embryo are higher than those physiological for human neutrophils. Antibodies against zebrafish SDF-1a, still unavailable, would be helpful to clarify this point.

To determine if the close structural conservation of the most distal serine rich parts of human CXCR4 and zebrafish CXCR4b is reflected by functional conservation we performed a similar mutant analysis for human CXCR4. To this end, we demonstrated not only that the same amino acids are essential for endocytosis of this protein but also that parts of the conserved region are redundant. These findings differ from previous results suggesting that specific amino acids within this region are essential for internalization [95]. Mutating these residues alone (serines 338 and 339 in the human receptor or the corresponding serines 339 and 340 in the zebrafish receptor) had no effect on internalization in our experimental systems. This discrepancy could derive from the use of different ways for estimating internalization potential of the receptor versions. We believe that the procedure that we used in our study when cells expressing certain versions of CXCR4 tagged with EGFP were fixed unmodified and observed right after incubation with the ligand was the most direct to attain our goal.

A rise in calcium levels is one of the earliest events following activation of CXCR4 by SDF-1 [123, 124] and such an increase was shown to be important for proper PGC migration in zebrafish [48]. We demonstrated *in vivo* that defects in receptor internalization are accompanied by increased signalling as manifested by higher calcium level in cells expressing mutant receptor as compared to the control. These results are consistent with previous findings [94], indicating that the internalization-defective receptor is active and provides a stronger signal than normal (reviewed in [98]). This increased signalling could be caused either by defective receptor desensitization or by the lack of CXCR4b internalization. In the first case, the signalling level could rise due to prolonged receptor coupling to G-proteins. In the second one, those receptor molecules that failed to internalize would accumulate on the plasma membrane and provide additional signalling. It is not clear whether chemokine receptors remaining on the plasma membrane after binding their ligand can proceed into a new cycle of activation. There is some

evidence that chemokine receptors are able to resensitize without leaving the membrane [138].

The results discussed above provided us with a powerful tool for investigating the role internalization plays in guided cell migration *in vivo.* Such an analysis could be performed by comparing the function of the 'non-internalizable' version of CXCR4b with that of the wild-type receptor in supporting directed PGC migration *in vivo*. Here we showed that the mutant receptor was less potent in complementing *ody* mutation than its wild-type counterpart. A considerable proportion of germ cells was found at ectopic positions in 1-day old embryos and cells that managed to arrive at the site of the gonad formed a dispersed cluster. Notably, the ectopic positions where some germ cells arrived instead of their correct target were characterized as sites of high expression of SDF-1a, which strengthens the notion that cells guided by mutant receptor, respond to SDF-1a by directed migration, but frequently miss their correct target and arrive at other sites where SDF-1a is expressed.

To prove that activity of wild-type or mutant CXCR4b was not affected by EGFP fusion we demonstrated that untagged, these proteins exhibited similar potential for *ody* complementation. Additionally, we confirmed the specificity of the effect of the serine exchange mutant on germ cell migration by reproducing similar 'internalization phenotype' using other internalization defective mutants for complementing *ody*.

Altogether these results emphasize the critical role the identified CXCR4b regulatory domain plays in arrival at the target of migrating cells. Therefore, we headed to investigate the basis for the defects in PGC arrival at the site of the gonad looking at the cells during the early stages of their active migration, which basically determine how successfully the cells reach their final goal.

As it was shown in a previous study, in the course of their migration germ cells alternate between run and tumbling phases, which constitutes the intrinsic germ cell behaviour that occurs independently of CXCR4b signalling [114]. During run phase cells are polarized and actively migrate. Tumbling phase is characterized by

loss of cell polarity and by immobility relative to surrounding tissues. Since the vast majority of corrections to the migration route are performed at the exit from the tumbling phase, the run-and-tumbling behavioural pattern constitutes a mechanism regulating the accuracy of PGC migration as they follow the dynamically changing expression of the chemokine [114]. As we demonstrated in our study, the 'internalization migration phenotype' does not affect SDF-1a gradient sensing but rather migration accuracy. Therefore, we hypothesized that run/tumbling bimodal behaviour might be involved in bringing cells guided by the mutant receptor to ectopic positions. Indeed we showed that these cells on average perform significantly longer runs. In additional data analysis we demonstrated that lack of CXCR4b internalization correlates with more than double increase in amount of very long runs of more than 15 minutes.

Consistent with our data are the results describing cells carrying a C-terminal truncation mutant CXCR4 that exhibit increased motility in wound healing and transwell assays [55, 107, 109]. The errors in arrival of PGCs at the site of the gonad, when guided by CXCR4b forms that lack a functional C-terminus could therefore result from cells 'over-shooting' their target due to abnormally long duration of run. Obviously, to run more does not mean to run better. The migration route of such cells could now be dictated by SDF-1a expression domains that normally function in other morphogenetic events (e.g., guidance of the lateral line primordium [125, 126]) as it is demonstrated in our data.

It would be interesting to determine the relative contribution of receptor internalization alone versus down-regulation of receptor signalling in controlling cell migration, two processes that depend on an intact cytoplasmic tail of CXCR4. However, specific inhibitors of internalization that could uncouple the two processes (e.g. [136]) cannot be employed in the *in vivo* experimental system used here. Specifically, expression of dominant-negative forms of proteins whose function is essential for internalization (e.g., dynamin, caveolin-1 as well as nonvisual arrestins 2 and 3) at levels that do not affect CXCR4b internalization already inflicts general toxicity on the developing embryos. Furthermore, even at lower concentrations that do not severely affect general embryonic development,

these agents strongly inhibit PGC motility signifying the general deleterious effect these reagents exert on cells.

The longer runs and increased calcium level in cells expressing the mutant CXCR4b and the enhanced G-protein activity induced by C-terminus mutated CXCR4 [55, 109] are consistent with the notion that this domain is important for down regulation of receptor signalling. In line with this notion was as well our finding that internalization defective mutant brings otherwise wild-type cells at ectopic positions at 24 hours of embryonic development i.e., overrides wild-type cell behaviour. Furthermore migration analysis of such cells at earlier stages replicated the 'internalization phenotype' observed when mutant receptor was expressed at *ody* background i.e., duration of run phase was increased. So here we can talk about a dominant effect of the introduced mutation. Importantly, wild-type receptor expressed in wild-type cells at very high concentrations could bring germ cells to ectopic locations in the embryo as well as resulted in higher proportion of very long runs at earlier stages i.e. phenocopied the internalization defective mutant. This supports the idea that the effect of the internalization defective mutant on cell behaviour is mediated by the increased receptor signalling.

Providing evidence for the role of CXCR4b C-tail domain in signalling down-regulation (measurements of the calcium level), our results can account for the dominant deleterious effect of receptor over-signalling on the arrival at the gonad. Moreover, these findings could pertain to the dominant WHIM syndrome disorder. WHIM syndrome is an immunological disease associated with C-terminal mutations eliminating 10 to 19 of the distal tail amino acids, including a number of potential phosphorylation sites [53, 107]. This leads to the expression of the receptor with altered regulation. Following activation by SDF-1a cells isolated from patients suffering from WHIM syndrome exhibit enhanced cell migration *in vitro* as well as a lack of desensitization, an increase in F-actin polymerization, enhanced calcium mobilization and a decrease in SDF promoted internalization [55, 107, 108]. Nevertheless, the precise effect on cell migration within the body and the basis for the observed pathology have remained unknown [53, 55, 107]. Data

presented in our work could serve as a head start for further investigations in the field.

According to our findings and previous studies [114] cells experiencing reduced levels of SDF-1a/CXCR4b signalling spend less time in the run phase. Conversely, increasing CXCR4b induced signalling (as manifested by enhanced calcium mobilization) drastically prolongs the duration of run. Therefore, expected would be to observe longer runs in the vicinity of their target, where the level of SDF-1a is the highest. This expectation comes into a logical contradiction with our results as prolongation of the run phase reduces the accuracy of cell arrival and therefore must be biologically unfavourable. Indeed we demonstrated that wild type cells decrease the duration of the runs as they approach a group of cells producing SDF-1a. Such behaviour would enable corrections to the migration path close to the target, thus reducing the chance of the cells arriving at other sites where SDF-1a is expressed (Figure 21). Strikingly, wild-type cells expressing the mutant CXCR4b increased the duration of run phases as they approach the source of SDF-1a. This is consistent with the idea that cells that are not able to internalize the receptor and reduce the intracellular response to the chemokine experience enhanced signalling level closer to the transplant, which is manifested in the increased duration of the run phase. Interestingly, in this “simplified” migration environment where the endogenous cues are knocked down and the directional information is provided by a single stationary source of SDF-1a, cells guided by the mutant receptor successfully arrive at the target (data not shown). It is likely that only when other targets are present in the migration field as is the case in the *in vivo* situation that the long runs result in arrival at other sources of SDF-1a (Figure 21). Thus, we propose chemokine receptor internalization and signalling down-regulation as a fundamental mechanism to ensure the precise arrival of cells at their migration target in the dynamic environment of a living organism.

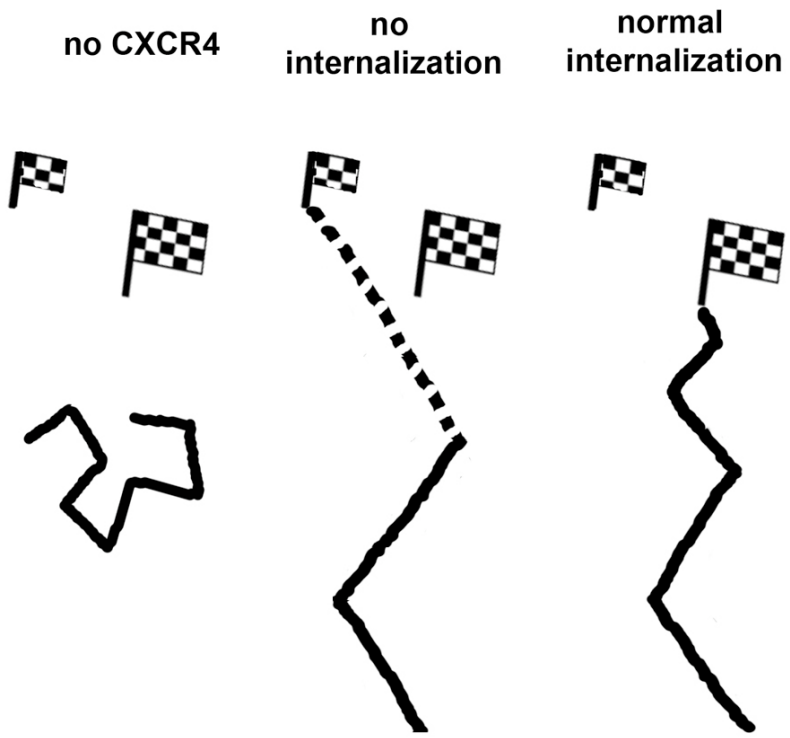

Figure 21. A model for the role of internalization in precise arrival of PGCs to their target. Sensing the SDF-1a cells migrate directionally performing relatively long run phases as compared to cells migrating in an environment lacking the directional cue. As they get closer to the target run phases become shorter in a process that depend on internalization. In the absence of internalization the run phase remains long and the cells may pass over their target. Large flags depict the PGC target where peak level of SDF-1a is produced. Smaller flags depict other locations in the embryo where SDF-1a is expressed.

4.0 Summary and Conclusion

By the end of the first day of embryonic development, zebrafish primordial germ cells (PGCs) arrive at the site where the gonad develops. In our study we investigated the mechanisms controlling the precision of primordial germ cell arrival at their target.

We found that in contrast with our expectations which were based on findings in *Drosophila* and mouse, the endoderm does not constitute a preferred migration substrate for the PGCs. Rather, endoderm derivatives are important for later stages of organogenesis keeping the PGC clusters separated. It would be interesting to investigate the precise mechanism by which endoderm controls germ cell position in the gonad.

In their migration towards the gonad, zebrafish germ cells follow the gradient of chemokine SDF-1a, which they detect using the receptor CXCR4b that is expressed on their membrane. Here we show that the C-terminal region of CXCR4b is responsible for down-regulation of receptor activity as well as for receptor internalization. We demonstrate that receptor molecules unable to internalize are less potent in guiding germ cells to the site where the gonad develops, thereby implicating chemokine receptor internalization in facilitating precision of migration during chemotaxis *in vivo*. We demonstrate that while CXCR4b activity positively regulates the duration of the active migration phases, the down-regulation of CXCR4b signalling by internalization limits the duration of this phase. This way, receptor signalling contributes to the persistence of germ cell migration, whereas receptor down-regulation enables the cells to stop and correct their migration path close to the target where germ cells encounter the highest chemokine signal.

Chemokine receptors are involved in directing cell migration in different processes such as lymphocyte trafficking, cancer and in the development of the vascular system. The C-terminal domain of many chemokine receptors was shown to be essential for controlling receptor signalling and internalization. It would therefore be

important to determine whether the role for receptor internalization *in vivo* as described here (allowing periodical corrections to the migration route) and the mechanisms involved (reducing the level of signalling) apply for those other events, too.

5.0 Zusammenfassung

Innerhalb des ersten Tages der embryonalen Entwicklung des Zebrafisches erreichen die primordialen Keimzellen die Gonaden. In dieser Arbeit haben wir die Kontroll-mechanismen untersucht, die die präzise Ziel-Ankunft dieser Zellen ermöglichen.

Wir stellen fest, dass das Endoderm entgegen vorheriger Erkenntnisse in *Drosophila* und Maus kein bevorzugtes Substrat für Keimzellmigration darstellt. Stattdessen halten Zellen endodermalen Ursprungs in späteren Phasen der Entwicklung die Teilung der beiden Keimzellverbände aufrecht. Was diese Art der Positionierung primordialer Keimzellen im Zebrafisch ermöglicht, verbleibt jedoch unbekannt und sollte Gegenstand weiterer Forschungen sein.

Während ihrer Wanderung zu den Gonadenanlagen wird die Richtung der Wanderung durch einen Gradienten des Chemokins SDF-1a gesteuert, den Keimzellen durch den in ihrer Zellmembran befindlichen Chemokinrezeptor CXCR4b erkennen. Wir zeigen, dass C-terminale Steuerungsdomänen von CXCR4b für die Reduktion der Rezeptoraktivität und der Rezeptorinternalisierung verantwortlich sind. Mutationen, die die Internalisierung von CXCR4b verhindern, stören die gerichtete Zellwanderung primordialer Keimzellen zu den Gonaden und weisen daher auf einen *in vivo* Zusammenhang zwischen Rezeptorinternalisierung und der Präzision von Zellwanderung hin. In unseren Versuchen verlängert CXCR4b-Aktivität die Dauer aktiver Wanderungsphasen, Reduktion der Aktivität von CXCR4b hingegen verkürzt diese Wanderungsphasen. Auf diese Art unterstützt das Rezeptorsignal die anhaltende Wanderung der Zellen zu ihrem Ziel, während die Reduktion der Rezeptoraktivität den Zellen eine Korrektur ihrer Wanderungsrichtung nahe ihres Ziels erlaubt, einer Umgebung mit hoher Signalkonzentration.

Chemokinrezeptoren sind in vielen gerichteten Migrationsprozessen involviert, darunter in der Lymphozytenwanderung, dem invasen Krebswachstum und der Metastasenbildung, sowie der Entwicklung und Ausformung des Gefäßsystems. Es wäre von grossem Interesse, ob die C-terminale Domäne anderer Chemokinrezeptoren die periodische Richtungskorrektur und Signalreduzierung *in vivo* regulieren könnte.

6.0 Experimental Procedures

6.1 Bacteria strain

E. Coli Top 10F'	Invitrogen

6.2 Chemicals

All chemicals, if not noted otherwise, were purchased from the companies Applichem, Merck, Roth and SIGMA.

anti-DIG antibody	Roche 1093274
anti-fluorescein antibody	Roche 1426338
DIG RNA labeling Mix	Roche 1277073
DAB Diaminobenzidine	SIGMA
Eukitt	Kindler
RNA isolation	Trizol, Invitrogen
DMEM	GIBCO, Invitrogen
FBS	GIBCO, Invitrogen

6.3 Kits

mMessage mMachine Kit	Ambion
Topo-TA Cloning Kit	Invitrogen
QIAquick Gel extraction Kit	Quiagen
OmniScript Kit	Quiagen
Advantage HF 2 PCR Kit	Clontech
QIAquick PCR purification Kit	Qiagen
QIAfilter Plasmid Mini/Midi/Maxi Kit	Qiagen
Phusion PCR Kit	Finnzym
Lipofectamine 2000	Invitrogen

6.4 Primary and Secondary Antibodies

Rabbit polyclonal anti-GFP antibodies (Santa Cruz Biotechnology) (P6) were used as primary antibody against GFP in working dilution 1:500. HRP conjugated goat anti-rabbit antibodies (S7) were used as secondary antibodies for immunostaining of GFP.

6.5 Antisense probes used for *in situ* RNA hybridization

Nanos1-Dig	Nanos1 RNA is localized in PGCs at stages of our interest. It

	was used to mark the germline in experiments described in Figure 6B, 6C, 6E, 6F, 6H, 6I, and Figure 17.
Nanos1-Fluo	The same probe marked with Fluo used in experiments described in Figure 8A
Sox17-Dig	Sox17 is a transcription factor, whose RNA is expressed in endodermal cells during gastrulation and beyond. It was used to mark endodermal lineage in experiments described in Figure 6B, 6E, 6H.
Fkd2-Fluo	Forkhead-2 is a transcription factor normally used as a late endodermal marker. We used to distinguish between wild-type and *cas* embryos in experiments described in Figure 8A.
SDF1a-Dig	SDF-1a antisense probe was used to detect *sdf-1a* expression pattern in experiments described in Figure 8A and Figure 17.

Table 1. Antisense probes used for in situ RNA hybridization

6.6 DNA Constructs used in this work

CXCR4b and human CXCR4 constructs produced in this work		
Plasmid No.	**Name**	**Description**
760	pSP6-CXCR4b-EGFP-3'UTRnos1	Wild type CXCR4b used for identification of CXCR4b localization as well as for complementation of *ody* mutant.
958	pSP6-CXCR4b-3'UTRnos1	EGFP-free analogues of some CXCR4b versions were used to confirm the unaltered efficiency of EGFP fusion proteins.
A136	pSP6-CXCR4b-(1-312)-EGFP-3'UTRnos1	CXCR4b truncation mutant (aa 1-312; at the end of the truncation three alanines were inserted to mimick the hydrophobic anchor of the C-tail) depicted in Figure 12 (construct 1)
A061	pSP6-CXCR4b-(1-312)-3'UTRnos1	The same construct without EGFP
956	pSP6-CXCR4b-(1-338)-EGFP-3'UTRnos1	CXCR4b truncation mutant (aa 1-338) depicted in Figure 12 (construct 2)
957	pSP6-CXCR4b-(1-338)-3'UTRnos1	The same construct without EGFP
185	pSP6-CXCR4b-trunc(1-347)-EGFP-3'UTRnos1	CXCR4b truncation mutant (aa 1-347) depicted in Figure 12 (construct 3)
981	pSP6-CXCR4b(1-347)-3'UTRnos1	The same construct without EGFP
A017	pSP6-CXCR4b-del(339-346)-	CXCR4b deletion mutant (deletion of aa

	EGFP-3'UTRnos1	339-346) depicted in Figure 12 (construct 4)
A006	pSP6-CXCR4b-del(339-346)-3'UTRnos1	The same construct without EGFP
A713	pSP6-CXCR4b-S 339 340 342 345 A-EGFP-3'UTRnos1	CXCR4b exchange mutant (aa 339, 340, 342 and 345 were exchanged for alanines) depicted in Figure 12 (construct 5)
A285	pSP6-CXCR4b-S 339 340 342 345 347 348 349 A-EGFP-3'UTRnos1	CXCR4b exchange mutant (aa 339, 340, 342, 345, 347, 348 and 349 were exchanged for alanines) depicted in Figure 12 (construct 6)
A367	pSP6-CXCR4b-S 339 340 342 345 347 348 349 A- 3'UTRnos1	The same construct without EGFP
A232	pSP6-CXCR4b-del(313-338)-EGFP-3'UTRnos1	CXCR4b deletion mutant (deletion of aa 313-338) depicted in Figure 12 (construct 7)
A007	pSP6-CXCR4b-del(313-338)-3'UTRnos1	The same construct without EGFP
A354	pSP6-CXCR4b-tailmut(1-7)-EGFP-3'UTRnos1	CXCR4b exchange mutant (aa 313, 315, 321, 323, 324, 326, 327 were exchanged for alanines) depicted in Figure 12 (construct 8)
A361	pSP6-CXCR4-trunc(1-347)-tailmut(1-7)-EGFP-3'UTRnos1	CXCR4b truncation mutant (aa 1-347) in which aa 313, 315, 321, 323, 324, 326, 327 were exchanged for alanines. This mutant is depicted in Figure 12 (construct 9)
A362	pSP6-CXCR4-del(339-346)-tailmut(1-7)-EGFP-3'UTRnos1	CXCR4b deletion mutant (deletion of aa 339-346) in which aa 313, 315, 321, 323, 324, 326, 327 were exchanged for alanines. This mutant is depicted in Figure 12 (construct 10)
A557	pcDNA3.1(-) HA hCXCR4 EGFP	Wild-type human CXCR4 tagged with HA at N-terminus and with EGFP at C-terminus that was used as a control in experiments with human CXCR4.
A574	pcDNA3.1(-) HA hCXCR4 mut7StoA EGFP	Human CXCR4 exchange mutant (aa 338, 339, 341, 344, 346, 347, 348 were exchanged for alanines) depicted in Figure 12 (construct 11) and used in experiments described in Figure 14.
A710	pcDNA3.1(-)HA hCXCR4 S3389A EGFP	Human CXCR4 exchange mutant (aa 338, 339 were exchanged for alanines) was used

		to repeat experiments presented by Orsini et al. [95].
A711	pcDNA3.1(-)HA hCXCR4 S3389A S3414A EGFP	Human CXCR4 exchange mutant (aa 338, 339, 341, 344 were exchanged for alanines) depicted in Figure 12 (construct 12).
A712	pcDNA3.1(-)HA hCXCR4 S34678A EGFP	Human CXCR4 exchange mutant (aa 346, 347, 348 were exchanged for alanines) depicted in Figure 12 (construct 13).
Other plasmids produced in this work		
A366	pCR-TOPO4-rDynDN-3'UTRnos1	Rat dominant negative dynamin-2 (K44A) used to suppress internalization in PGCs. It has a general deleterious effect on PGC migration at concentrations not sufficient to affect CXCR4b endocytosis.
A729	pSP6-zf caveolin1 P135L - 3'UTRnos1	Zebrafish dominant negative caveolin-1 (P135L) used to suppress internalization in PGCs. It has a general deleterious effect on PGC migration at concentrations not sufficient to affect CXCR4b endocytosis.
A751	pSP6-z-nonvis arrestin-2 319-418 3'UTR-nos1	Zebrafish dominant negative nonvisual arrestin-2 (a protein fragment aa319-418) used to suppress internalization in PGCs. Has a general deleterious effect on PGC migration at concentrations not sufficient to affect CXCR4b endocytosis.
A752	pSP6-z-nonvis arrestin-3 284-408 3'UTR-nos1	Zebrafish dominant negative nonvisual arrestin-3 (a protein fragment aa284-408) used to suppress internalization in PGCs. Has a general deleterious effect on PGC migration at concentrations not sufficient to affect CXCR4b endocytosis.
Other plasmids used in this work		
40	pCS2+	Expression vector for DNA driven by the simian CMV IE94 enhancer/promoter and for RNA transcription from SP6 (sense) or T7, T3 (antisense)
355	pSP6-GFP-nos1 3'UTR	GFP fused to nos1 3'UTR for expression of GFP in the PGCs specifically
363	Supergerm Red	N-terminal Vasa protein fragment sufficient

		for localization to germ granules fused to DsRed, RNA stabilized in PGCs by nanos 3'UTR; efficiently labeling of PGCs in red
651	pSP6-nanos1-pT7	Nanos1 without 3'UTR; for antisense probe
493	pSP64 EGFP-F nos1 3'UTR	Expression of farnesylated EGFP to label membrane-localized germ cells by the nos1 3'UTR
66	taramA*	Activated TARAM-A used to convert an injected blastomere to endodermal fate in an experiment described in Figure 11 and in Experimental Procedures below.
345	Zf H1M GFP globin 3'UTR	Zebrafish histone protein used to mark endodermal cells in experiments described in Figure 6A, 6D, 6G.

Table 2. DNA constructs used in this work

6.7 Equipment

Cameras	- RT slider Spot, Diagnostic Instruments
	- Leica DC 300, Leica
	- RT SE Spot, Diagnostic Instruments
Injector	- PV830 Pneumatic PicoPump, World
	- Precision Instruments (USA)
Needle puller	PN-30 Microelectrode Puller, Science Products
PCR machines	- Cyclone 96, Peqlab, Erlangen
	- Mastercycler Personal, Eppendorf
Microscopes	- Leica MZ FLIII, Leica
	- Zeiss Axioplan 2, Zeiss
	- LSM 510 Meta, Zeiss
	- Leica confocal microscope DMRXE
	- Olympus SZX12
Centrifuges	- Eppendorf 5415D, Eppendorf
	- Centrifuge Biofuge primo R, Heraeus
Spectrophotometer	- Eppendorf 6131, Eppendorf
water bath WB-7	- Memert GmbH
pH-meter MP220	- Mettler Toledo
Electroporation MicroPulser	- Bio Rad
Gel chambers ComPhor L Mini, Midi	- Bioplastics BV

Power supply EC105	- E-C Apparatus Corporation
Cooling block Thermomixer comfort	- Eppendorf
Fish incubator BK600	- Heraeus, Kendro
Bacteria incubator Type 3031	- GFL
Microtome	- Leica

6.8 Programs, Databases

Image processing	Adobe Photoshop 7.0, Adobe
Microscopy	Metamorph, Universal Imaging Corp.
	Leica confocal software, Leica
	LSM 510 Meta, Zeiss
Cloning	Vector NTI, Invitrogen (USA)
Office application	Microsoft
Literature	PubMed www.ncbi.nln.nih.gov
Databases	Endnote 8.0, Thomson
	FileMaker Pro 7, FileMaker Inc.
BLAST-programs	www.ncbi.nlm.nih.gov
	- blastn
	- blastp
	- tblastn
1/2/3D protein analysis	ExPASy Proteomics Server
	www.expasy.org
Multiple sequence alignment	AlignX, InforMax

6.9 Molecular Biology – general protocols

6.9.1 RNA extraction and cDNA synthesis

RNA extraction from zebrafish embryos:

About 50 embryos were grown to a certain stage of development, transferred into 200 mL Trizol reagent (Gibco BRL-Life Technologies) and homogenized with a glass-teflon pistil. Following homogenization, 800 mL Trizol reagent were added then the cell suspension was centrifuged (12 min, 12000 rpm, 4°C) to further process the liquid phase and to discard the pellet. Next, the liquid phase was incubated at RT for about 5 min to dissociate associated proteins on the RNA. 200 mL of chloroform was added, shacked and incubated for about 2

min at RT followed by spinning (15 min, 12000 rpm, 4°C). The upper (aqueous phase including the RNA) was transferred into a new Eppendorf-tube and 500 mL iso-propyl alcohol was added before shacking and spinning (10 min, 12000 rpm, 4°C). The supernatant was discarded and the residual RNA pellet was washed with 1 mL 75% ethanol/water before spinning again (5 min, 7000 rpm, 4°C). The ethanol was removed, the pellet got air-dried and finally the RNA was dissolved in 20 mL HEPES solution (10mM, pH 7.4).

First-strand cDNA synthesis (reverse-transcription):

1. Thaw template RNA on ice.
2. Thaw the primer solutions, 10x Buffer RT, dNTP Mix, and RNase-free water at room temperature
3. Prepare a fresh master mix on ice according to bellow's Table 1.
   Note: The protocol is optimized for use with 50 ng to 2 mg RNA.
4. Add template RNA to the individual tubes containing the master mix.
5. Incubate for 60 min at 37°C.
6. Store the cDNA at -20°C (can be used directly for amplifications by PCR)

Master mix (standard example):

Component	**Vol/Reaction**	**Final Concentration**
10x Buffer RT	2 mL	1x
dNTP Mix (5 mM each dNTP)	2 mL	0.5 mM each dNTP
Oligo-dT primer (10 mM)	2 mL	1 mM
RNase inhibitor (10 units/ML)	1 mL	10 units (per 20 mL reaction)
Omniscript Reverse Transcriptase	1 mL	4 units (per 20 mL reaction)
RNase-free water	Variable	
Template RNA,	Variable	Up to 2 mg (per 20 mL reaction)
Total volume	**20 mL**	

Table 3. Reverse-Transcription Reaction Components

6.9.2 Polymerase chain reaction (PCR)

Any primer, which was used for PCR amplification and sequencing was produced by the following manufacturers; IBA (Göttingen, Germany), MWG (Ebersberg, Germany) and VBC-Genomics (Vienna, Austria).

Three different PCR conditions, respectively DNA polymerases were used; Taq-Polymerase (Invitrogen), HF-Polymerase (Clontech), Phusion-Polymerase (Finnzymes). The Taq- and HF-polymerase provide the PCR product with adenine overhangs whereas the Phusion-Polymerase give rise to blunt-ended DNA strands. Standard PCR mixture and a standard PCR program are shown in the following two Tables (A, B correspond to different DNA templates and 1, 2 and 3 depict different DNA polymerases).

Component	**Conc.**	**Volume**
Template: [(A)]Plasmid-DNA [(B)]cDNA	50 ng/ Reaction	1 mL
Primer1	10 mM	1 mL
Primer 2	10 mM	1 mL
[(1, 2)] dNTPs	2.5 mM	1.5 mL
[(1, 2)] PCR buffer	10x	2 mL
[(1)]Taq [(2)]HF [(3)]Phusion	5U/mL, 5U/mL, 2U/mL	0.5 – 1 mL 7mL
dH2O		10 – 13 mL
Total		**20 mL**

Table 4. PCR reaction mix

Temp	**Time**	**Cycles**
[(1)]94 - [(2,3)]98°C	[(A)]2 - [(B)]10 min	1x
94 - 98°C	20-30 s	20 – 30x
50-60°C	20-30s	
[(2)]68 - [(1,3)]72°C	800-2000 bp/min	
[(2)]68 - [(1,3)]72°C	4-7 min	1x
4°C	hold	

Table 5. Standard PCR program

Step	Description	Temp.	Time
1	Excise the DNA fragment from the agarose gel with a clean, sharp scalpel.	RT	
2	Weigh the gel slice in an Eppendorf tube. Add 3 volumes of Buffer QG to 1 volume of gel (100 mg ~ 100 ml).	RT	
3	Dissolve the gel; mix by vortexing the tube every 2–3 min during the incubation.	50°C	10 min
4	After the gel slice has dissolved completely, add 1 gel volume of isopropanol to the sample and mix. (100 mg gel = 100 ml isopropanol)	RT	
5	To bind the DNA, apply the sample to the QIAquick column, which was inserted into a provided 2 mL collection tube, wait 5 min and centrifuge (13000 rpm).	RT	1 min
6	Discard the flow-through and place the QIAquick column back in the same collection tube.	RT	
7	To wash, add 750 mL of Buffer PE to the QIAquick column, wait 5 min and centrifuge (13000 rpm).	RT	1 min
8	Discard the flow-through and place the QIAquick column back in the same collection tube and centrifuge again to remove residual PE traces (13000 rpm).	RT	2 min
9	Place the QIAquick column into a clean 1.5 mL Eppendorf tube.	RT	
10	To elute DNA, add 30 - 50 mL of Buffer EB (10 mM Tris·Cl, pH 8.5) to the center of the QIAquick membrane, wait for 1 – 5 min and centrifuge the column (13000 rpm).	RT	1.5 min

Table 6. DNA extraction from agarose gels

6.9.3 DNA separation on agarose gels

TAE Agarose Gel (standard example):

2,5 g SeaKem LE-Agarose (Biozyme) was dissolved in 250 mL TAE agarose running buffer by heating in a microwave. The agarose solution was cooled down to about 40 - 50°C before 15 mL of a 1% Ethidium-bromide solution (Merck) was added before the viscous mixture was poured into the sledge of a ComPhor Gel chamber. Combs of different sizes (vary in loading volume) are provided by the supplier. After the agarose gel polymerized, the chamber was filled with TAE running buffer until the gel was covered by a 3-5 mm. DNA got supplemented

with 6x blue loading dye (Fermentas) and loaded into the slots of the gel. To compare the sizes of the loaded DNA fragments, a 'DNA ladder' (Fermentas; lDNA-EcoRI/HindIII, 100 bp, 1 kb) was loaded into an empty slot next to the DNA samples. The power-supply was used between 50-120 milliamps to run the DNA through the agarose gel.

6.9.4 Enzymatic DNA digestions and modifications for cloning purposes

Restriction enzyme digest:

Enzymes were provided by NEB (New England Biolabs, Frankfurt, Germany) and Fermentas (St. Leon-Rot, Germany).

Component	**Concentration**	**Volume**
Sample: (1) Plasmid-DNA (2) PCR product	2-5 μg/Reaction	1 - 5 μL
Reaction buffer	10x	10 μL
BSA (optional)	100x	1 μL
Enzyme	5-20 U/μL	1 - 2 μL per enzyme
dH2O		82 μL
Total		**100 μL**

Table 7. Restriction Enzyme reaction mix

Duration: 1-3 hours depending on the amount of DNA and the enzyme especially about the enzyme activity. The reactions were incubated at 25°C, 37°C or 50°C corresponding to the optimal activity of the used enzymes. Most of the restriction enzymes can be heat inactivated at 65 - 80°C for 10 – 20 min. Digested DNA was purified by using the PCR-Purification Kit from Qiagen.

CIAP (Calf Intestine Alkaline Phosphatase, Fermentas):

CIAP catalyzes the release of 5'- and 3'-phosphates from DNA, RNA, NTPs, dNTPs, and proteins.

Component	**Concentration**	**Volume**
Sample: (1) linearized Plasmid-	2-5 μg/Reaction	30 μL

DNA (2) PCR product		
CIP reaction buffer	10x	4 µL
CIP enzyme	10 U/µL	1 µL
dH2O		5 µL
Total		**40 µL**

Table 8. Standard CIAP reaction mix

Duration: 30 min incubation at 37°C and heat inactivated at 85°C. Modified DNA was purified by using the PCR-Purification Kit from Qiagen.

T4 PNK (T4 Phosphonucleotide Kinase, NEB)

T4 PNK adds phosphate to the 5'-carboxyl terminus of polynucleotides. It is used to allow subsequents ligation of otherwise non-phosphorylated DNA fragments.

Component	**Concentration**	**Volume**
Sample: (1) linearized Plasmid-DNA (2) PCR product	2-5 µg/Reaction	30 µL
T4 PNK reaction buffer	10x	4 µL
T4 PNK enzyme	10 U/µL	1 µL
dH2O		5 µL
Total		**40 µL**

Table 9. Standard T4 PNK reaction mix

Duration: 30 min incubation at 37°C and heat inactivated at 65°C for 20 min. Modified DNA was purified by using the PCR-Purification Kit from Qiagen.

6.9.5 Purification of linearized DNA or PCR products

Step	**Description**	**Temp.**	**Time**
1	Add 5 volumes of Buffer PB to 1 volume of the PCR sample	RT	

	and mix.		
2	Place a QIAquick spin column in a provided 2 mL collection tube and apply the DNA on the column. Bind the DNA by centrifugation (13000 rpm).	RT	1 min
3	Discard the flow-through and place the QIAquick column back in the same collection tube.	RT	
4	To wash, add 750 μL of Buffer PE to the QIAquick column, wait 5 min and centrifuge (13000 rpm).	RT	1 min
5	Discard the flow-through and place the QIAquick column back in the same collection tube and centrifuge again to remove residual PE traces (13000 rpm).	RT	2 min
6	Place the QIAquick column into a clean 1.5 mL Eppendorf tube.	RT	
7	To elute DNA, add 30 - 50 μL of Buffer EB (10 mM Tris·Cl, pH 8.5) to the center of the QIAquick membrane, wait for 1 – 5 min and centrifuge the column (13000 rpm).	RT	1.5 min

Table 10. Purification of linearized DNA or PCR products

6.9.6 DNA ligation reaction

Component	**Concentration**	
Vector DNA	100 ng/μL	1 μL
Insert DNA	100 ng/μL	3 μL
T4-ligation buffer	5x	2 μL
dH2O		3.5 μL
T4-DNA Ligase (Invitrogen)	1U/μL	0.5 μL
Total		**10 μL**
Duration: 1-3 hours at RT or o/n at 15°C		

Table 11. T4-Ligase reaction mix

Components	Concentration	Volume
PCR product	100 ng/μL	2 μL
Salt solution	1:4 dilution	0.5 μL
TOPO-system mix (Invitrogen)		0.5 μL
Total		**3 μL**
Duration: 20 min at RT		

Table 12. TOPO Ligation mix

6.9.7 Competent Cells

A single colony of *E.coli* cells was inoculated in 10-15mL LB-medium (+Tetracycline in the medium for the TOP 10 F' cells) and grown over night (o/n), shaking (200 rpm) at 37°C.
10 mL o/n grown bacteria were inoculated in 1 L of pre-warmed (37°C) LB-medium and grown at 37°C, shaking 250 - 300 rpm, to an OD_{600} of = 0.5 - 0.6. The OD was measured by using a spectrophotometer at 600 nm (simply LB-medium was used for the blank-value). The cells got chilled on ice for 10 to 15min and transferred to pre-chilled 0.5 L centrifuge bottles (cells were kept at 2°C for all subsequent steps).

Afterwards, the cells were centrifuged for 15 min at 5000g. The supernatant was poured off and the cells got re-suspended in 5 mL of pre-cooled fresh water, then the centrifuge bottles got filled up to 1 L before the centrifuge step above was repeated. The supernatant got immediately discharged following re-suspension of the pellet in 5 mL cold fresh water, then the centrifuge bottles got filled up to 500 mL before the centrifuge step above was repeated once more. The supernatant got decanted following the addition of 15 mL 10% cold glycerol and transferred into two 50 mL falcon-tubes to centrifuge again as mentioned before. The supernatant got discharged and the pellet was re-suspended in 2.5 – 3 mL 10% glycerol. 40 – 50 µL aliquots of the competent cells were immediately thrown into a bucket with liquid nitrogen and frozen at -80°C.

6.9.8 DNA transformation into bacteria strains (electro-competent cells)

Step	Description	Temp.	Time
1	Thaw competent cells on ice. (one tube contains about 40-50 μL)	4°C	

2	Add 2 µL of pCR-TOPO-ligation or 2 – 4 µL of T4-ligation to the competent cells and mix thoroughly with a pipette tip.	4°C	
3	Transfer the cell suspension including the DNA-ligation to a electroporation cuvette and transform the cells by using the MicroPulser of BioRad (Program EC2)		
4	Add 300 µL of LB-bacteria medium to the cells and transfer everything into a pre-cooled Eppendorf tube.	4°C	
5	Store the tube including the transformed cells on ice.	4°C	2 min
6	Incubate the cells before plating.	37°C	30-60 min
7	50 – 100 µL of the total 300 µL got plated on a LB-bacteria plate supplemented with Ampicillin (Ampicillin stock 100 mg/mL => final conc. 1000x diluted)	37°C	o/n

Table 13. DNA transformation into bacteria strains (electro-competent cells)

6.9.10 Bacteria mini-culture and plasmid DNA isolation

Single colonies of *E.coli* cells were picked with sterile pipette-tips were inoculated in LB-medium (Luria-Bertani medium) supplemented with Ampicillin 100 µg/mL (2-3mL for mini, 50-100 mL for midi) and grown over night (o/n), shaking (200 rpm) at 37°C.

Protocol (Plasmid DNA Purification Using the QIAprep Spin Miniprep Midiprep Kit and a Microcentrifuge, according to Qiagen):

Miniprep protocol is marked in red and the Midiprep protocol in blue. Step 1-4 are common for both applications.

Step	Description	Temp.	Time
1	Transfer the bacteria culture in Eppendorf-tubes/Falcon-Tubes and centrifuge the bacteria culture at 5000 rpm/4000 rpm and discard the supernatant.	RT	5-10 min
2	Resuspend the pelleted bacterial cells in 250 µL/6 mL Buffer P1 (includes RNase A) by vortexing.	RT	1-2 min
3	Add 250 µL/6 mL Buffer P2 and mix thoroughly by inverting the tube 4–6 times.	RT	max. 5 min
4	Add 350 µL/6 mL chilled Buffer N3/P3 and mix immediately and thoroughly by inverting the tube	RT	5 min

	4–6 times. Incubate the reaction.		
5	Centrifuge at 13,000 rpm.	RT	10 min
6	To bind the DNA, apply the supernatants from step 5 to the QIAprep spin column by decanting or pipetting and let the column soak.	RT	5 min
7	Centrifuge at max. speed and discard the flow-through.	RT	30–60 s
8	Wash QIAprep spin column by adding 750 μL Buffer PE, wait 5 min and centrifuging at max speed.	RT	30–60 s.
9	Discard the flow-through, and centrifuge again to remove residual wash buffer.	RT	2 min
10	Place the QIAprep column in a clean 1.5 mL Eppendorf-tube. To elute DNA, add 50 μL Buffer EB (10 mM Tris·Cl, pH 8.5) to the center of the QIAprep spin column, let stand for 5 min, and centrifuge (13000 rpm).	RT	2 min
5	Pour the lysate into the barrel of the QIAfilter Cartridge and incubate. Do not insert the plunger!	RT	10 min
6	Equilibrate a HiSpeed Midi Tip by applying 4 mL QBT Buffer and allow the column to empty by gravity flow.	RT	
7	Insert the plunger into the QIAfilter Cartridge and filter the cell lysate into the previously equilibrated HiSpeed Tip. Allow the cleared lysate to enter the resin by gravity flow.	RT	
8	Wash the HiSpeed Midi Tip with 20 mL Buffer QC. Allow Buffer QC to move through the HiSpeed Tip by gravity flow.	RT	
9	Elute DNA with 5 ml Buffer QF. Collect the eluate in a tube with a minimum capacity of 10 mL.	RT	
10	Precipitate DNA by adding 3.5 mL (0.7 volumes) roomtemperature isopropanol to the eluted DNA. Mix and incubate.	RT	5 min
11	During the incubation, attach a 20 mL syringe to the QIAprecipitator Midi Module.	RT	
12	Transfer the eluate/isopropanol mixture into the 20 mL syringe and filter the mixture through the QIAprecipitator using constant pressure.	RT	
13	Add 2 mL 70% ethanol to the syringe and wash the DNA by	RT	

	pressing the ethanol through the QIAprecipitator using constant pressure.		
14	Dry the membrane by pressing air through the QIAprecipitator quickly and forcefully. Repeat this step.	RT	
15	To elute the DNA, add 200 - 400 µL of Buffer EB (10 mM Tris·Cl, pH 8.5) to syringe/QIAprecipitator, and collect the DNA in a 1.5 mL Eppendorf-tube.	RT	1.5 min

Table 14. Plasmid DNA Purification Using the QIAprep Spin Miniprep Midiprep Kit and a Microcentrifuge, according to Qiagen

6.9.11 Diagnostic Restriction digest to verify plasmid DNA

Component	Concentration	Volume
Plasmid-DNA	200 – 400 ng	1 - 3 µL
Reaction buffer	10x	2 µL
BSA (optional)	100x	0.2 µL
Enzyme	5-20 U/µL	0.3 µL per enzyme
dH2O		14.5 – 16.5 µL
Total		**20 µL**

Table 15. Diagnostic restriction enzyme mix

6.9.12 Sequencing of plasmid DNA

Plasmids used for this work were verified by sequencing performed by Seqlab (Göttingen, Germany) and MWG (Ebersberg, Germany).

6.9.13 Sense- and anti-sense RNA production

Sense RNA:

First, purified Midi plasmid-DNA was linearized as described in chapter 6.10.5 to produce the template for sense RNA. The Message machine kit (Ambion) was used to produce capped sense RNA for injection.

1.) Set up the transcription reaction mix

Sense RNA reaction:

Component	Concentration	Volume

Linearized DNA	50 - 500 ng	1 - 3 μL
NTP mix, Cap analog	2x	5 μL
GTP (optional for long transcripts only)		1 μL
T3, T7 or SP6 buffer	10x	1 μL
dH2O		variable
T3, T7 or SP6 RNA-Polymerase	1U/□L	0.8 μL
Total		**10 μL**
Duration: 2 – 3.5 hours at 37°C		

Table 16. Sense RNA reaction mix

2.) Removal of the template

add 0,5 μL DNAseI (Ambion), mix well and incubate for 20 min at 37°C

3.) Phenol-Chloroform extraction

1) add 260 μL DEPC water (AppliChem) to the sense reaction
2) add 30 μL Ammonium Acetate Stop Solution (Message Machine Kit)
3) add 300 μL PCI (Phenol-Chloroform-Isoamylalcohol, 25: 24 : 1, pH=6,6, Ambion)
4) vortex for about 10 s, spin for 15 min at 13000 rpm at RT
5) carefully transfer the upper phase to a new Eppendorf tube and discard the lower phase.
6) add 300 μL CI (Chloroform-Isoamylalcohol, 24:1), shake vigorously and spin for 7 min at 13000 rpm at RT
7) transfer the upper phase to new Eppendorf tube
8) repeat step 5 – 7 again

4.) Precipitation

1) add equal volume of 100% Isopropanol
2) centrifuge immediately for 40 min at 13000 rpm., cool down to 4°C while spinning
3) carefully remove the supernatant
4) wash 2x with 80% EtOH
5) after the second wash, remove large drops and air dry the RNA pellet for a minimum time
6) dissolve the RNA in 20 μL HEPES (10mM, pH 7,4, DEPC water)

5.) Analysis of the RNA

- Spectrophotometer:

  dissolve 1 μL in 99 μL DEPC water, use the RNA mode of the spectrometer

- Agarose gel:

  1 μL RNA + 1μL Ambion RNA loading buffer

  heat the mixture for 3 min at 85°C, put on ice for 2 min and load the gel

Antisense RNA:

First, purified Midi plasmid-DNA was linearized as described in chapter 6.10.5 to produce the template for anti-sense RNA.

1.) Set up the anti-sense reaction mix

Anti-sense RNA reaction:

Components	**Concentration**	**Volume**
Linearized DNA	500 – 1000 ng	2 μL
Dig- or Fluo-labeled NTPs	10x	2 μL
T3, T7 or SP6 buffer	5x	4 μL
RNAse Inhibitors		1 μL
dH2O		variable
T3, T7 or SP6 RNA-Polymerase	1U/μL	2 μL
Total		**20 μL**

Table 17. Anti-sense RNA reaction mix

Preparation of the 10x NTP-Mix:

- Roche:

pre-mixed Dig-or Fluo-labeled NTP-Mixes

- Lab mix: (50 μl)

ATP (Stock: 100mM):	5 μl	final conc.= 10 mM
GTP (Stock: 100mM):	5 μl	final conc.= 10 mM
CTP (Stock: 100mM):	5 μl	final conc.= 10 mM

UTP (Stock: 100mM):	3,25 µl	final conc.= 6,5 mM
Dig- or Fluo-UTP (Stock: 10 mM):	17,5 µl	final conc.= 3,5 mM
H_2O (can be DEPC- H_2O):	14,25 µl	

2.) Removal of the template

add 1 µL of DNAse I (Ambion), mix well and incubate for 30 min at 37°C

3.) NH_4 Ac-Precipitation

1) add 11 µL of NH_4Ac (7,8 M)
2) add 63 µL of 100% EtOH
3) mix well by using the vortex and spin at 13000 rpm at RT
4) let the RNA precipitate for 30 - 50 min at RT (keep dark)
5) discard supernatant
6) wash the RNA pellet 1x with 1 mL 80% EtOH at RT
7) spin for 5 – 10 min at 13000 rpm
8) discard supernatant
9) remove big residual drops and air dry the RNA pellet for a minimum time
10) dissolve the RNA in 20 µL H_2O + 80 µL Hyb-buffer

4.) Analysis of the RNA

- Agarose gel:

  3 µL RNA + 3 µL Ambion RNA loading buffer

  heat the mixture for 3 min at 85°C, put on ice for 2 min and load the gel

6.10 Zebrafish – experimental animal model

6.10.1 Zebrafish strain and fish maintenance

Zebrafish (*Danio rerio*) of the AB and TL genetic background were maintained, raised and staged as previously described in [139] and [140] and as it is described below. *Odysseus* mutant fish [47] *Casanova* mutant fish [112] were kindly provided by C. Nusslein-Volhard**.**

6.10.2 Injection of sense RNA and dyes into the zebrafish embryo

Injection protocol:

The day before injection:

- set-up 1 L of 0.3x Danieau's solution (for pouring and overlaying the injection ramps where the embryos are placed during the injection)

- set-up fish: fill tanks with water from the fish-facility and bring one female and one male together in one tank but they have to be divided by the separation inserts (mesh).

The day of injection:

- Dilute RNA in HEPES (10 mM) to the appropriate concentration and keep on ice.
- Add Penicillin/Streptomycin (P/S) to 0.3x Danieau's solution and use it to exchange the 0.3x Danieau's solution on the ramps from the day before.
- cross the fish-couple by removing the inserts (mesh) which separates the female from the male. One mesh remains in the tank, which will keep the fish away from already laid eggs.
- after a couple laid eggs collect the clutch in a sieve and transfer the eggs in a clean Petri dish containing 1x methylene blue/egg water solution.
- collect the embryos using a pasteur pipette and transfer them into the ramps (overlayed with fresh 0.3x Danieau's solution P/S) and use the metal needle to orient the embryos in the ramps.
- cut the tip of the glass-needle off with a scalpel and load the sample into the injection-needle
- the injection itself: pierce the chorion membrane and inject RNA or dye (or a mix) into the yolk or the cell. The RNA will get into the cell by streaming from the yolk. Usually around 5 nL RNA is injected per embryo.
- after finishing the injection: get the embryos out of the ramps and transfer them (not more than 50-80 embryos) into a new clean Petri dish containing 0.3x Danieau's solution with P/S.
- transfer the embryos into the appropriate incubator (25°C, 28°C or 30°C)
- after 2-3 hours take a look at the embryos and place the fertilized into a new Petri dish with 0.3x Danieau's solution P/S. Incubate them further at 25°C - 30°C.

Progress to perform live imaging of embryos:

- chorions which surround the embryo are removed by hand (forceps) and embryos are transferred and oriented into small agarose ramps.

Table 18. Reagents/Materials for injection

30x Danieau's solution pH 7.6 (stock solution):	
Reagents	**for 1 liter**
1.74 M NaCl (MW = 58.44 g/mol)	101.7 g
21 mM KCl (MW = 74.56 g/mol)	1.57 g

12 mM $MgSO_4[7H_2O]$ (MW = 246.48 g/mol)	2.96 g
18 mM $Ca(NO_3)2[4H_2O)]$ (MW = 236.15 g/mol)	4.25 g
150 mM HEPES (MW = 238.31 g/mol)	35.75 g

Ramps:

Set them up on the day before injection! Use a Erlenmeyer flask (should not been washed with detergents) and set up 100 ml 1.5% agarose in 0.3x Danieau's solution (this agarose should only be used for this purpose) sufficient for pouring 3-4 ramps. Place the ramp template (contains 6 rows for about 50 embryos each) carefully in the center of the petridish and avoid making bubbles. Remove the ramp template carefully when the agarose becomes solid. Overlay the agarose with 0.3x Danieau's solution to prevent it from getting dried. Longer storage should be at 4˚ C with 0.3x Danieau's solution on top.

HEPES:

Stock solution:	500 mM, pH 7.4 (HEPES, sodium salt; MW = 260,28 g/mol)
Working solution for RNA injections:	10 mM HEPES, pH 7.4

Pen/Strep stock solution (penicillin and streptomycin):

Add 2 tubes of stock solution (2.5 ml each, 100x Pen/Strep concentration, final concentration 0.5x) into 1 liter of 0.3x Danieau's solution.

RNA injection:

Work was done always on ice!
Dilute RNA to a concentration of 50 - 200 ng/µL in HEPES 10mM, pH 7.4. By using concentrations over 200 ng/µL it will become more and more toxic for the embryo. Before use, centrifuge the diluted RNA at maximum speed in a conventional tabletop microcentrifuge for a minimum of 10 min.

Injection needles:

To inject the RNA/DNA into the embryos one has to prepare injection needles with the needle puller. Use a sharp scalpel to cut off the tip of the needle.

Generation of needles with an almost defined opening-width:

- cut the tip of the needle
- put a drop (20-50 µl) DEPC-water into a clean small petridish

- place the needle into the needle holder of the micromanipulator
- adjust pressure of the pneumatic picopump to 15 to 20 psi
- place the tip of the needle in the waterdrop
- the psi value at which air-bubbles will just leave the needle gives you an approximate estimation of the opening of the needle
  for example: is it a value around 15 psi the opening is wider than it is the case at a value around 20
  Choose a value, which is appropriate for your experiment.

Methylene blue solution and egg water (blue water):

salt/water solution containing methylene blue (prevents contamination with fungi)

- stock solution of methylene blue:
  add 1 g methylene blue to 1 liter reverse osmosis water
- 4x methylene blue/egg water solution:
  add 20 ml of methylene stock solution to 10 liter egg water
- 1x methylene blue/egg water ready-to-use solution:
  add 250 ml 4x methylene blue solution to 750 ml egg water

6.10.3 Fixation of embryos

For in situ hybridization:

- Embryos 24 hpf and older: chorion was removed by using forceps before fixation. Fixation overnight at 4°C in 4% PFA in PBS.
- Embryos younger than 1-2 somite stage were fixed for 2 days.
  After fixation the embryos were rinsed 2-3 times in PBT and the chorion was removed by using forceps.
- Embryos got transferred to 100% MeOH by passing them through a gradient of MeOH/PBT; 25%, 50%, 75% and 100%.
- Embryos were stored in 100% MeOH at –20°C for several weeks or months.

For immunohistochemistry:

- chorion was removed with forceps before fixation. Embryos were transferred in pre-warmed (RT) PFA (4%) in PBS and fixed for 2-3 h at RT.

6.10.4 *In situ* RNA hybridization of whole mount zebrafish embryos

One- and two-colour whole-mount in situ hybridization was performed as described previously [141] with modifications described elsewhere [142] and [45]. To perform double staining *in situ* hybridization with a mix of different Dig- and Fluo-labeled probes, the antibody- and

subsequent staining-steps are performed individually because both antibodies are coupled to the same enzyme (alkaline phosphatase). This enzyme was used with different dye combinations, here we used X-phosphate/NBT (blue) and X-phosphate/INT (red). Doing the blue staining as a first step has the advantage that the embryos can be cleared in EtOH (reduces dark background in the yolk) before the second antibody application.

In situ Day 1:

Step	Description	Temp.	Time
1	Rehydration 75% MetOH - 25% PBT	RT	5 min
2	Rehydration 50% MetOH - 50% PBT	RT	5 min
3	Rehydration 25% MetOH - 75% PBT	RT	5 min
4	Rehydration 100% PBT	RT	4x5 min
5	Proteinase K (5 µg/ml in PBT): - before shield: no treatment - shield - bud: 0 - 30 sec - 1 somite: 30 - 60 sec - 5 somite: 3 - 4 min - 24 hpf embryo: 4 - 5 min - 36 -72 hpf embryo: 10 - 20 min with 10µg/ml	RT	
6	PBT	RT	10 s
7	PBT	RT	10 s
8	PBT	RT	1 min
9	PBT	RT	5 min
10	Refixation in 4% PFA in PBS	RT	20 min
11	Wash in PBT	RT	5x5min
12	Prehybridization: incubate in 200 □L of Hyb-buffer	67°C	2 – 5 h
13	Hybridization: 0,5 µL – 3 µL of antisense probe in 200 µl of Hyb-buffer to replace the prehybridization. *Heat the hybridization mix to 67°C (water bath) for about 10 min.*	67°C	12 h

Table 19. RNA *in situ* hybridization – Day 1

Solutions:

PBS 10x for 1L

- 80 g NaCl
- 2 g KCl
- 18 g Na_2HPO_4 (2 H_2O)
- 2,4 g KH_2PO_4
- adjust to pH 7,2

PBT 1x for 1L

- 100 ml 10x PBS
- 900 ml H_2O
- adjust to pH 7,4 (by adding 15% HCl)
- add 10 ml 10% Tween20

SSC 20x for 8L

- 1400 g NaCl
- 704 g Trisodium Citrate[$2H_2O$]
- adjust to pH 7,0 (by adding 15% HCl)

Hyb-buffer for 1L

- 250 ml 20x SSC
- 500 mg tRNA* (Sigma)
- 50 mg Heparin (Sigma)
- 10 ml 10% Tween20 (Sigma)
- 1,89 g Citric Acid (Monohydrate) to pH 6,0 – 6,5
- H_2O to 500 mL
- last: add 500 mL deionized formamide
- store at –20°C

* Rnase free tRNA: torula yeast RNA (Sigma R6625)

- 500 mg tRNA in 20 mL 10x SSC extracted with Phenol/Chloroform – Chloroform/Isoamylalcohol (see protocol for purifying sense or antisense RNA)
- after 2x wash with 80% EtOH, air dry and resuspend in 5 mL 10x SSC

In situ Day 2:

- Recover the probes!
- Always preheat the washing solutions to hybridization temperature!

Step	Description	Temp.	Time
1	Wash with Hyb-buffer	67°C	20 min

2	Wash with 50% SSCT 2x / 50% Formamide	67°C	3x20 min
3	Wash with 75% SSCT 2 x / 25% Formamide	67°C	20 min
4	Wash with SSCT 2x	67°C	2x20 min
5	Wash with SSCT 0.2x	67°C	4x30 min
6	PBT	67°C	5 min
7	Blocking: 5% sheep serum + 10 mg/ml BSA in PBT *Slow agitation and keep dark*	RT	> 1 h
8	Antibody-incubation I: Incubate in 100 - 200 µL antibody solution. *Antiserum pre-absorbed against embryos, 1:2000- 1:4000 in PBT + 2 mg/mL BSA (optional: +2% sheep serum). For storage at 4°C: add Sodium Azide to 0,02%*	4°C	14 h

Table 20. RNA *in situ* hybridization – Day 2

In situ Day 3:
- Recover the antibody!

Step	**Description**	**Temp.**	**Time**
1	Wash with PBT with slow agitation, dark	RT	2x5 min
2	Wash with PBT with slow agitation, dark	RT	8x20 min
3	Wash with NTMT buffer	RT	3x5 min
5	Transfer embryos to a 24 well plate		
6	Staining reaction: add 500 µL of BCIP/NBT mix *Staining at 4°C overnight is also possible.*	37°C	
7	Stop the reaction: removing of the staining solution and wash in Stop-Solution	RT	3x1min
8	Removal of the first antibody: add 0,1 M Glycin/HCl, pH 2.2 + 0.1% Tween20, *shake well*	RT	2x5 min
9	Wash with PBT with slow agitation, dark	RT	4x5 min
10	Clearing (optional): incubate embryos in 100% EtOH with slow agitation *This step cannot be performed after the red staining reaction.*	RT	2x10 min

	(The red stain dissolves in ETOH very fast.)		
11	75% EtOH / 25% PBT	RT	5 min
12	50% EtOH /50% PBT	RT	5 min
13	25% EtOH / 75% PBT	RT	5 min
14	PBT	RT	4x5min
15	Antibody-incubation II: Incubate in 100 - 200 µL antibody solution. No additional blocking step is required prior to the second antibody incubation. *Antiserum pre-absorbed against embryos, 1:2000- 1:4000 in PBT + 2 mg/mL BSA (optional: +2% sheep serum). For storage at 4°C: add Sodium Azide to 0,02%*	4°C	14 h

Table 21. RNA *in situ* hybridization – Day 3

Solutions:

NTMT staining buffer for 20 mL

- 2 mL Tris HCl pH 9.5, 1M
- 1 mL $MgCl_2$, 1M
- 2 mL NaCl, 1M
- 200 µL 10% Tween20
- add 14.8 mL H_20

Staining solution BCIP/NBT (blue staining):

- 4.5 µL NBT (Nitro Blue Tetrazolium, Sigma; 75 mg/mL in 70% DMF / 30% H_2O)
- 3,5 µL X-phosphate (=BCIP) (50 mg/mL in 100% DMF)
- 1 mL NTMT buffer

Stop-Solution

- 0.05M phosphate buffer pH 5.8
- 1mM EDTA
- 0.1% Tween20

for 200mL: 92mL 0.1M NaH2PO4
8mL 0.1M Na2HPO4
(this mixture should produce a pH of 5.8)

0,1 M Glycin HCl, pH 2,2 + 0,1% Tween20 (for 500 mL):

- 3,75 g Glycin
- add H_2O to 400 mL
- adjust to pH 2,2

- fill to 500 mL with H_2O
- add 5 ml 10% Tween20

In situ Day 4:

- Recover the antibody!

Step	Description	Temp.	Time
1	Wash with PBT with slow agitation, dark	RT	2x5 min
2	Wash with PBT with slow agitation, dark	RT	8x20 min
3	Wash with NTMT buffer	RT	3x5 min
5	Transfer embryos to a 24 well plate		
6	Staining reaction: add 500 µL of BCIP/INT mix *Staining at 4°C overnight is also possible.*	37°C	
7	Stop the reaction: removing of the staining solution and wash in Stop-Solution	RT	3x1min
8	Transfer embryos to 6-well plates in 80% Glycerol – 20% Stop-Solution.	RT	

Table 22. RNA *in situ* hybridization – Day 4

Staining solution BCIP/INT (red staining):

- 3,5 µL INT (Iodonitrotetrazolium violet, Sigma; 50 mg/mL in DMSO)
- 3,5 µL X-phosphate (=BCIP) (50 mg/mL in 100% DMF)
- 1 mL NTMT buffer

6.10.5 Immunochemistry of whole mount embryos

After whole mount in situ hybridization, specimens were blocked with calf serum and DMSO. Endoderm was fluorescently labeled as described below and then visualized using anti-GFP polyclonal rabbit antibody (P7) and secondary anti-rabbit (S7) antibody with DAB staining.

Below is the general protocol for immunostaining of whole mount zebrafish embryos. We used this protocol for post *in situ* embryos skipping the first day and starting with the steps of the Day 2.

Step	Description	Temperature	Time
Day 1			
1	Obtain fertilized eggs in the morning		

2	Manually dechorionate embryos at some point prior to fixation		
3	Fix embryos in 4% PFA in PBS	4ºC or RT	o/n 1-5 h
Day 2			
1	Wash in PBS	RT	2 x 5 min
2	Wash in distilled water		5 min
3	Incubate in pre-cooled acetone	-20ºC	2 min
4	Wash in distilled water	RT	5 min
5	Wash in PBS		5 min
6	Transfer into blocking solution*		30' or more
7	Add fresh blocking solution containing antiserum at appropriate dilution	4ºC or RT	8 h o/n
Day 3			
1	Wash with blocking solution	RT	4 x 20 min or more
2	Prepare dilution of secondary antibody in blocking solution. Add to embryos.		4h or more
3	Wash with blocking solution each one at least 20'		4 x 20 min or more
4	Prepare peroxidase staining solution (DAB**) (without H_2O_2). Preincubate.		10 min
5	Stain in peroxidase solution with H_2O_2 until cells are labelled		usually 15 min

Table 23. Protocol for antibody staining of whole zebrafish embryos and DAB staining

Solutions:

***blocking solution**:

20% calf serum, 1% DMSO, 0.1% Tween-20 in PBS

(for 25ml: 5ml calf serum, 250μl DMSO, 25μl Tween20)

****DAB** is a carcinogen. Wear gloves. Work on safety paper. Discard all washes in bleach and soak all tubes, pipette tips, etc in bleach before rinsing and discarding.

DAB: 30mg in 100ml PBS (0.03% w/v). Add 1μl of 1/10 diluted H_2O_2 to 200μl DAB solution

6.10.6 Histology: paraffin sections and Eosin staining

We fixed embryos at the stage of 75% epiboly in 4% paraformaldehyde for 24 h. After whole mount in situ hybridization, dehydration in ethanol, and clearing in toluene, the specimens were infiltrated with paraffin, embedded, and sectioned using Microtome (Leica). The sections were stained with eosin and visualized by using an Axioplan2 microscope.

Wild-type, *cas*, and *ody* embryos were fixed for 24h in 4% PFA at 4°C washed 3x with PBS and dehydrated in increasing ethanol solutions:

3x 50% EtOH for 1h
3x 70% EtOH for 1h
3x 90% EtOH for 1h
3x 100% EtOH for 1h

and then cleared in 100% toluene for 1h.
The dehydrated embryos were infiltrated with hot paraffin for several hours, embedded in paraffin blocks and sectioned on a microtome. The sections (8 µm thick) were transferred onto superfrost objective slides, dried for 1h at 40°C and then at 37° o/n.
The paraffin from the slides was removed by dipping them 2x 100% Xylol for 2'. The tissue was rehydrated in decreasing ethanol solutions:

2x100% EtOH for 2'
2x90% EtOH for 2 min
2x75% EtOH for 2 min
2x50% EtOH for 2 min
and 2x in water for 2 min each step.

Cytoplasmic staining (Pink):

The sections were incubated 2x in water for 2 min and stained in Eosin solution for 2-6 min, washed briefly in water 2x and dehydrated by dipping them in reverse order in the above EtOH solutions for about 20 sec and incubating them 2x in 100% Xylol for 2 min each step. Finally the sections were dried and mounted with Eukitt (Kindler).

6.10.7 Generation of CXCR4, CXCR4 mutants and other constructs

Different mutant versions of CXCR4b and human CXCR4 were generated by PCR. Truncation and deletion mutations were introduced by amplification of CXCR4 ORF excluding the region of truncation or deletion correspondingly. Point mutations were obtained by PCR using partially complementary oligonucleotides that contain those mutations.

Human CXCR4 N-terminally tagged with HA was amplified from a construct kindly provided by Jeffrey Benovic and cloned into pcDNA3.1(-) plasmid (Clontech). Below the cloning procedures and the primers for PCR are listed.

Wild type CXCR4b was amplified using oligonucleotides AAAGGATCCGAACAAAATGGAATTT and TTTGGATCCCCACTCGTCAGTGCACTGGACGAC cut with BamHI and inserted in-frame with *egfp* into pSP64 vector containing *egfp-nos1*-3'UTR which resulted in a plasmid wt CXCR4b-*egfp-nos1*-3'UTR.

CXCR4b truncation mutants were amplified from the wt CXCR4b-*egfp-nos1*-3'UTR plasmid, then cut with BamHI, and inserted into pSP64 vector as substitutes for wt CXCR4 (cut out with BamHI) in-frame with *egfp*. The following reverse primers were used: GGATCCCCAGCAGCAGCGAACCTGAC (for the construct (1), Figure 12); GGGATCCCCTATAGGCCCCCTTTTCTTGGTCA (for the construct (2), Figure 12); AAAGGATCCCCCTCTGATTCAGTAGATAC (for the construct (3), Figure 12).

To generate the truncation mutant (9) (Figure 12), the same oligonucleotides as for the construct (3) were used. The construct (8) (see below) was used as a template for the amplification reaction in this case.

CXCR4b deletions were amplified from the wt CXCR4b-*egfp-nos1*-3'UTR construct into two pieces excluding the region of the deletion with oligonucleotides that had an overlapping overhang. The second piece would start after the region of deletion and end in the *nos1*-3'UTR of the plasmid (the reverse oligonucleotide: TCTAGAGAAAATGTTTATATTTTCC). These two pieces were consequently fused by amplification with the forward primer of the first piece and the reverse primer of the second piece. Then they were amplified with the primers used for amplification of wt CXCR4b (see above), cut with BamHI and inserted in-frame with *egfp* into pSP64 vector containing *egfp-nos1*-3'UTR. The following pairs of oligonucleotides flanking the region of deletion were used:
TATAGGCCCCCTTTTCTTGGTC and AGGGGGCCTATATCGTCCAGTGCACTGACGAGT (for the construct (5), Figure 12);
GAACCTGACGCCTAGGAAAGCA and GGCGTCAGGTTCTCATCTGTATCTACTGAAT (for the construct (7), Figure 12)

To generate the deletion mutant (10) (Figure 12), the same oligonucleotides as for the construct (5) were used. The construct (8) (see below) was used as a template for the amplification reactions.

CXCR4b serine mutants were constructed by oligonucleotide-directed polymerase chain reaction mutagenesis. In order to work with primers not exceeding the length of 40nt, serine-to-alanine mutations were introduced in several steps for both plasmids #6 and #8. For each step there was a pair of complementary oligonucleotides containing mutations of certain region. Two pieces would be amplified in each step, then fused by co-amplification and used for the next step. The second piece would start with the region of mutations and end in the *nos1*-3'UTR of the plasmid (the reverse oligonucleotide: TCTAGAGAAAATGTTTATATTTTCC).The final amplicon that contained all planned mutations would be cut with BamHI and inserted in-frame with *egfp* into pSP64 vector containing *egfp-nos1*-3'UTR. The following pairs of mutagenic oligonucleotides were used:
To generate the construct (6) the following oligonucleotides were used:
Step 1:
CAGTAGATACAGCTGCTATAGGCCCCC and GGGGGCCTATAGCAGCTGTATCTACTG;
Step 2:
GGACGACTCTGCTTCAGTAGCTACAG and CTGTAGCTACTGAAGCAGAGTCGTCC;
Step 3:
CGTCAGTGCAGCGGCCGCCTCTGC and GCAGAGGCGGCCGCTGCACTGACG.
To generate the construct (8) the following oligonucleotides were used:
Step1:
ACGGGCAGCTTTAGCGAACCT and AGGTTCGCTAAAGCTGCCCGT;
Step 2:
TTGTGAGCGGCTCTAGCGGCGATGGCCAGAG and CTCTGGCCATCGCCGCTAGAGCCGCTCACAA.

As mentioned above constructs (9) and (10) were generated by PCR using construct (8) as a template and the oligos used to generate constructs (3) and (5) correspondingly.

Human HA-tagged CXCR4 was amplified with oligonucleotides AATCTAGAATGGCTTACCCGTATGACGT and AAAAAGCTTTTAGCTGGAGTGAAAACTTG, cut with XbaI and HindIII and inserted into pcDNA3.1(-) plasmid (Clontech).

To produce construct (11) in Figure 12 the serine-to-alanine mutations were introduced into wild-type human CXCR4 at positions 338, 339, 341, 344, 346, 347, 348 by oligonucleotide-directed polymerase chain reaction mutagenesis using oligonucleotides containing the mutations and partially complementary. Two pieces were amplified and then fused by co-amplification. The first piece started at ATG at the start of the HA-tagged CXCR4 molecule and ended in the region of the mutations. The second piece started at the region of mutations and ended in the SV40 promoter of the vector (reverse primer: GCTCCCGGGAGCTTTTTGCAAAAGCCTAGGCCTC). The final amplicon was cut with XbaI

and XmaI and inserted as a substitute for the wild type human HA-tagged CXCR4 in the pcDNA3.1(-) vector. The oligonucleotides used for the mutagenesis were the following: CTCAGCCTCAGTGGCAACAGCTGCATGTCCACC (reverse) and TGAGGCTGAGGCTGCAGCTTTTCACTCCAGCTAA (forward).

To generate the exchange mutant in which serine residues at positions 338 and 339 are exchanged for alanines the mutations were introduced into wild-type human CXCR4 by PCR amplification of the plasmid containing the wild-type version of CXCR4 with the following oligonucleotides:
CATGCAGCTGTTTCCACTGAGTCTGAGTCT (forward);
TCCACCTCGCTTTCCTTTGGAGAGGATC (reverse).
Then the amplicon was isolated from gel, phosphorylated with a T4-PNK (phosphonucleotide kinase) (NEB Biolabs) and ligated.

To generate the exchange mutant depicted as construct (12) in Figure 12 the serine-to-alanine mutations were introduced into wild-type human CXCR4 at positions 338, 339, 341, 344 by PCR amplification of the plasmid containing the wild-type version of CXCR4 with the following oligonucleotides:
CATGCAGCTGTTGCCACTGAGGCTGAGTCT (forward);
TCCACCTCGCTTTCCTTTGGAGAGGATC (reverse).
Then the amplicon was isolated from gel, phosphorylated with a T4-PNK (phosphonucleotide kinase) (NEB Biolabs) and ligated.

To generate the exchange mutant depicted as construct (13) in Figure 12 the serine-to-alanine mutations were introduced into wild-type human CXCR4 at positions 346, 347, 348 by PCR amplification of the plasmid containing the wild-type version of CXCR4 with the following oligonucleotides:
GAGTCTGAGGCTGCAGCTTTTCACTCC (forward)
AGTGGAAACAGATGAATGTCCACCTC (reverse).
Then the amplicon was isolated from gel, phosphorylated with a T4-PNK (phosphonucleotide kinase) (NEB Biolabs) and ligated.

Dominant negative rat dynamin-2 was amplified from a plasmid kindly provided by C-P. Heisenberg with the following oligonucleotides:
ATGGGCAACCGCGGGATGGA (forward) and CTAGTCGAGCAGGGACGGCT (reverse),
cloned into TOPOII vector, then cut with EcoRV and NotI and used as a vector in which 3'UTRnos1 flanked with identical restriction ends was inserted. To optimize transcription of this construct dominant negative Dynamin together with 3'UTRnos1 was amplified from this original plasmid with following oligos:

ACCATGGGCAACCGCGGGATG (forward oligo that contains Kozak sequence in it to improve transcription)
GGCCGCTTTTTTTTTTTTTT (reverse)
and cloned into TOPO4 vector.

To generate dominant negative caveolin-1 we used the following strategy. First the wild-type caveolin was amplified from cDNA obtained from RNA of zebrafish embryos at shield stage. This was done using the following oligonucleotides:
ATGACTAGCGGATACAAGGA (forward) and TTACACCACCTTAGTAGCAG (reverse)
Into this PCR product mutations were introduced by first amplifying two pieces overlapping in the region of the mutation. Complementary oligonucleotides carrying the mutation were the following:
CTTCACGCAAAGCACCACGGCCCAGA and TCTGGGCCGTGGTGCTTTGCGTGAAG.
Then the two pieces were merged by another PCR reaction where they were used as the templates and the following oligonucleotides flanked with restriction sites were used:
AAAGGATCCGAACAAAATGACTAGCGGATACAAGGA (forward)
AAACTCGAGACATGCACACATTACACCACCTTAGTAGCAG (reverse)
The resulting amplicon was restricted with BamHI and XhoI and inserted into pSP64 vector containing 3'UTRnos1 cut with the identical enzymes by ligation.

Dominant negative forms of nonvisual arrestins 2 and 3 were generated by PCR reaction using the following pairs of oligonucleotides:
For nonvisual arrestin-2:
AAAGGATCCGAACAAAATGGTATCTTATAAGGTGAAAGTTA (forward)
AAACTCGAGACATGCACACACTATCTGTCGTTCAATTTGGGC (reverse)
For nonvisual arrestin-3:
AAAGGATCCGAACAAAATGGAGAAGAGGGGTCTGGCTCTGG (forward)
AAACTCGAGACATGCACACATTAGCAGAAGTGGTCGTCCTCT (reverse)
Then the resulting amplicons were restricted with BamHI and XhoI and inserted into a pSP64 vector containing 3'UTRnos1 by ligation.

6.10.8 Expression of specific proteins in zebrafish embryos

To direct protein expression to the PGCs, the corresponding open reading frames (ORFs) were fused to the 3'UTR of the *nanos*1 gene, facilitating translation and stabilization of the RNA in these cells [17].
To fluorescently label PGCs, *gfp-nos*1-3'UTR RNA was injected (150 pg per embryo) [17].
For the functional analysis of different CXCR4b versions, 90 pg of RNA encoding the EGFP tagged proteins were injected into embryos homozygous for the *odysseus* mutation [47].
For ectopic expression of SDF-1a in the endoderm (Figure 1D, E), the endogenous SDF-1a was knocked down by SDF-1a-2-MO at 1-cell stage and 1 pg of activated TARAM-A that

directs blastomeres toward the endodermal fate [143] was coninjected with 20 pg of morpholino-resistant *sdf-1a* RNA (MO number 2 in [46]) and with 8 pg of *dsRed-ex1-f-globin*-3'UTR (serving as a clonal marker; [144] into a marginal blastomere of 16-cell stage embryos. Since germ cells never originate from corner blastomeres (of 16-cell blastula) we aimed to inject one of these to avoid the fate conflict.

6.10.9 Fluorescent live imaging

Epifluorescence:

Images were obtained using a Zeiss Axioplan2 microscope controlled by the Metamorph software (Universal Imaging). Low magnification time-lapse movies were generated using a 10x objective at a rate of one frame per minute. High magnification time-lapse movies were generated using a 63x or 40x objective capturing frames at 20-second or 2-minutes intervals. Speed measurements of migrating PGCs and colour-alignments were performed using the Metamorph software (Universal Imaging).

Confocal-Microscopy:

Images were obtained using a Leica TCS Confocal microscope controlled by the internal Leica software. High magnification time-lapse movies (for PGC/endoderm mutual disposition presented in Figure 6 and for calcium measurements presented in Figure 15) were generated using a 40x objective capturing frames at 20-second intervals. The laser intensity, potentiometer, gain and offset were adjusted according to the individual conditions of the experiments (fluorescent intensity based on the probe characteristics). The recorded frames of migrating germ cells were processed using the Quantity-Mode (Stack profile/Statistics) of the TCS SL confocal software provided by Leica.

6.10.10 Cell transplantation

To observe CXCR4 internalization in real-time and to track PGCs migrating towards a source of SDF-1a we transplanted cells expressing the chemokine from dome stage donor embryos (4.3 hpf) into host embryos at the 60 to 75 % epiboly stage (7 to 8 hpf). In both experiments the transplant cells were marked with dextran Alexa Fluor 568 (10,000 kDa; Molecular Probes) by injecting it into 1-cell stage donor embryos (0.15 ng per embryo). Donor embryos were also injected with 300 pg (for the internalization assay) or 60 pg (to observe internalization at low levels of SDF-1a and for cell attraction assays) of SDF-1a at the 1-cell stage. Based on comparative *in situ* hybridization experiments, the latter amount of injected *sdf-1a* RNA is similar to endogenous *sdf-1a* levels expressed in embryos and is thus considered physiological (personal communication). To follow CXCR4b internalization, host PGCs expressed CXCR4b-EGFP and the transplant was placed in the vicinity of the cells.

6.10.11 Time-Lapse Analysis and Tracking of PGC Migration

For time-lapse movie analysis, PGCs were labeled by microinjecting one-cell stage embryos with 150 pg *gfp-nanos*-1 RNA [45]. Movies and PGC migration tracks and speed were obtained using MetaMorph software (Universal Imaging). Duration of run and tumbling phases performed by PGCs were calculated by analyzing migrating cells traveling on their delineated tracks. Mean duration of individual runs and tumblings performed by *ody* or wild type cells expressing either wild type or mutant forms of CXCR4b-EGFP were compared using the T-test.

6.10.12 Measurement of calcium levels

Determination of calcium levels in migrating PGCs was performed as previously described [48]. Three groups of cells– *ody* PGCs, *ody* PGCs expressing RNA encoding the wild-type CXCR4b and *ody* PGCs expressing the internalization-defective mutant CXCR4b were compared using Tukey HSD test and all pairwise differences between the three experimental groups were found to be statistically significant ($p<0.0001$). Tukey HSD test was performed with a 95% familywise confidence level using the stats package of R software (www.r-project.org). T-test was used to compare the calcium level when different amounts of wild-type CXCR4b were expressed in wild-type PGCs and the difference was found significant ($p<0.005$).

6.11 Cell culture experiments

HEK-293 cells were cultured in DMEM (GIBCO Invitrogen) supplemented with 10% fetal-bovine serum (FBS) (GIBCO Invitrogen) in a humidified incubator with 5% CO2 at 37°C. 24 hours after being plated cells that have reached 50% confluency by that time were transfected with wild-type or mutated human CXCR4 tagged with EGFP using the Lipofectamine 2000 (Invitrogen) reagent. Transfected and starved (30 min) HEK-293 cells were incubated for 45 min at 37°C with 1mg/ml dextran Alexa Fluor 680 10000MW (Molecular Probes, Invitrogen) with or without 200 nM SDF-1 (Peprotech, London) in DMEM, washed with PBS, fixed with 4% paraformaldehyde for 30 minutes at 4°C, and imaged by confocal microscopy.

6.11.1 Cell Revival

Cells from liquid nitrogen were revived in a 37 °C water bath as quickly as possible, then transferred into a 15 ml Falcon tube containing 5 ml proper culture medium, and centrifuged at 1,000 rpm for 5 minutes. The supernatant medium was aspirated, 5 ml fresh medium was added to the cell pellet and pipetted up and down for at least 15 times to break cell aggregates. The, the cell resuspension was distributed in a 10 cm petridish containing 5 ml culture medium (10 ml in total). The dish was gently shaken left-right and backward-forward

to achieve equally distribution of cells. Then, the cells were cultured in a BBD 6220 incubator (Heraeus) at 37 °C under 5% CO_2 concentration.

6.11.2 Cell Passage and Freeze

The medium of cultured 70-95% confluent cells in a 10 cm dish was aspirated. Cells were washed with 10 ml PBS, which was then aspirated from the dish. 2.5 ml 1×Trypsin-EDTA solution (Gibco BRL) was equally distributed onto the washed cells, and incubatd at 37 °C for about 5 minutes. The dish was shaken until all the cells became floating. 5 ml culture medium with 10 % FBS was added to stop the trypsin digestion, pipetted up and down for several times to blow the cells, and then transferred into a 15 ml Falcon tube. Centrifugation was carried out at 1,000 rpm for 5 minutes to pellet the cells, followed by aspirating the supernatant.

For passage, the cell pellet was resuspended in required amount of culture medium by pipetting 15 to 20 times to break cell aggregates. Resuspension was pipetted into a 10 cm dish (for cell line maintenance) or 12-well plate (for consequent transfection) containing culture medium, gently shaken and incubated.

For freeze, the cell pellet was resuspended in 2 ml culture medium, and every 500 μl cell resuspension was transferred into a cryotube (Nunc) containing 500 μl culture medium and 10% DMSO, mixed well by inverting, and sequentially frozen at –20 °C overnight, at –80 °C for a week to a month, and finally in liquid nitrogen.

6.11.3 Cell Transfection with plasmids

Step No	Step description
1	The day before transfection, trypsinize and count the cells, plating them on 12-well plate so that they are 50% confluent on the day of transfection. Each plate should contain a 10mm round coverslip for consequent imaging. Cells are plated in their normal growth medium containing serum.
2	For each well (12-well plate) of cells to be transfected, dilute 500ng of DNA into 125L of OptiMEM (Invitrogen).
3	For each well of cells, dilute 5 µl of Lipofectamine 2000 Reagent into 125 ml of OptiMEM (Invitrogen) and incubate for 5 min at RT.
4	Once the LF2000 Reagent is diluted, combine it with the DNA and incubate at RT for 20 min to allow DNA-LF2000 Reagent complexes to form..
5	Add 250 L of the mix to each plate. The removal of culture medium is not required.
6	Incubate the cells at 37°C in a CO2 incubator for 4-5 h. Incubate cells until they are ready for further experiments. It is not necessary to remove the complexes or change the medium. Alternatively, growth medium may be replaced after 4-5 h without loss in

	transfection activity.

Table 24. Cell transfection with plasmids

Transfection Mix

(Per 1 well in a 12-well plate)

DNA	500 ng
Lipofectamine 2000	5 μL
OptiMEM	250 μL

7.0 References

1. Molyneaux, K., and Wylie, C. (2004). Primordial germ cell migration. Int J Dev Biol *48*, 537-543.
2. Santos, A.C., and Lehmann, R. (2004). Germ cell specification and migration in Drosophila and beyond. Curr Biol *14*, R578-589.
3. Starz-Gaiano, M., and Lehmann, R. (2001). Moving towards the next generation. Mech Dev *105*, 5-18.
4. Goto, T., Adjaye, J., Rodeck, C.H., and Monk, M. (1999). Identification of genes expressed in human primordial germ cells at the time of entry of the female germ line into meiosis. Mol Hum Reprod *5*, 851-860.
5. McLaren, A. (1998). Germ cells and germ cell transplantation. Int J Dev Biol *42*, 855-860.
6. Wylie, C. (1999). Germ cells. Cell *96*, 165-174.
7. Ohinata, Y., Payer, B., O'Carroll, D., Ancelin, K., Ono, Y., Sano, M., Barton, S.C., Obukhanych, T., Nussenzweig, M., Tarakhovsky, A., Saitou, M., and Surani, M.A. (2005). Blimp1 is a critical determinant of the germ cell lineage in mice. Nature.
8. Saitou, M., Barton, S.C., and Surani, M.A. (2002). A molecular programme for the specification of germ cell fate in mice. Nature *418*, 293-300.
9. Tanaka, S.S., Yamaguchi, Y.L., Tsoi, B., Lickert, H., and Tam, P.P. (2005). IFITM/Mil/fragilis family proteins IFITM1 and IFITM3 play distinct roles in mouse primordial germ cell homing and repulsion. Dev Cell *9*, 745-756.
10. Yoshimizu, T., Obinata, M., and Matsui, Y. (2001). Stage-specific tissue and cell interactions play key roles in mouse germ cell specification. Development *128*, 481-490.
11. Hashimoto, Y., Maegawa, S., Nagai, T., Yamaha, E., Suzuki, H., Yasuda, K., and Inoue, K. (2004). Localized maternal factors are required for zebrafish germ cell formation. Dev Biol *268*, 152-161.
12. Knaut, H., Pelegri, F., Bohmann, K., Schwarz, H., and Nusslein-Volhard, C. (2000). Zebrafish vasa RNA but not its protein is a component of the germ plasm and segregates asymmetrically before germline specification. J Cell Biol *149*, 875-888.
13. Houston, D., and King, M. (2000). Germ plasm and molecular determinants of germ cell fate. Curr Top Dev Biol *50*, 155-181.
14. Knaut, H., Steinbeisser, H., Schwarz, H., and Nusslein-Volhard, C. (2002). An Evolutionary Conserved Region in the vasa 3'UTR Targets RNA Translation to the Germ Cells in the Zebrafish. Curr Biol *12*, 454-466.
15. Seydoux, G., and Fire, A. (1994). Soma-germline asymmetry in the distributions of embryonic RNAs in Caenorhabditis elegans. Development *120*, 2823-2834.
16. Seydoux, G., and Strome, S. (1999). Launching the germline in Caenorhabditis elegans: regulation of gene expression in early germ cells. Development *126*, 3275-3283.

17. Köprunner, M., Thisse, C., Thisse, B., and Raz, E. (2001). A zebrafish nanos-related gene is essential for the development of primordial germ cells. Genes Dev *15*, 2877-2885.
18. Wolke, U., Weidinger, G., Köprunner, M., and Raz, E. (2002). Multiple levels of post-transcriptional control lead to germ line specific gene expression in the zebrafish. Current Biology *12*, 289-294.
19. Olsen, L.C., Aasland, R., and Fjose, A. (1997). A vasa-like gene in zebrafish identifies putative primordial germ cells. Mech Dev *66*, 95-105.
20. Yoon, C., Kawakami, K., and Hopkins, N. (1997). Zebrafish vasa homologue RNA is localized to the cleavage planes of 2- and 4-cell-stage embryos and is expressed in the primordial germ cells. Development *124*, 3157-3165.
21. Braat, A., Zandbergen, T., van de Water, S., Goos, H., and Zivkovic, D. (1999). Characterization of zebrafish primordial germ cells: morphology and early distribution of vasa RNA. Dev Dyn *216*, 153-167.
22. Knaut, H., Pelegri, F., Bohmann, K., Schwarz, H., and Nusslein-Volhard, C. (2000). Zebrafish vasa RNA but not its protein is a component of the germ plasm and segregates asymmetrically before germline specification. J Cell Biol *149*, 875-888.
23. Mishima, Y., Giraldez, A.J., Takeda, Y., Fujiwara, T., Sakamoto, H., Schier, A.F., and Inoue, K. (2006). Differential regulation of germline mRNAs in soma and germ cells by zebrafish miR-430. Curr Biol *16*, 2135-2142.
24. Schupbach, T., and Wieschaus, E. (1986). Maternal-effect mutations altering the anterior-posterir pattern of the Drosophila embryo. Roux's Arch.Dev. Biol. *195*, 302-317.
25. Lehmann, R., and Nusslein-Volhard, C. (1991). The maternal gene nanos has a central role in posterior pattern formation of the Drosophila embryo. Development *112*, 679-691.
26. Wang, C., and Lehmann, R. (1991). Nanos is the localized posterior determinant in Drosophila [published erratum appears in Cell 1992 Mar 20;68(6):1177]. Cell *66*, 637-647.
27. Weidinger, G., Stebler, J., Slanchev, K., Dumstrei, K., Wise, C., Lovell-Badge, R., Thisse, C., Thisse, B., and Raz, E. (2003). *dead end*, a novel vertebrate germ plasm component, is required for zebrafish primordial germ cell migration and survival. Current Biology *13*, 1429-1434.
28. Youngren, K.K., Coveney, D., Peng, X., Bhattacharya, C., Schmidt, L.S., Nickerson, M.L., Lamb, B.T., Deng, J.M., Behringer, R.R., Capel, B., Rubin, E.M., Nadeau, J.H., and Matin, A. (2005). The Ter mutation in the dead end gene causes germ cell loss and testicular germ cell tumours. Nature *435*, 360-364.
29. Horvay, K., Claussen, M., Katzer, M., Landgrebe, J., and Pieler, T. (2006). Xenopus Dead end mRNA is a localized maternal determinant that serves a conserved function in germ cell development. Dev Biol.
30. Tsuda, M., Sasaoka, Y., Kiso, M., Abe, K., Haraguchi, S., Kobayashi, S., and Saga, Y. (2003). Conserved role of nanos proteins in germ cell development. Science *301*, 1239-1241.

31. Kunwar, P.S., Siekhaus, D.E., and Lehmann, R. (2006). In Vivo Migration: A Germ Cell Perspective. Annu Rev Cell Dev Biol.
32. Van Doren, M., Broihier, H.T., Moore, L.A., and Lehmann, R. (1998). HMG-CoA reductase guides migrating primordial germ cells [see comments]. Nature *396*, 466-469.
33. Starz-Gaiano, M., Cho, N.K., Forbes, A., and Lehmann, R. (2001). Spatially restricted activity of a Drosophila lipid phosphatase guides migrating germ cells. Development *128*, 983-991.
34. Zhang, N., Zhang, J., Purcell, K.J., Cheng, Y., and Howard, K. (1997). The Drosophila protein Wunen repels migrating germ cells. Nature *385*, 64-67.
35. Kunwar, P.S., Starz-Gaiano, M., Bainton, R.J., Heberlein, U., and Lehmann, R. (2003). Tre1, a G Protein-Coupled Receptor, Directs Transepithelial Migration of Drosophila Germ Cells. PLoS Biol *1*, E80.
36. Tanaka, S.S., and Matsui, Y. (2002). Developmentally regulated expression of mil-1 and mil-2, mouse interferon-induced transmembrane protein like genes, during formation and differentiation of primordial germ cells. Mech Dev *119 Suppl 1*, S261-267.
37. Gomperts, M., Garcia-Castro, M., Wylie, C., and Heasman, J. (1994). Interactions between primordial germ cells play a role in their migration in mouse embryos. Development *120*, 135-141.
38. Molyneaux, K.A., Stallock, J., Schaible, K., and Wylie, C. (2001). Time-lapse analysis of living mouse germ cell migration. Dev Biol *240*, 488-498.
39. Wylie, C. (2005). IFITM1-mediated cell repulsion controls the initial steps of germ cell migration in the mouse. Dev Cell *9*, 723-724.
40. Ara, T., Nakamura, Y., Egawa, T., Sugiyama, T., Abe, K., Kishimoto, T., Matsui, Y., and Nagasawa, T. (2003). Impaired colonization of the gonads by primordial germ cells in mice lacking a chemokine, stromal cell-derived factor-1 (SDF-1). Proc Natl Acad Sci U S A *100*, 5319-5323.
41. Molyneaux, K., Zinszner, H., Kunwar, P., Schaible, K., Stebler, J., Sunshine, M., O'Brien, W., Raz, E., Littman, D., Wylie, C., and Lehmann, R. (2003). The chemokine SDF1/CXCL12 and its receptor CXCR4 regulate mouse germ cell migration and survival. Development *130*, 4279-4286.
42. Weidinger, G., Wolke, U., Koprunner, M., Klinger, M., and Raz, E. (1999). Identification of tissues and patterning events required for distinct steps in early migration of zebrafish primordial germ cells. Development *126*, 5295-5307.
43. Blaser, H., Eisenbeiss, S., Neumann, M., Reichman-Fried, M., Thisse, B., Thisse, C., and Raz, E. (2005). Transition from non-motile behaviour to directed migration during early PGC development in zebrafish. J Cell Sci *118*, 4027-4038.
44. Raz, E. (2003). Primordial germ-cell development: the zebrafish perspective. Nature Reviews Genetics *4*, 690-700.
45. Weidinger, G., Wolke, U., Koprunner, M., Thisse, C., Thisse, B., and Raz, E. (2002). Regulation of zebrafish primordial germ cell migration by attraction towards an intermediate target. Development *129*, 25-36.

46. Doitsidou, M., Reichman-Fried, M., Stebler, J., Koprunner, M., Dorries, J., Meyer, D., Esguerra, C.V., Leung, T., and Raz, E. (2002). Guidance of Primordial Germ Cell Migration by the Chemokine SDF-1. Cell *111*, 647-659.
47. Knaut, H., Werz, C., Geisler, R., and Nusslein-Volhard, C. (2003). A zebrafish homologue of the chemokine receptor Cxcr4 is a germ-cell guidance receptor. Nature *421*, 279-282.
48. Blaser, H., Reichman-Fried, M., Castanon, I., Dumstrei, K., Marlow, F.L., Kawakami, K., Solnica-Krezel, L., Heisenberg, C.P., and Raz, E. (2006). Migration of zebrafish primordial germ cells: a role for Myosin contraction and cytoplasmic flow. Dev Cell *11*, 613-627.
49. Horuk, R. (2001). Chemokine receptors. Cytokine Growth Factor Rev *12*, 313-335.
50. Lusso, P. (2006). HIV and the chemokine system: 10 years later. Embo J *25*, 447-456.
51. Muller, A., Homey, B., Soto, H., Ge, N., Catron, D., Buchanan, M.E., McClanahan, T., Murphy, E., Yuan, W., Wagner, S.N., Barrera, J.L., Mohar, A., Verastegui, E., and Zlotnik, A. (2001). Involvement of chemokine receptors in breast cancer metastasis. Nature *410*, 50-56.
52. Scotton, C.J., Wilson, J.L., Milliken, D., Stamp, G., and Balkwill, F.R. (2001). Epithelial cancer cell migration: a role for chemokine receptors? Cancer Res *61*, 4961-4965.
53. Hernandez, P.A., Gorlin, R.J., Lukens, J.N., Taniuchi, S., Bohinjec, J., Francois, F., Klotman, M.E., and Diaz, G.A. (2003). Mutations in the chemokine receptor gene CXCR4 are associated with WHIM syndrome, a combined immunodeficiency disease. Nat Genet *34*, 70-74.
54. Diaz, G.A., and Gulino, A.V. (2005). WHIM syndrome: a defect in CXCR4 signaling. Curr Allergy Asthma Rep *5*, 350-355.
55. Balabanian, K., Lagane, B., Pablos, J.L., Laurent, L., Planchenault, T., Verola, O., Lebbe, C., Kerob, D., Dupuy, A., Hermine, O., Nicolas, J.F., Latger-Cannard, V., Bensoussan, D., Bordigoni, P., Baleux, F., Le Deist, F., Virelizier, J.L., Arenzana-Seisdedos, F., and Bachelerie, F. (2005). WHIM syndromes with different genetic anomalies are accounted for by impaired CXCR4 desensitization to CXCL12. Blood *105*, 2449-2457.
56. Vila-Coro, A.J., Rodriguez-Frade, J.M., Martin De Ana, A., Moreno-Ortiz, M.C., Martinez, A.C., and Mellado, M. (1999). The chemokine SDF-1alpha triggers CXCR4 receptor dimerization and activates the JAK/STAT pathway. Faseb J *13*, 1699-1710.
57. Angers, S., Salahpour, A., and Bouvier, M. (2002). Dimerization: an emerging concept for G protein-coupled receptor ontogeny and function. Annu Rev Pharmacol Toxicol *42*, 409-435.
58. Manes, S., Lacalle, R.A., Gomez-Mouton, C., del Real, G., Mira, E., and Martinez, A.C. (2001). Membrane raft microdomains in chemokine receptor function. Semin Immunol *13*, 147-157.
59. Nguyen, D.H., and Taub, D. (2002). CXCR4 function requires membrane cholesterol: implications for HIV infection. J Immunol *168*, 4121-4126.

60. Lauffenburger, D.A., and Horwitz, A.F. (1996). Cell migration: a physically integrated molecular process. Cell *84*, 359-369.
61. Franca-Koh, J., Kamimura, Y., and Devreotes, P. (2006). Navigating signaling networks: chemotaxis in Dictyostelium discoideum. Curr Opin Genet Dev *16*, 333-338.
62. McKay, D.A., Kusel, J.R., and Wilkinson, P.C. (1991). Studies of chemotactic factor-induced polarity in human neutrophils. Lipid mobility, receptor distribution and the time-sequence of polarization. J Cell Sci *100 (Pt 3)*, 473-479.
63. Nieto, M., Frade, J.M., Sancho, D., Mellado, M., Martinez, A.C., and Sanchez-Madrid, F. (1997). Polarization of chemokine receptors to the leading edge during lymphocyte chemotaxis. J Exp Med *186*, 153-158.
64. Vicente-Manzanares, M., Montoya, M.C., Mellado, M., Frade, J.M., del Pozo, M.A., Nieto, M., de Landazuri, M.O., Martinez, A.C., and Sanchez-Madrid, F. (1998). The chemokine SDF-1alpha triggers a chemotactic response and induces cell polarization in human B lymphocytes. Eur J Immunol *28*, 2197-2207.
65. Pelletier, A.J., van der Laan, L.J., Hildbrand, P., Siani, M.A., Thompson, D.A., Dawson, P.E., Torbett, B.E., and Salomon, D.R. (2000). Presentation of chemokine SDF-1 alpha by fibronectin mediates directed migration of T cells. Blood *96*, 2682-2690.
66. van Buul, J.D., Voermans, C., van Gelderen, J., Anthony, E.C., van der Schoot, C.E., and Hordijk, P.L. (2003). Leukocyte-endothelium interaction promotes SDF-1-dependent polarization of CXCR4. J Biol Chem *278*, 30302-30310.
67. Xiao, Z., Zhang, N., Murphy, D.B., and Devreotes, P.N. (1997). Dynamic distribution of chemoattractant receptors in living cells during chemotaxis and persistent stimulation. J Cell Biol *139*, 365-374.
68. Servant, G., Weiner, O.D., Neptune, E.R., Sedat, J.W., and Bourne, H.R. (1999). Dynamics of a chemoattractant receptor in living neutrophils during chemotaxis. Mol Biol Cell *10*, 1163-1178.
69. Dumstrei, K., Mennecke, R., and Raz, E. (2004). Signaling Pathways Controlling Primordial Germ Cell Migration in Zebrafish. Journal of Cell Science *117*, 4787-4795.
70. Ganju, R.K., Brubaker, S.A., Meyer, J., Dutt, P., Yang, Y., Qin, S., Newman, W., and Groopman, J.E. (1998). The alpha-chemokine, stromal cell-derived factor-1alpha, binds to the transmembrane G-protein-coupled CXCR-4 receptor and activates multiple signal transduction pathways. J Biol Chem *273*, 23169-23175.
71. Kucia, M., Jankowski, K., Reca, R., Wysoczynski, M., Bandura, L., Allendorf, D.J., Zhang, J., Ratajczak, J., and Ratajczak, M.Z. (2004). CXCR4-SDF-1 signalling, locomotion, chemotaxis and adhesion. J Mol Histol *35*, 233-245.
72. Krupnick, J.G., and Benovic, J.L. (1998). The role of receptor kinases and arrestins in G protein-coupled receptor regulation. Annu Rev Pharmacol Toxicol *38*, 289-319.
73. Fong, A.M., Premont, R.T., Richardson, R.M., Yu, Y.R., Lefkowitz, R.J., and Patel, D.D. (2002). Defective lymphocyte chemotaxis in beta-arrestin2- and GRK6-deficient mice. Proc Natl Acad Sci U S A *99*, 7478-7483.

74. DeFea, K.A., Zalevsky, J., Thoma, M.S., Dery, O., Mullins, R.D., and Bunnett, N.W. (2000). beta-arrestin-dependent endocytosis of proteinase-activated receptor 2 is required for intracellular targeting of activated ERK1/2. J Cell Biol *148*, 1267-1281.
75. Luttrell, L.M., Ferguson, S.S., Daaka, Y., Miller, W.E., Maudsley, S., Della Rocca, G.J., Lin, F., Kawakatsu, H., Owada, K., Luttrell, D.K., Caron, M.G., and Lefkowitz, R.J. (1999). Beta-arrestin-dependent formation of beta2 adrenergic receptor-Src protein kinase complexes. Science *283*, 655-661.
76. Lefkowitz, R.J., and Shenoy, S.K. (2005). Transduction of receptor signals by beta-arrestins. Science *308*, 512-517.
77. Cheng, Z.J., Zhao, J., Sun, Y., Hu, W., Wu, Y.L., Cen, B., Wu, G.X., and Pei, G. (2000). beta-arrestin differentially regulates the chemokine receptor CXCR4-mediated signaling and receptor internalization, and this implicates multiple interaction sites between beta-arrestin and CXCR4. J Biol Chem *275*, 2479-2485.
78. Sun, Y., Cheng, Z., Ma, L., and Pei, G. (2002). Beta-arrestin2 is critically involved in CXCR4-mediated chemotaxis, and this is mediated by its enhancement of p38 MAPK activation. J Biol Chem *277*, 49212-49219.
79. Roland, J., Murphy, B.J., Ahr, B., Robert-Hebmann, V., Delauzun, V., Nye, K.E., Devaux, C., and Biard-Piechaczyk, M. (2003). Role of the intracellular domains of CXCR4 in SDF-1-mediated signaling. Blood *101*, 399-406.
80. Busillo, J.M., and Benovic, J.L. (2006). Regulation of CXCR4 signaling. Biochim Biophys Acta.
81. Freedman, N.J., and Lefkowitz, R.J. (1996). Desensitization of G protein-coupled receptors. Recent Prog Horm Res *51*, 319-351; discussion 352-313.
82. Pitcher, J.A., Freedman, N.J., and Lefkowitz, R.J. (1998). G protein-coupled receptor kinases. Annu Rev Biochem *67*, 653-692.
83. Ferguson, S.S. (2001). Evolving concepts in G protein-coupled receptor endocytosis: the role in receptor desensitization and signaling. Pharmacol Rev *53*, 1-24.
84. Benovic, J.L., Kuhn, H., Weyand, I., Codina, J., Caron, M.G., and Lefkowitz, R.J. (1987). Functional desensitization of the isolated beta-adrenergic receptor by the beta-adrenergic receptor kinase: potential role of an analog of the retinal protein arrestin (48-kDa protein). Proc Natl Acad Sci U S A *84*, 8879-8882.
85. Lohse, M.J., Benovic, J.L., Codina, J., Caron, M.G., and Lefkowitz, R.J. (1990). beta-Arrestin: a protein that regulates beta-adrenergic receptor function. Science *248*, 1547-1550.
86. Pippig, S., Andexinger, S., Daniel, K., Puzicha, M., Caron, M.G., Lefkowitz, R.J., and Lohse, M.J. (1993). Overexpression of beta-arrestin and beta-adrenergic receptor kinase augment desensitization of beta 2-adrenergic receptors. J Biol Chem *268*, 3201-3208.
87. Peacock, J.W., and Jirik, F.R. (1999). TCR activation inhibits chemotaxis toward stromal cell-derived factor-1: evidence for reciprocal regulation between CXCR4 and the TCR. J Immunol *162*, 215-223.

88. Guinamard, R., Signoret, N., Ishiai, M., Marsh, M., Kurosaki, T., and Ravetch, J.V. (1999). B cell antigen receptor engagement inhibits stromal cell-derived factor (SDF)-1alpha chemotaxis and promotes protein kinase C (PKC)-induced internalization of CXCR4. J Exp Med *189*, 1461-1466.
89. Li, B.Q., Wetzel, M.A., Mikovits, J.A., Henderson, E.E., Rogers, T.J., Gong, W., Le, Y., Ruscetti, F.W., and Wang, J.M. (2001). The synthetic peptide WKYMVm attenuates the function of the chemokine receptors CCR5 and CXCR4 through activation of formyl peptide receptor-like 1. Blood *97*, 2941-2947.
90. Selleri, C., Montuori, N., Ricci, P., Visconte, V., Carriero, M.V., Sidenius, N., Serio, B., Blasi, F., Rotoli, B., Rossi, G., and Ragno, P. (2005). Involvement of the urokinase-type plasminogen activator receptor in hematopoietic stem cell mobilization. Blood *105*, 2198-2205.
91. Richardson, R.M., Tokunaga, K., Marjoram, R., Sata, T., and Snyderman, R. (2003). Interleukin-8-mediated heterologous receptor internalization provides resistance to HIV-1 infectivity. Role of signal strength and receptor desensitization. J Biol Chem *278*, 15867-15873.
92. Suratt, B.T., Petty, J.M., Young, S.K., Malcolm, K.C., Lieber, J.G., Nick, J.A., Gonzalo, J.A., Henson, P.M., and Worthen, G.S. (2004). Role of the CXCR4/SDF-1 chemokine axis in circulating neutrophil homeostasis. Blood *104*, 565-571.
93. Hecht, I., Cahalon, L., Hershkoviz, R., Lahat, A., Franitza, S., and Lider, O. (2003). Heterologous desensitization of T cell functions by CCR5 and CXCR4 ligands: inhibition of cellular signaling, adhesion and chemotaxis. Int Immunol *15*, 29-38.
94. Haribabu, B., Richardson, R.M., Fisher, I., Sozzani, S., Peiper, S.C., Horuk, R., Ali, H., and Snyderman, R. (1997). Regulation of human chemokine receptors CXCR4. Role of phosphorylation in desensitization and internalization. J Biol Chem *272*, 28726-28731.
95. Orsini, M.J., Parent, J.L., Mundell, S.J., Benovic, J.L., and Marchese, A. (1999). Trafficking of the HIV coreceptor CXCR4. Role of arrestins and identification of residues in the c-terminal tail that mediate receptor internalization. J Biol Chem *274*, 31076-31086.
96. Signoret, N., Oldridge, J., Pelchen-Matthews, A., Klasse, P.J., Tran, T., Brass, L.F., Rosenkilde, M.M., Schwartz, T.W., Holmes, W., Dallas, W., Luther, M.A., Wells, T.N., Hoxie, J.A., and Marsh, M. (1997). Phorbol esters and SDF-1 induce rapid endocytosis and down modulation of the chemokine receptor CXCR4. J Cell Biol *139*, 651-664.
97. Signoret, N., Rosenkilde, M.M., Klasse, P.J., Schwartz, T.W., Malim, M.H., Hoxie, J.A., and Marsh, M. (1998). Differential regulation of CXCR4 and CCR5 endocytosis. J Cell Sci *111 (Pt 18)*, 2819-2830.
98. Neel, N.F., Schutyser, E., Sai, J., Fan, G.H., and Richmond, A. (2005). Chemokine receptor internalization and intracellular trafficking. Cytokine Growth Factor Rev *16*, 637-658.
99. Marchese, A., Chen, C., Kim, Y.M., and Benovic, J.L. (2003). The ins and outs of G protein-coupled receptor trafficking. Trends Biochem Sci *28*, 369-376.

100. Tarasova, N.I., Stauber, R.H., and Michejda, C.J. (1998). Spontaneous and ligand-induced trafficking of CXC-chemokine receptor 4. J Biol Chem *273*, 15883-15886.
101. Marchese, A., and Benovic, J.L. (2001). Agonist-promoted ubiquitination of the G protein-coupled receptor CXCR4 mediates lysosomal sorting. J Biol Chem *276*, 45509-45512.
102. Marchese, A., Raiborg, C., Santini, F., Keen, J.H., Stenmark, H., and Benovic, J.L. (2003). The E3 ubiquitin ligase AIP4 mediates ubiquitination and sorting of the G protein-coupled receptor CXCR4. Dev Cell *5*, 709-722.
103. Sbaa, E., Dewever, J., Martinive, P., Bouzin, C., Frerart, F., Balligand, J.L., Dessy, C., and Feron, O. (2006). Caveolin plays a central role in endothelial progenitor cell mobilization and homing in SDF-1-driven postischemic vasculogenesis. Circ Res *98*, 1219-1227.
104. Nguyen, D.H., and Taub, D. (2002). Cholesterol is essential for macrophage inflammatory protein 1 beta binding and conformational integrity of CC chemokine receptor 5. Blood *99*, 4298-4306.
105. Venkatesan, S., Rose, J.J., Lodge, R., Murphy, P.M., and Foley, J.F. (2003). Distinct mechanisms of agonist-induced endocytosis for human chemokine receptors CCR5 and CXCR4. Mol Biol Cell *14*, 3305-3324.
106. Orsini, M.J., Parent, J.L., Mundell, S.J., Marchese, A., and Benovic, J.L. (2000). Trafficking of the HIV coreceptor CXCR4: role of arrestins and identification of residues in the C-terminal tail that mediate receptor internalization. J Biol Chem *275*, 25876.
107. Gulino, A.V., Moratto, D., Sozzani, S., Cavadini, P., Otero, K., Tassone, L., Imberti, L., Pirovano, S., Notarangelo, L.D., Soresina, R., Mazzolari, E., Nelson, D.L., Notarangelo, L.D., and Badolato, R. (2004). Altered leukocyte response to CXCL12 in patients with warts hypogammaglobulinemia, infections, myelokathexis (WHIM) syndrome. Blood *104*, 444-452.
108. Kawai, T., Choi, U., Whiting-Theobald, N.L., Linton, G.F., Brenner, S., Sechler, J.M., Murphy, P.M., and Malech, H.L. (2005). Enhanced function with decreased internalization of carboxy-terminus truncated CXCR4 responsible for WHIM syndrome. Exp Hematol *33*, 460-468.
109. Ueda, Y., Neel, N.F., Schutyser, E., Raman, D., and Richmond, A. (2006). Deletion of the COOH-terminal domain of CXC chemokine receptor 4 leads to the down-regulation of cell-to-cell contact, enhanced motility and proliferation in breast carcinoma cells. Cancer Res *66*, 5665-5675.
110. Ramirez-Weber, F.A., and Kornberg, T.B. (1999). Cytonemes: cellular processes that project to the principal signaling center in Drosophila imaginal discs. Cell *97*, 599-607.
111. Kikuchi, Y., Agathon, A., Alexander, J., Thisse, C., Waldron, S., Yelon, D., Thisse, B., and Stainier, D.Y. (2001). casanova encodes a novel Sox-related protein necessary and sufficient for early endoderm formation in zebrafish. Genes Dev *15*, 1493-1505.
112. Alexander, J., Rothenberg, M., Henry, G.L., and Stainier, D.Y. (1999). casanova plays an early and essential role in endoderm formation in zebrafish. Dev Biol *215*, 343-357.

113. Alexander, J., and Stainier, D.Y. (1999). A molecular pathway leading to endoderm formation in zebrafish. Curr Biol *9*, 1147-1157.
114. Reichman-Fried, M., Minina, S., and Raz, E. (2004). Autonomous Modes of Behavior in Primordial Germ Cell Migration. Developmental Cell *6*, 589-596.
115. Jekely, G., Sung, H.H., Luque, C.M., and Rorth, P. (2005). Regulators of endocytosis maintain localized receptor tyrosine kinase signaling in guided migration. Dev Cell *9*, 197-207.
116. Mueller, S.G., White, J.R., Schraw, W.P., Lam, V., and Richmond, A. (1997). Ligand-induced desensitization of the human CXC chemokine receptor-2 is modulated by multiple serine residues in the carboxyl-terminal domain of the receptor. J Biol Chem *272*, 8207-8214.
117. Richardson, R.M., Pridgen, B.C., Haribabu, B., Ali, H., and Snyderman, R. (1998). Differential cross-regulation of the human chemokine receptors CXCR1 and CXCR2. Evidence for time-dependent signal generation. J Biol Chem *273*, 23830-23836.
118. Oppermann, M., Mack, M., Proudfoot, A.E., and Olbrich, H. (1999). Differential effects of CC chemokines on CC chemokine receptor 5 (CCR5) phosphorylation and identification of phosphorylation sites on the CCR5 carboxyl terminus. J Biol Chem *274*, 8875-8885.
119. Kraft, K., Olbrich, H., Majoul, I., Mack, M., Proudfoot, A., and Oppermann, M. (2001). Characterization of sequence determinants within the carboxyl-terminal domain of chemokine receptor CCR5 that regulate signaling and receptor internalization. J Biol Chem *276*, 34408-34418.
120. Huttenrauch, F., Nitzki, A., Lin, F.T., Honing, S., and Oppermann, M. (2002). Beta-arrestin binding to CC chemokine receptor 5 requires multiple C-terminal receptor phosphorylation sites and involves a conserved Asp-Arg-Tyr sequence motif. J Biol Chem *277*, 30769-30777.
121. Mokros, T., Rehm, A., Droese, J., Oppermann, M., Lipp, M., and Hopken, U.E. (2002). Surface expression and endocytosis of the human cytomegalovirus-encoded chemokine receptor US28 is regulated by agonist-independent phosphorylation. J Biol Chem *277*, 45122-45128.
122. Richardson, R.M., Marjoram, R.J., Barak, L.S., and Snyderman, R. (2003). Role of the cytoplasmic tails of CXCR1 and CXCR2 in mediating leukocyte migration, activation, and regulation. J Immunol *170*, 2904-2911.
123. Bleul, C.C., Farzan, M., Choe, H., Parolin, C., Clark-Lewis, I., Sodroski, J., and Springer, T.A. (1996). The lymphocyte chemoattractant SDF-1 is a ligand for LESTR/fusin and blocks HIV-1 entry. Nature *382*, 829-833.
124. Oberlin, E., Amara, A., Bachelerie, F., Bessia, C., Virelizier, J.L., Arenzana-Seisdedos, F., Schwartz, O., Heard, J.M., Clark-Lewis, I., Legler, D.F., Loetscher, M., Baggiolini, M., and Moser, B. (1996). The CXC chemokine SDF-1 is the ligand for LESTR/fusin and prevents infection by T-cell-line-adapted HIV-1. Nature *382*, 833-835.
125. David, N.B., Sapede, D., Saint-Etienne, L., Thisse, C., Thisse, B., Dambly-Chaudiere, C., Rosa, F.M., and Ghysen, A. (2002). Molecular

basis of cell migration in the fish lateral line: Role of the chemokine receptor CXCR4 and of its ligand, SDF1. Proc Natl Acad Sci U S A.
126. Gilmour, D., Knaut, H., Maischein, H.M., and Nusslein-Volhard, C. (2004). Towing of sensory axons by their migrating target cells in vivo. Nat Neurosci *7*, 491-492.
127. Bendel-Stenzel, M.R., Gomperts, M., Anderson, R., Heasman, J., and Wylie, C. (2000). The role of cadherins during primordial germ cell migration and early gonad formation in the mouse. Mech Dev *91*, 143-152.
128. Sano, H., Renault, A.D., and Lehmann, R. (2005). Control of lateral migration and germ cell elimination by the Drosophila melanogaster lipid phosphate phosphatases Wunen and Wunen 2. J Cell Biol *171*, 675-683.
129. Loetscher, P., Moser, B., and Baggiolini, M. (2000). Chemokines and their receptors in lymphocyte traffic and HIV infection. Adv Immunol *74*, 127-180.
130. Baggiolini, M., and Loetscher, P. (2000). Chemokines in inflammation and immunity. Immunol Today *21*, 418-420.
131. Carlos, T.M. (2001). Leukocyte recruitment at sites of tumor: dissonant orchestration. J Leukoc Biol *70*, 171-184.
132. Dormann, D., and Weijer, C.J. (2006). Imaging of cell migration. Embo J *25*, 3480-3493.
133. Devreotes, P., and Janetopoulos, C. (2003). Eukaryotic Chemotaxis: Distinctions between Directional Sensing and Polarization. J Biol Chem *278*, 20445-20448.
134. Merlot, S., and Firtel, R.A. (2003). Leading the way: Directional sensing through phosphatidylinositol 3-kinase and other signaling pathways. J Cell Sci *116*, 3471-3478.
135. Manes, S., Gomez-Mouton, C., Lacalle, R.A., Jimenez-Baranda, S., Mira, E., and Martinez, A.C. (2005). Mastering time and space: immune cell polarization and chemotaxis. Semin Immunol *17*, 77-86.
136. Yang, W., Wang, D., and Richmond, A. (1999). Role of clathrin-mediated endocytosis in CXCR2 sequestration, resensitization, and signal transduction. J Biol Chem *274*, 11328-11333.
137. Fan, G.H., Yang, W., Wang, X.J., Qian, Q., and Richmond, A. (2001). Identification of a motif in the carboxyl terminus of CXCR2 that is involved in adaptin 2 binding and receptor internalization. Biochemistry *40*, 791-800.
138. Rose, J.J., Foley, J.F., Murphy, P.M., and Venkatesan, S. (2004). On the mechanism and significance of ligand-induced internalization of human neutrophil chemokine receptors CXCR1 and CXCR2. J Biol Chem *279*, 24372-24386.
139. Westerfield, M. (1995). The Zebrafish Book (Oregon: University of Oregon Press).
140. Kimmel, C., Ballard, W., SR, K., B, U., and TF, S. (1995). Stages of embryonic development of the zebrafish. Developmental Dynamics *203*, 253-310.
141. Jowett, T., and Lettice, L. (1994). Whole-mount in situ hybridizations on zebrafish embryos using a mixture of digoxigenin- and fluorescein-labelled probes. Trends Genet *10*, 73-74.

142. Hauptmann, G., and Gerster, T. (1994). Two-color whole-mount in situ hybridization to vertebrate and Drosophila embryos. Trends Genet *10*, 266.
143. Peyrieras, N., Strahle, U., and Rosa, F. (1998). Conversion of zebrafish blastomeres to an endodermal fate by TGF-beta-related signaling. Curr Biol *8*, 783-786.
144. Müller, K., Thisse, C., Thisse, B., and Raz, E. (2002). Expression of a linker histone-like gene in the primordial germ cells in zebrafish. Mechanisms of Development *117*, 253-257.

8.0 Acknowledgements

I would like to thank Erez Raz who supported my work and my ideas, from whom I basically learnt everything professionally starting with molecular cloning and up to writing this thesis, to correctly address scientific questions and not to lose time on unnecessary points. To distinguish those was a great lesson that I learnt from Erez.

I am also grateful to him and to other lab members for the warmest atmosphere in the lab during the years of my PhD. Here I would like to express my special gratitude to Karin, Natalia and Elena who became my close friends with whom on one hand we had tons of fun and who on the other hand supported me in my bitter moments. Elena thank you so much for not letting me forget Russian during these years! Natalia dear good luck with your new career !

Thank you dear Michal for your warmth, friendship, fruitful collaboration, the best dinners at your place and especially for bringing me to this lab, which was really a great turn in my career that determined my future life directions. Besides, Goettingen is a marvellous place. How could it be that I would miss it? However it sounds, you were a *deadend* for me, a real fate determinant.

Dear Heiko, Markus, Bijan and Harsha, thank you very much for being in the lab. You were the best collegues and friends. Am I going to have such nice people around me at my future job? I can only hope for that! Heiko I am very grateful to you for teaching me things in the lab in those first months and later whenever I would need it. I will never step away from the rules you imprinted on me. Better kill me but I will never collect eggs before 5 minutes have passed! Bijan thank you so much for your help with this manuscript.

My special thanks are owed to Julia, Helene and Ursula for their technical support and readiness to help.

9.0 Affidavit

Hiermit versichere ich, dass ich die vorliegende Dissertation selbständig und ohne unerlaubte Hilfe angefertigt und andere als die in der Dissertation angegebenen Hilfsmittel nicht benutzt habe. Alle Stellen, die wörtlich oder sinngemäß aus veröffentlichten oder unveröffentlichten Schriften entnommen sind, habe ich als solche kenntlich gemacht. Kein Teil dieser Arbeit ist in einem anderen Promotions- oder Habilitationsverfahren verwendet worden.

Here I declare that my thesis entitled “Molecular Mechanisms controlling the Precision of Chemokine Guided Cell Migration” has been done independently and with no other sources and aids than quoted and listed below.

Göttingen, 25.04.2007

Signature: Sofia Minina